

ENGINEERING

EDGE

Accelerate Innovation with CFD & Thermal Characterization

Curiosity: Life on Mars

Page 18

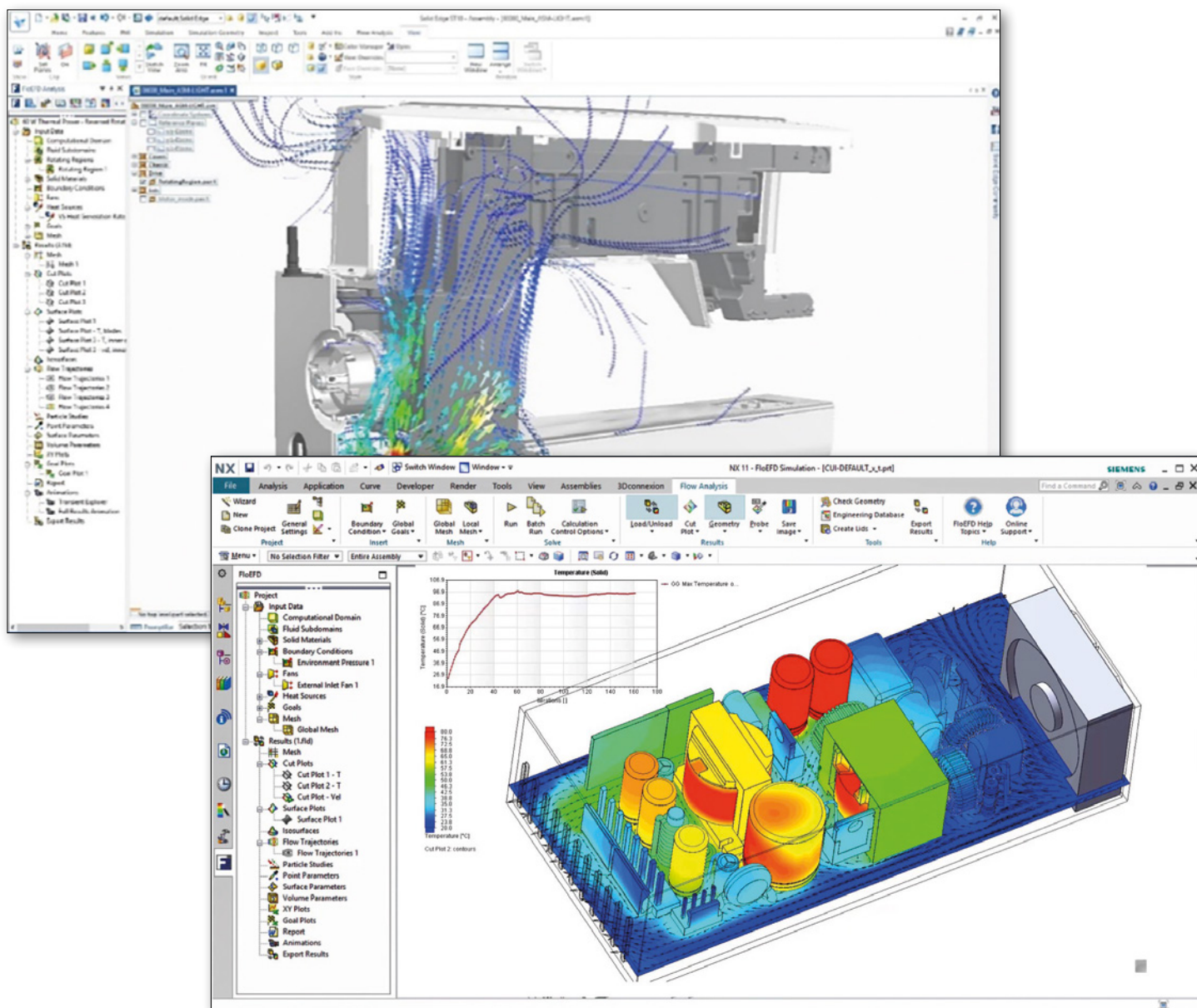
Intel Corporation:
Thermal-Power
Page 24

Hitachi Corporation:
Medical Ultrasound Probes
Page 44

Mentor[®]
A Siemens Business

mentor.com/mechanical
Vol. 06 / Issue. 02 / 2017

FloEFD™ - Frontloading CFD inside Siemens NX and Solid Edge





Vol. 06, Issue. 02

Greetings readers! A lot has happened since our last Newsletter. Mentor Graphics Corporation is now a Siemens company having been acquired by Siemens AG in April 2017, and is now part of the Digital Factory Division of the Siemens PLM Group. This pioneering foray into the EDA sector by a PLM company, the first of its kind, opens up a whole new chapter in our journey and some exciting new directions for our product lines that I touch on in an editorial article on page 6 of this magazine. Siemens PLM's vision of digital twins, predictive engineering analytics, simulation & test, and systems driven product development very much echo where we have been going for the last five years. In addition, my colleague, Puneet Sinha, our new Automotive Electrification Manager, also offers insights into our autonomous vehicle activities in this emerging electric powertrain area (page 9). My colleague, Lazlo Tolnay, also introduces a new concept for MicReD Industrial, a Volume Tester, with real benefits to many different electronic application areas in terms of applying T3Ster's unprecedented thermal analysis methodology into production lines for large samples in short testing windows.

Moving on to product news, we have some exciting major software product releases in the form of FloTHERM® 12 and FloEFD™ 17. Both have exciting 'big stone' features such as a new improved Command Center, phase change materials and ODB++ import inside FloTHERM, and free surface, turbomachinery periodicity and a myriad of user experience enhancements in FloEFD. My congratulations to our development teams for such big releases. I would also like to recognize our MicReD Product Manager, Zoltan Sakarny, who was given the 'Outstanding Technical Paper' award at the ICEP 2016 conference for his co-authored work with Marta Rencz and Gabor Farkas on "Thermal Characterization of Capacitors".

We have a wealth of customer stories in this edition of Engineering Edge covering an amazing range of applications. We lead with INTA in Spain who worked with NASA to develop the sensors for the Curiosity Mars rover, plus Intel and Iceotope deal with

the fast-emerging Internet of Things (IoT). There are also stories from Fiat, Infineon and Hitachi that I commend to you.

Finally, we can announce the winner of this year's Don Miller Award is an excellent piece of work from Hyundai Heavy Industries in Korea where FloMASTER was cleverly used to model the fuel system of a satellite launching rocket. This year's Frontloading CFD Award will be announced at our FloEFD Conference in Berlin in November. I look forward to meeting a number of you there.

**Roland Feldhinkel, General Manager,
Mechanical Analysis Division,
Mentor – A Siemens Company**

Mentor, a Siemens Business

Pury Hill Business Park,
The Maltings,
Towcester, NN12 7TB,
United Kingdom
Tel: +44 (0)1327 306000
email: ee@mentor.com

Editor:

Keith Hanna

Managing Editor:

Natasha Antunes

Copy Editor:

Jane Wade

Contributors:

A. A. Sobachkin, A.V. Ivanov, A.V. Rubekina, Doug Kolak, G.E. Dumnov, John Parry, Keith Hanna, Laszlo Tolnay, Mike Croegeart, Mike Gruetzmacher, Puneet Sinha and Roland Feldhinkel.

With special thanks to:

Centro de Astrobiologia (INTA-CSIC), Creative Solutions, DATADVANCE, Fiat Chrysler Automobiles Italy, FLIR Systems, Hitachi Ltd., Japan, IC Blue ICEOTOPE, UK, Infineon Technologies AG, Intel Corporation, JS Pump and Fluid System Consultants, Kehoe Myers Consulting Engineers, Korean Aerospace Research Institute, KTH Royal Institute of Technology, Mobilis, PAO NPO Saturn, Russia, Team Bath Racing, Technion-Israel Institute

Technology, Technische Universitat Chemnitz, Voxdale Bvba, Watson-Marlow Fluid Technology Group and Wendy Luiten Consulting.

©2017 Mentor, a Siemens Business, all rights reserved. This document contains information that is proprietary to Mentor, a Siemens Business and may be duplicated in whole or in part by the original recipient for internal business purposes only, provided that this entire notice appears in all copies. In accepting this document, the recipient agrees to make every reasonable effort to prevent unauthorized use of this information.

All trademarks mentioned in this publication are the trademarks of their respective owners.

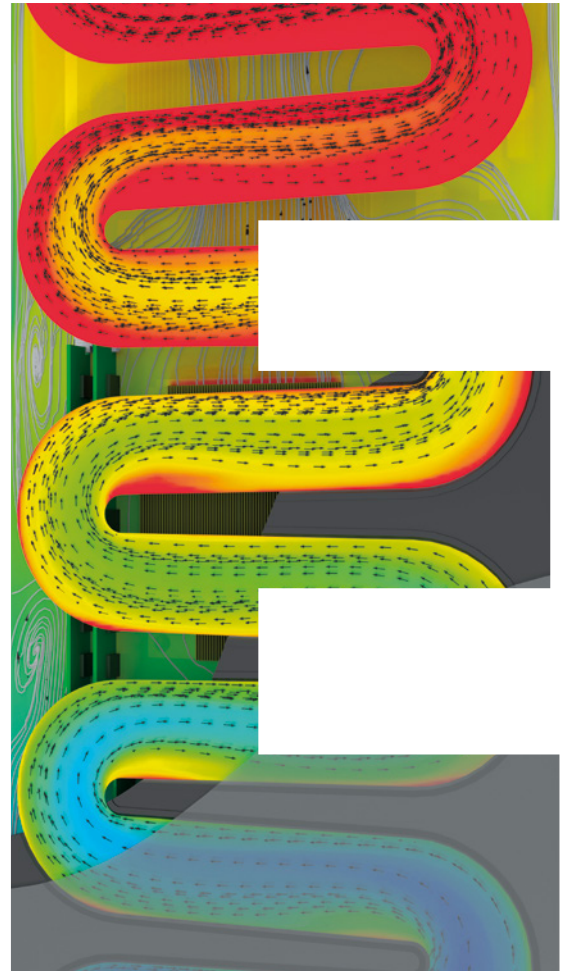


News

- 06** Design-Centric Simulation & Test
- 09** Autonomous Vehicle Systems
- 12** Don Miller Award 2017
- 14** New Release: FloEFD 17.0
- 15** New Release: FloTHERM 12
- 16** Introduction to Industrial Volume Testing

Engineering Edge

- 18** Curiosity: Life on Mars
- 24** Thermal-Power: Envelopes in IoT Solutions
- 28** IR-Camera Thermal Management
- 34** Up in the Cloud: Turbo Charging FloEFD Usage
- 38** Rocket Science and FloMASTER
- 44** Fast Design of Medical Ultrasound Probes
- 46** Evaluation of Characterization Methods for Solid TIMs
- 50** Peristaltic Pump Electronics Thermal Design
- 52** Team Bath Race Car Cooling & Lubrication Simulation



56 Transonic Micro-turbine Test Rig Validation

60 Keeping it Cool in Gas Turbines

68 Design for Six Sigma in Electronics Cooling

72 Liquid Cooled Computing

76 Designing a Water Supply System for Australia's Newest Airport

80 The Evolution of One-dimensional Simulation for Automotive Thermal Management Systems

84 CAD-Embedded Battery Pack Design Optimization

Regular Features

30 How to: Optimize an IGBT Cold Plate

42 Interview: Wendy Luiten, Wendy Luiten Consulting

65 Ask the GSS Expert

88 Geek Hub

90 Brownian Motion

Design-Centric Simulation & Test and the Digital Twin

By Roland Feldhinkel, GM, Mechanical Analysis Division, Mentor, a Siemens Business



Many of you will now know that Mentor Graphics Corporation was acquired by Siemens PLM in April 2017 becoming part of its Digital Factory Division, and this event is being seen, by analysts in our sector, as a tectonic plate shift for the PLM, CAE, and arguably the EDA landscape. This is all being driven by external trends, I believe, because electronics is increasingly being embedded into everything mechanical, as indeed we experience on a daily basis in our cars and with an ever-growing array of consumer products. Moreover, we are about to see waves of new technologies coming into the mainstream of our societies such as autonomous vehicles, the Internet of Things (IoT), robotics, big data analytics, cloud computing, artificial intelligence (AI) and additive manufacturing; all are contributing to this blurring of the historic electronics/mechanical divide in products.

You may have heard of the phrase 'Industrie 4.0' (Figure 1) which refers to a German-government-sponsored vision for the fourth industrial revolution – the first being water/steam power, the second being mass production and automation, the third being IT and robotics - and now we have the emerging concept of 'cyber-physical systems', i.e. 'digital twins', to differentiate this new evolutionary phase from the electronic automation that has gone before [1]. The 4th Industrial Revolution is going to create enormous upheaval and it's coming at a massive rate. It will be disruptive because it will take out the weakest links in all sorts of value chains, and I suspect that companies we are familiar with today will likely disappear. It will be a massive paradigm shift for all manufacturing enterprises because every device in the world will be designed in the virtual space. And with the emergence of the IoT, there will be worldwide connectivity of these devices; whether we like it or not. Ultimately, the 4th Industry Revolution will be about Software and Electrification, Automation, and Digitalization (EAD). This is a vision that very much resonates with the 2020 vision of Siemens AG, who uniquely have hardware manufacturing, automation, and now Mechanical Design Automation (MDA) and Electric/Electronic Design Automation (EDA) software all under one roof [2].

Siemens has spent nearly \$6.5Bn since 2013 in expanding its software portfolio for MDA and EDA, acquiring LMS (1D and CAE/3D Simulation and Test, 2013), CD-adapco



(CFD Market Leader, 2016) and now Mentor Graphics (EDA, 2017). Siemens is now vying for first place in the Product Lifecycle Management (PLM) space. Incidentally, with the acquisition of CD-adapco and the Mechanical Analysis Division in Mentor Graphics, with our 1D and 3D CFD products, it also means that Siemens PLM is definitely ruling the CFD market as well, with the broadest industry offering to support all enterprise needs in simulation. Moreover, I genuinely believe that Siemens now has the chance to truly bridge the gap between the EDA (Electronics Design Automation) sector and our mechanical design and simulation domain.

With Siemens PLM's vision for 'Predictive Data Analytics' to enable verification and

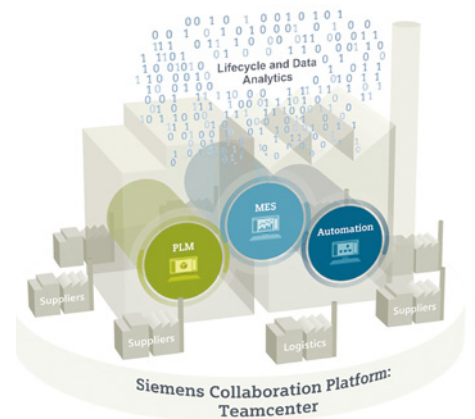


Figure 1. Siemens' Digital Factory 'Industrie 4.0' Conception

validation for Systems Driven Product Development (SDPD), manifested as the Simcenter™ portfolio launched in 2016, we are further setting the pace for innovation in the Simulation and Analysis market. Siemens already has supporting Simulation Data Management (SDM) in its PLM backbone software, Teamcenter™, together with geometry sourced from its NX or Solid Edge CAD engines, and the LMS acquisition is helping to pull together the fields of 1D systems and 3D multi-discipline mechanical simulation. Siemens PLM also has unique Testing equipment plus its existing factory automation software. It therefore means that Siemens offers a big unifying vision of the ‘digital factory’ spanning hardware, manufacturing software, engineering simulation & test including 1D-3D CAE software (Figure 4), and post-sales service software; all in an open architecture conception (Figure 2).

It is fair to say that engineering simulation software, including CFD, is a big key to enabling manufacturers to bring better products to the market faster, and at less cost. And typically frontloading of simulation yields the largest return in investment (ROI) in engineering simulation. If we consider the 3D CFD landscape, suddenly over a one year period Siemens now provides the most comprehensive CFD solution suite in the world and is the market leader in electronics cooling and CAD-embedded CFD with the acquisition of FloTHERM® and FloEFD™ products (Figure 5). Market leading CFD products such as STAR-CCM+®, STAR-CD®, the existing Simcenter 3D Flow, and now also FloTHERM®, and FloEFD™ applications expand Siemens’ CAE simulation portfolio Simcenter™. These applications cover the full spectrum of CFD user profiles extending from R&D engineers & CFD simulation engineers, to design engineers & designers for both general purpose CFD and electronics thermal applications. Siemens’ suite of CFD products offer unprecedented user workflow and productivity benefits encompassing accurate frontloading, CAD-embedding and design space exploration. Siemens PLM has, I believe, the largest CFD knowledgebase in the world with many industry thought-leaders collaborating together. There is also the realistic prospect of accelerating the democratization of CFD usage like never before within real-world manufacturing PLM workflows [3].

I stated in the last Engineering Edge [3] that embedding CFD into native CAD software will be one of the biggest factors driving the democratization of CFD in the next ten years, and products like our FloEFD suite of tools will



Figure 2. Siemens Digital factory Software Portfolio for the Digital Enterprise

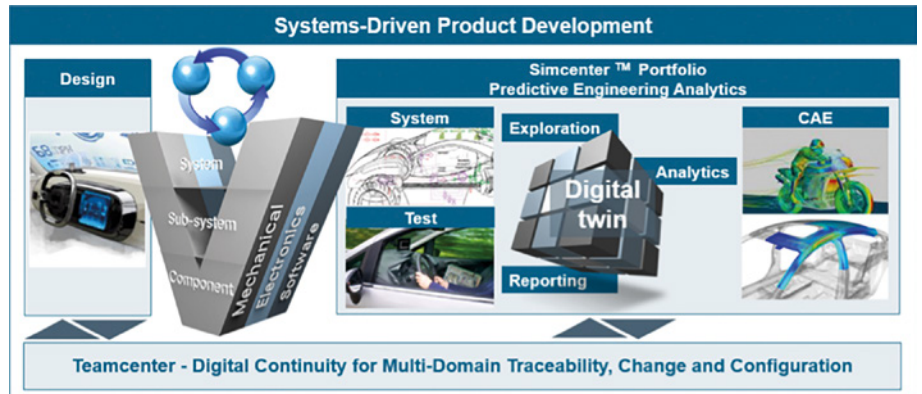


Figure 3. Simcenter™ from Siemens PLM for Predictive Data Analytics - Verification & Validation in the age of Systems Engineering

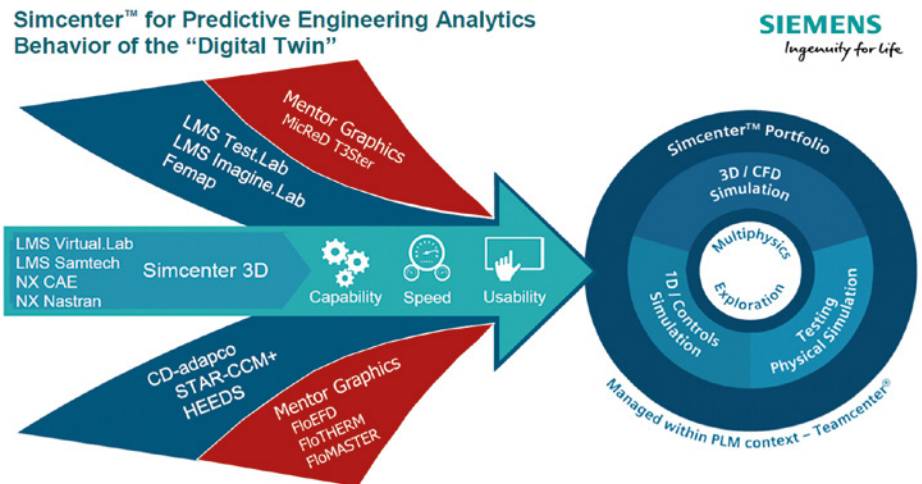


Figure 4. Products contributing to the Simcenter™ Portfolio from Siemens PLM and schematic of Mentor's Mechanical Analysis software & test equipment offerings

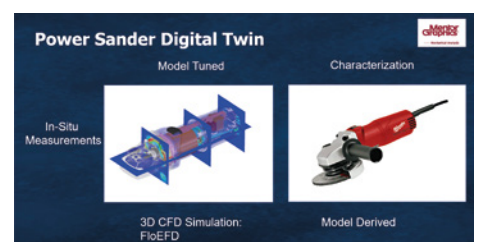
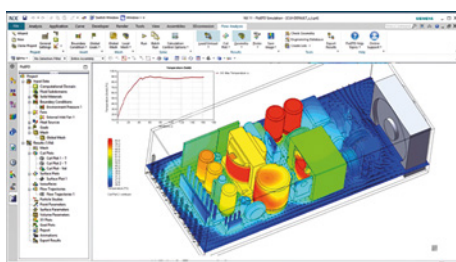


Figure 5. NX CAD-embedded CFD implementation of FloEFD and a typical Power Sander ‘Digital Twin’

Unique Challenges

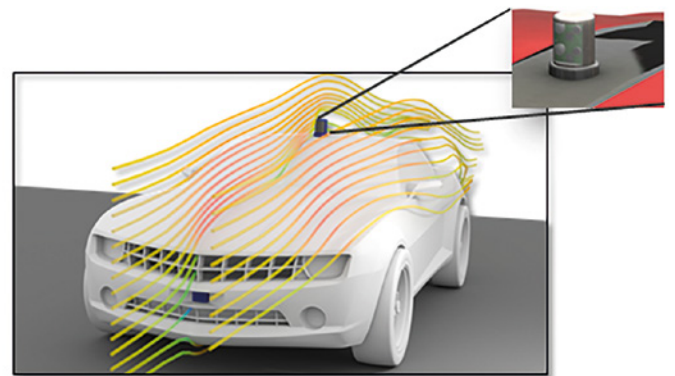
with Autonomous Vehicle Systems
Design and Integration

By Puneet Sinha, Automotive Manager, Mentor, a Siemens Business



S stories about autonomous vehicles are regular fare in the tech news cycle and usually include forecasts about the eventual ascendancy of self-driving cars. It is projected that by 2035, 25% of all cars will have partial or full autonomy [1]. In the short few years since the Google concept car, auto manufacturers new and old have announced their plans [2] for commercializing autonomous vehicles starting as early as 2021. That's disruption! So what will it take to deliver on this future? Without a doubt, artificial intelligence with robust machine algorithms to comprehend road and traffic conditions and make appropriate decisions is the most critical. However, it will take a lot more than artificial intelligence to build commercially-viable autonomous vehicles.

To deliver, the automotive supply chain will reshape very drastically in the coming years, where necessary component-level technology (sensors/fusion box/new electronics) will be driven by the new entrants (technology/electronics startups or large organizations) but the responsibility of vehicle integration will continue to be with auto OEMs. This fast evolving supply chain coupled with a paradigm shift in desired vehicle functionalities, pose unique challenges to autonomous vehicle engineering. In this article, I highlight the key challenges and Mentor's solutions to address them.



Sensor Design Exploration

Design goals for lidars, radars and cameras, three of the most critical sensors for autonomous vehicles, are largely centered on size and cost reduction without sacrificing high resolution and the high range necessary to support various levels of vehicle autonomy. Additionally, these sensors when integrated in vehicles, must function reliably in an automotive environment and in all-weather conditions. Desired small form factors and functionality consolidation for signal processing in the sensors may cause significant heat build-up that may be detrimental to performance and/or reliability of sensors. This may deter sensor size (and cost) reduction efforts. Thermally-conscious designs for sensor electronics as well as for

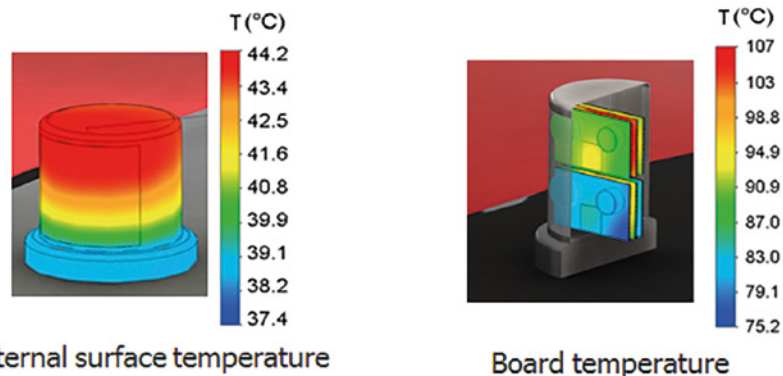


Figure 1. FloTHERM XT CAD-embedded thermal simulation of a rotating lidar mounted on a vehicle. Vehicle is moving at 10m/s and the ambient temperature is 25°C.

their enclosures, while taking into account their vehicle integration locations, is critical to achieve the desired size (and cost) reduction while achieving high resolution and range goals are met. Mentor's EDA-centric, CAD-embedded softwares are ideally positioned to address these challenges from the early design stages. Figure 1 exhibits thermal simulation of autonomous vehicle lidar, accounting for its vehicle integration location using FloTHERM XT. In this Engineering Edge, there is also an article on IR camera thermal management design exploration based on the Masters' thesis of Hugo Falk from KTH Industrial Engineering and Management Institute. Reliable estimation of thermal behavior for lidars (solid-state lidars and/or mechanical rotating lidars) allow hardware engineers to achieve the desired size (and therefore cost) reduction without jeopardizing sensor life, due to undesired hotspots, in the automotive environment. Lidar integration in headlights, pursued by many companies, may pose additional challenges to lidar thermal footprint, as well as may impact lidar performance with headlight fogging or icing. FloEFD™, with its design-centric headlight design simulation capabilities, is helping companies to account for such vehicle integration issues. Additionally, heat build-up in sensors, especially in cameras, can negatively impact output quality, posing challenges to building reliable a 360° view around the vehicle. Sensor thermal simulation, therefore, taking its vehicle integration location and real world driving scenarios, impacts autonomous vehicle virtual testing, verification and validation.

Sensor Fusion Box Reliability and Power Consumption

Most of today's autonomous test vehicles have a trunk full of computers to ensure data from multiple vision and non-vision sensors can be efficiently fused together to create an accurate 360° view around a vehicle. However, for a commercial ready vehicle, desired processing efficiency must accompany size reduction for the fusion box for easy integration in a vehicle. This poses a significant challenge to sensor fusion electronics board design, as well as box enclosure design to ensure robust active cooling design considerations are taken into account. Our electronic cooling software FloTHERM™, a de facto standard for electronic cooling for the last 30 years, and its seamless integration with T3ster®, is ideally suited to address shrinking geometry related design challenges for sensor fusion box. With an electric powertrain, sensor fusion box will likely be powered by high voltage battery, through a DC-DC converter, and that can

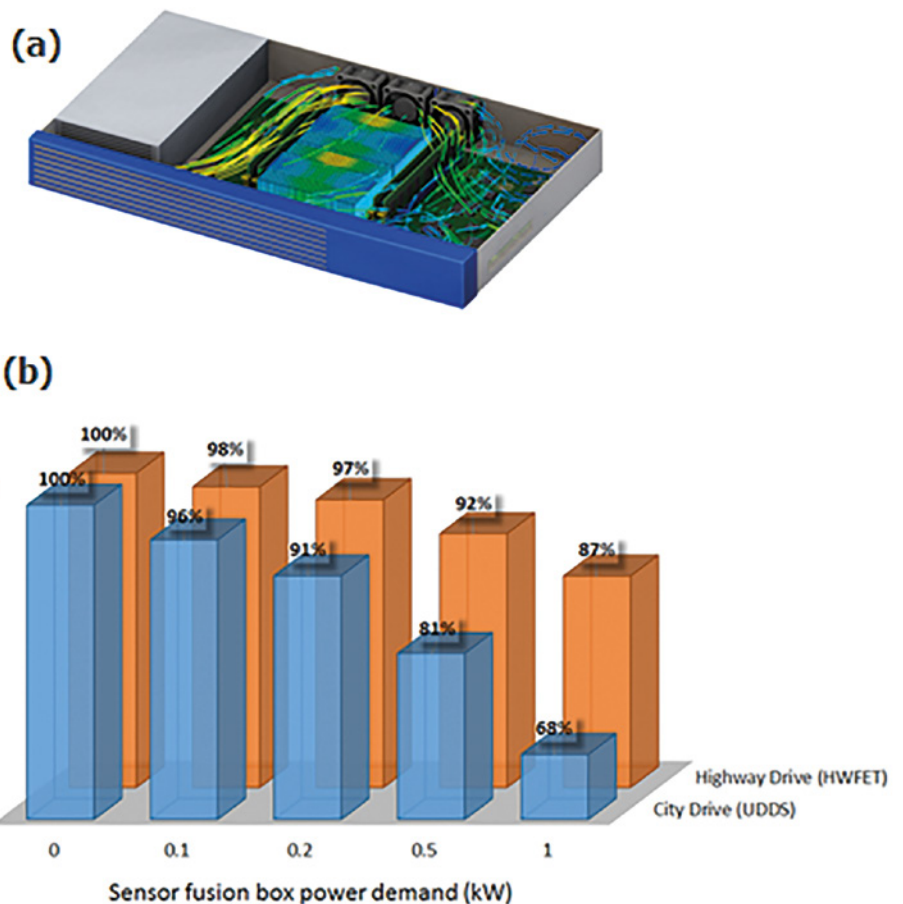


Figure 2. (a) CAD-embedded electronics cooling simulation of sensor fusion box using FloTHERM XT (b) FloMASTER autonomous vehicle system simulation to evaluate sensor fusion box power demand on electric drive range. Sensor fusion box is powered by the high voltage battery via DC-DC converter, in this example

impact electric drive range. This makes power consumption of the sensor fusion box a key criterion for vehicle integration. However, there is no publicly mentioned target for sensor fusion box maximum power consumption. FloMASTER™ system simulation can evaluate the impact of the sensor fusion box power demand impact on battery drive range and can empower suppliers and auto OEMs alike to develop and integrate a sensor fusion box that can deliver the required intelligence without impacting on vehicle performance/range. For instance, Figure 2 shows a 250W (NVIDIA PX2) or higher power consumption sensor fusion box can reduce electric drive range by 10% or more, especially in city drive. This analysis further highlights the advantage of Mentor's DRS360 sensor fusion platform, which consumes no more than 100W- for commercially-viable autonomous vehicles.

Vehicle Integration and E-Powertrain Implications

Electric powertrain is indispensable for autonomous vehicles as it offers a) higher fuel efficiency and reduced CO₂ emissions, b) an easier platform to support drive-by-wire

FloTHERM, a de facto standard for electronics cooling for the last 30 years, and its seamless integration with T3ster®, is ideally suited to address shrinking geometry related design challenges for sensor fusion boxes.

systems needed for vehicle autonomy, and c) as battery prices keep dropping sharply, an attractive proposition of lower cost of ownership and maintenance, especially for fleet owners in a ride-sharing ecosystem. However, integrating vehicle autonomy with electrification will not be simple additive manufacturing. Vehicle autonomy poses additional challenges as well as unique opportunities to optimize electric powertrain size and energy management. For instance, the tremendous increase of vehicle electronics can impact electric drive range, especially in city drive. Whereas, autonomous vehicles are expected to be driven in a pre-determined way, especially Level 4 and Level 5 autonomous vehicles, that eliminate the need to account for 90th percentile driver (with highly aggressive driving pattern) and its impact on electric powertrain sizing and operation. Additionally, in a ride-sharing city-centric usage of autonomous vehicle, power demand to support cabin comfort is expected to challenge the available drive range and may warrant a complete redesign of cabin comfort. For these and many other aspects of autonomous electric vehicle, Mentor's frontloading e-powertrain simulation capabilities in FloMASTER and FloEFD allow users to define, design and evaluate electric powertrain architectures in the early phase of design. To learn more about Mentor's e-powertrain component to system simulation and reliability characterization offering, refer to our very recent white paper [3].

Vehicle Safety and In-Cabin Experience

With the increase in vehicle autonomy, safety-critical functions of steering and

braking will depend on electronic control units (ECU). One of the biggest challenges for ECU design engineers is to manage power (and hence thermal) load on electronics, especially in harsh automotive operation. It has been demonstrated that thermal problems with ECUs invariably lead to electronic failures, which for autonomous vehicles will have severe safety implications. Mentor's Mechanical Analysis Division has been empowering major suppliers all over the world in developing reliable ECUs [4]. Additionally, as vehicles evolve towards Level 5 autonomy, passengers' expectations from in-cabin experience are expected to go through a paradigm shift. Infotainment systems are very likely to evolve towards thin large screens that may be integrated in the vehicle interior in ways that haven't been done to date. To meet these challenges, ECU and infotainment systems design engineers are exploring electronics consolidation. This can pose unique electronics cooling challenges for such systems. Mentor's T3Ster products are one-of-a-kind tools for non-destructive reliability characterization of PCB/semiconductors that allow suppliers to accurately quantify their product's life in real world drive cycle conditions. This coupled with FloTHERM XT/FloEFD electronic cooling software, benefit users to significantly compress time to design and develop ECUs for the drive-by-wire units and new infotainment systems.

As mentioned before, autonomous vehicles warrant technology integration from two vastly different verticals: electronics/technology and automotive. Historically, the two industries have very different product lifecycle requirements and product

development trajectories. Simulations are, therefore, expected to play a critical role to connect these two industry verticals from component level design exploration to vehicle integration to vehicle-level verification and validation. Mentor's Mechanical Analysis Division frontloading, design-centric software, as shown through some of the examples in this article, are well-suited to address the challenges for autonomous vehicle engineering. Various customer stories in this edition of Engineering Edge and in the previous ones showcase the improvement in design efficiency our softwares are bringing to the customers in automotive and electronics industries all over the world. Extrapolating these benefits to autonomous vehicle engineering promises to bring a significant reduction in time and cost for design and vehicle integration for autonomous vehicle hardware.

References:

- [1] <https://www.bcg.com/expertise/industries/automotive/autonomous-vehicle-adoption-study.aspx>
- [2] <http://www.businessinsider.com/companies-making-driverless-cars-by-2020-2017-1/>
- [3] "E-Vehicle Thermal Management Powertrain Simulation", a Mentor White Paper (Link)
- [4] "ECU Thermal Reliability Becomes Mission Critical", a Mentor White Paper (Link)

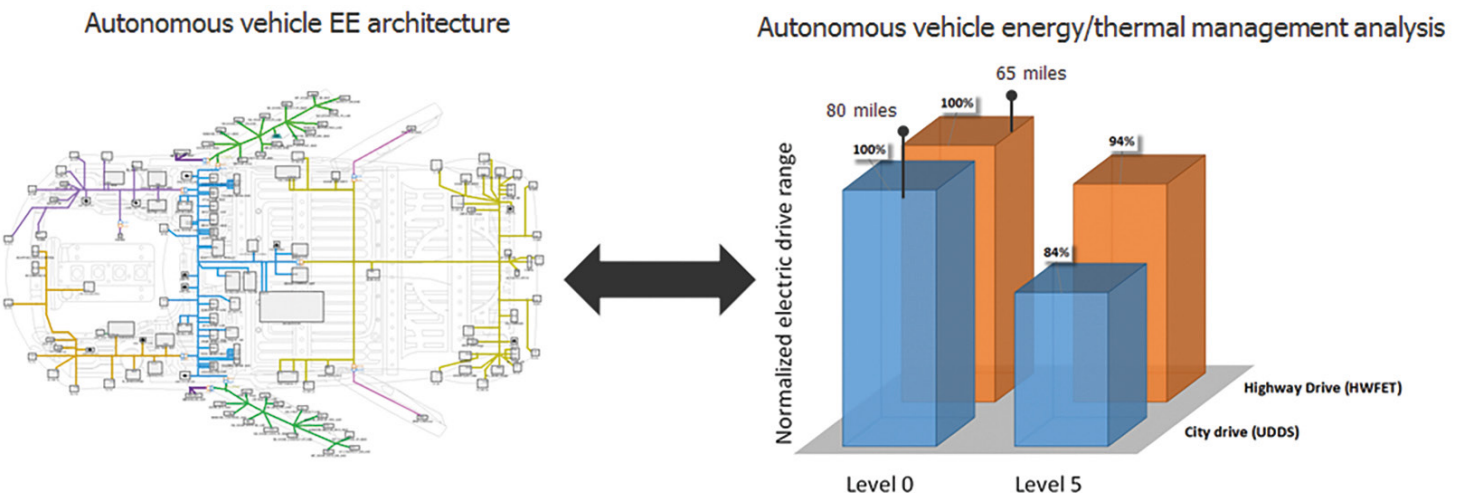


Figure 3. Impact of Level 5 autonomous vehicle system integration on electric drive range. In this example, Level 5 autonomous electric vehicle (80 miles electric range with 80kW front motor drive unit) is simulated where vehicle EE architecture (simulated using Mentor's Captil software) includes 30 sensors, DRS360 centralized sensor fusion and ECUs for steering and braking. Electric drive range is simulated at 25°C ambient conditions using FloMASTER based e-powertrain simulation framework.

2017 Don Miller Award **Winners** Showcase

the Diversity and the Accuracy that FloMASTER is Renowned for



Each year the candidates for the Don Miller Award prove how diverse and flexible FloMASTER is for providing reliable accurate results. This year is no different with submissions came from Korea, China, United States, and Australia. The 2017 Don Miller Award winners were selected based on their demonstration of excellence for a range of thermo-fluid design applications, including waste water reclamation, gas turbine blade cooling, and fueling of a space launch vehicle.

A team comprising Hwayoung Oh, and Sunil Kang from the Korean Aerospace Research Institute, and Jaejun Lee, Sangmin Park, and Eun Sang Jung of Hyundai Heavy Industries received the first place award for their design featured in the Journal of the Korean Society of Propulsion Engineers paper, "Analysis on the Filling Mode of Propellant Supply System for the Korea Space Launch Vehicle". Their analysis used a FloMASTER simulation model to verify the fueling scenarios to be used for fueling the Korean NARO rocket.

The important objective of this work was to develop a FloMASTER simulation model of the liquid oxygen (LOX) and Kerosene fueling systems of the NARO rocket designed and built by the Korean Aerospace Research Institute. It could verify the fueling scenarios that are required to safely transfer the liquid oxygen and kerosene from the ground storage tanks to the on-board fuel tanks for each of the three stages of the rocket. This is particularly critical for the liquid oxygen which is extremely volatile and can quickly boil off to a vapor if the system operation is not handled properly. Additionally as a result of the extremely low temperature required to maintain the oxygen in a liquid state, it can cause thermal shock

to the system if the LOX is pumped into the system too quickly.

KARI took full advantage of FloMASTER's capabilities to validate their design. First they utilized the steady state capability to predetermine the proper valve settings for each of the three stage tanks to fill at respective rates that will allow them to run full, simultaneously. Secondly, they ran a transient simulation to verify that the fuel tanks were filling as per design and that the overall fill time was reasonable. The analyses showed that the performance of the fill scenarios were well within the safety factor range.

Two runners up were selected by the panel of judges. Jurgen Sprengel from JS Pump and Fluid System Consultants in Australia received his award for a complex application of the FloMASTER tool, used to understand the water hammer and distribution issues that can occur in a waste water reclamation system. The application was described in the Engineering Edge article, "FloMASTER for Water Treatment Plant Hydraulic Simulations".

This particular Water Treatment Plant (WTP) design is one that treats saline water

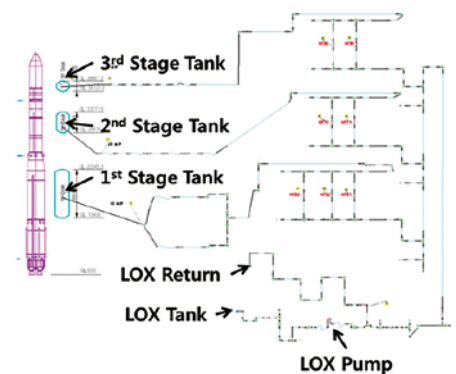


Figure 1. 1D analysis model of LOX filling system

produced from the coal seam methane gas extraction process. It receives raw water from the gas field's water gathering system which typically contains a significant amount of salt per liter. The raw water is collected in a storage dam adjacent to the WTP. The treated water and brine that result from the treatment process are temporarily stored in local storage dams. The treated water is then dispatched for beneficial use on an as-need basis, while the brine can be further treated in a brine concentrator. This paper is an excellent example of how FloMASTER can easily handle very large systems for, not only steady state, but transient systems as well. It provided the author with the detailed simulation results for liquid level and pressure needed to make critical operational decisions.

The second joint runner-up award went to the team of Batchu Suresh, V Kesavan, Ainapur Brijesh and S. Kishore Kumar from Gas Turbine Research Establishment, in Bangalore, India.

They investigated the interaction between the internal geometry and the internal air flow cooling of gas turbine rotor blades. They described it in their paper, "Heat Transfer and Flow Studies of Different Cooling Configurations for Gas Turbine Rotor Blade".

This is a very detailed paper that describes how the authors utilized FloMASTER's unique Internal Duct component to model the internal flow passage of a blade and estimate flow distributions. The temperature of the gas leaving the combustor and entering the turbine section of a gas turbine directly relates to the power output and the efficiency of the engine. The higher the temperature, the higher the efficiency and power. This causes an issue where the temperatures exiting the combustor are higher than the melting temperature of the material used to construct the turbine blades. Therefore the turbine blades must be cooled to keep them below the melting temperature. This is done by forcing cooler air through a series of passageways and holes inside the blade. The positioning and geometry of these passageways are critical for maintaining the integrity of the blades. They constructed a detailed model using the internal duct component that allows them to consider the geometric cross-section and enhanced heat transfer surfaces such as chevron fins and pin fins to predict the pressure drop and heat transfer to the cooling air.

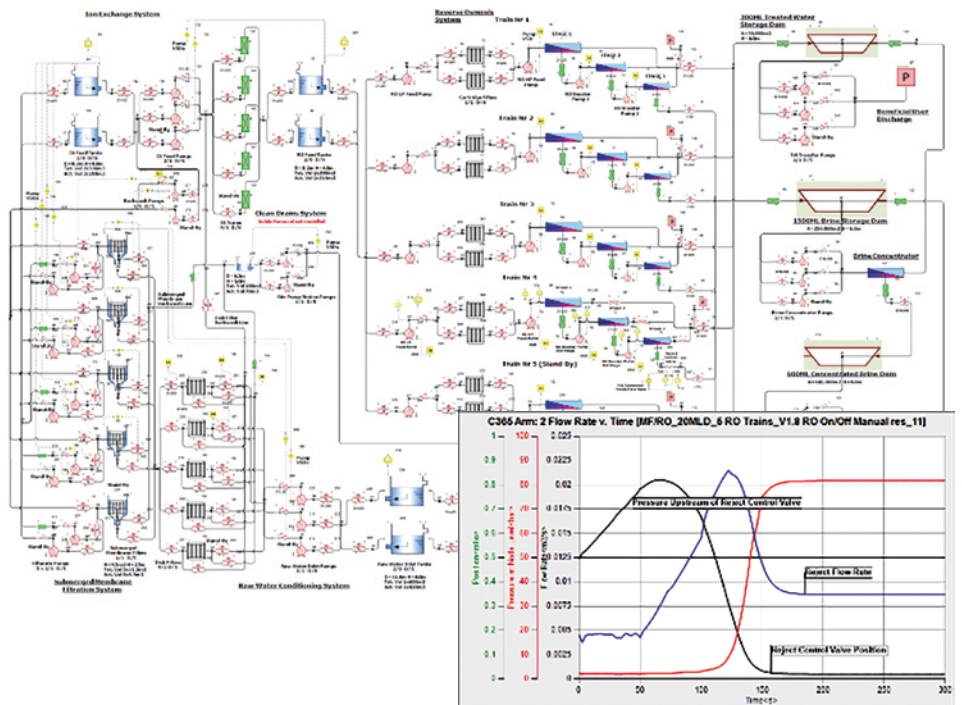


Figure 2. WTP Integrated Hydraulic Model

From these award winning papers it is easy to see the diversity of applications of FloMASTER and how creative engineers from around the world leverage it in innovative ways to solve their simulation and design problems.

New Release:

FloEFD™ 17

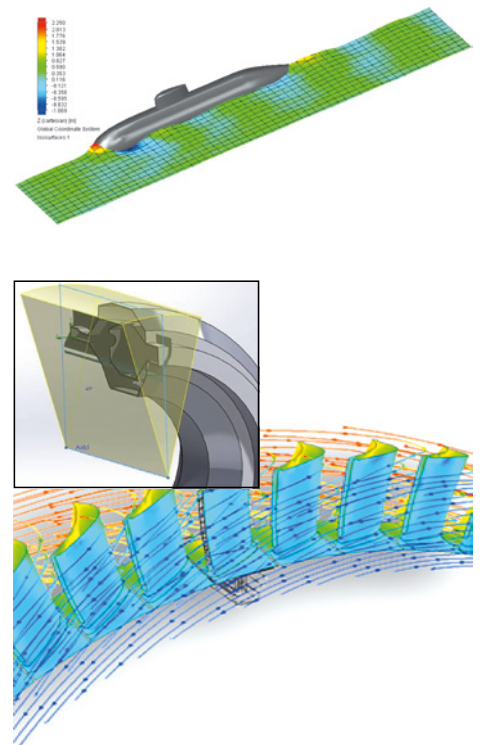
- **New FloEFD functionality includes enhanced geometry handling, new physics and results visualization tools for faster analysis and greater productivity**
- **FloEFD is embedded in popular CAD tools including Siemens NX, Solid Edge, Creo, and CATIA V5, as well as a stand-alone version**
- **The feature-rich FloEFD product is recommended for design engineers working in the automotive, aerospace, electronics and industrial process and heavy machinery industries**

Mentor, a Siemens business, is pleased to announce the latest release of its award-winning frontloading FloEFD computational fluid dynamics (CFD) product with new functionality for geometry handling, physics and results visualization. Featuring intelligent technology enabling fast and accurate simulation, the FloEFD solution helps users frontload CFD simulation early into the design process to understand the behavior of their concepts and eliminate the less attractive options. It is unique and market proven technology, FloEFD can reduce the overall simulation time by as much as 65-75%; thus, helping engineers in the automotive, aerospace, electronics and industrial equipment markets optimize product performance and reliability, reduce physical prototyping, and development costs.

The FloEFD product includes a large selection of powerful features and functionalities for easy-to-use, fast and accurate simulation. Among the significant new additions are the following:

- **Free surface simulation:** The new functionality enables users to simulate surface flows to observe fluid movement, such as flow of liquids into a storage tank. This important feature is useful for several industries including food and beverage processing equipment as well as automotive, and mil/aero.
- **FloEDA Bridge:** The FloEDA Bridge allows users to import EDA geometry into CAD with different levels of geometry resolution from compact to fully explicit including all the layers and vias. With the latest release, in addition to the geometry, material properties and heat power can be added to the FloEFD project.
- **Enhancements to LED module:** Definition of radiation spectrum and setting intensity of radiation can now be dependent on the angle. With that data defined, FloEFD now automatically applies the calculated radiant flux on top of the LED.
- **Stand-alone viewer:** A powerful viewer is now offered by FloEFD to help engineers share analysis results with those who do not have a copy of the FloEFD product. For example, an engineer can use the viewer to share the analysis results with clients or group managers for final approval.
- **Sector periodicity:** The FloEFD product now includes an efficient geometry handling feature which allows users to model only a fraction or section of large cylindrical shapes. This functionality helps reduce the model and mesh size, enables faster analysis and is especially useful for industrial design applications such as turbo-machinery, pumps, fans and compressors.

“Our continued investment in FloEFD by offering a host of powerful enhancements is in direct response to our customers’ needs,” stated Roland Feldhinkel, general manager of the Mentor Mechanical Analysis Division. “Our new release addresses the challenges our customers face in order to meet competitive time-to-market schedules with fast and accurate simulation results.”



New Release: FloTHERM® 12

with New Command Center for Productivity and Performance

Mentor, a Siemens business, is pleased to announce the latest release of its market-leading FloTHERM product, the industry's most powerful and accurate computational fluid dynamics (CFD) software for electronics cooling simulation. The latest product offers new functionality aimed at increasing user effectiveness and productivity. FloTHERM 12 includes Command Center, which allows users to understand the product design space by defining variations of the base models. The Command Center design window streamlines the interface and user work to achieve productivity gains. Addressing the needs of industries which demand product reliability including automotive, aerospace, and electronics, FloTHERM 12 quickly identifies potential thermal problems early in the design stage to significantly lower the costs of thermal testing and design re-work, enabling customers to get their products to market more quickly.

The Command Center is used to create and solve variants of a FloTHERM model. This enables a complete understanding of the product design space and allows the thermal engineer to make informed design decisions. Automatic design optimization tools can be deployed in Command Center to systematically design aspects of the product. The Command Center also supports calibration tasks using T3Ster® thermal characterization-based models for even greater accurate thermal simulations.

"I find the Command Center indispensable for running the many scenarios that I need to make sure that I do not just have a working design, but the best working design possible for my circumstances," said Wendy Luiten, Thermal Design, Electronics Cooling Specialist, at Wendy Luiten Consultancy.

The new functionality in the Command Center tool is based on customer feedback for usability and productivity and introduces several critical features that make scenario definition and design space exploration intuitive and fast: easy-to-find objects, attributes and settings; "find" tool with multiple applications for variant creation; easy interaction with spreadsheet tools; and efficient simulation of hundreds of models.

Additional FloTHERM product features

The new FloTHERM release provides additional features for productivity and accurate thermal simulation, including:

- Support for Phase Change Materials (PCM). Encapsulated PCMs have become a common thermal solution for consumer applications, and have been difficult to simulate in the past. FloTHERM now accepts latent heat and melt temperature as inputs and utilizes these values automatically in transient applications. The impact of PCMs on component and touch temperatures can now be fully explored and optimized in FloTHERM.
- Industry standard ODB++ data can now be used to bring printed circuit board (PCB) designs into FloTHERM. FloTHERM will now fit alongside any PCB Layout tool in the design flow.
- Blind and buried vias are fully supported in PCB model definition. This greatly improves results accuracy when conduction into the PCB is on the critical heat flow path.
- Improved parallel solver that produces faster and more scalable results for a broader range of applications.

"Our new FloTHERM product with Command Center addresses the thermal design challenges of today's advanced products, with automated features to make ideal design decisions for optimal product performance with confidence," stated Roland Feldhinkel, general manager of the Mentor Mechanical Analysis Division.

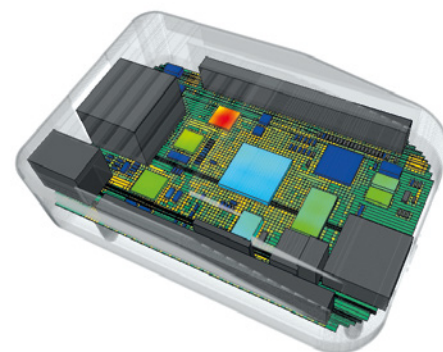


Figure 1. FloTHERM Command Center

An Introduction to Industrial Volume Testing

By Laszlo Tolnay, MicReD Product Line Director, and Dr. John Parry, Senior Industry Manager



There is a growing need to automate not just the performance thermal tests but also the evaluation of the results. Besides the general need for testing bigger and bigger number of samples and integrating T3Ster to larger set-ups, a clear driver is coming from manufacturing environments.

One of the challenges in building electronics in volume is ensuring the quality of components or products that enter the market. Changes happen over time due to changes in raw materials and process window variations across the production line. Consequently the risk of defects in the product that might result in reduced lifetime in the field, and even infant mortality where components fail very early in their expected useful lifetime, are ever present.

Testing components and assemblies in volume testing is one approach that component suppliers and systems integrators can take to de-risk the release of products into the supply chain. Volume can mean testing a statistically large batch or even every product or critical component in the manufacturing line. No matter whether the products are tested sequentially or in batches, large number of samples require that the tests and their evaluation are quick, automated and integrated as much as possible.

Unfavorable change of lifetime and reliability is in many cases induced thermally and the root cause can also be detected thermally. Examples are voids in the die attach in a component, and voids in the solder attachment of a power component to a PCB or inconsistent quality of TIM application. Where components are bought in and used within a product, changes in the thermal performance of the component due to material or manufacturing changes can be detected such as die size changes due to die shrink by the component supplier. Another

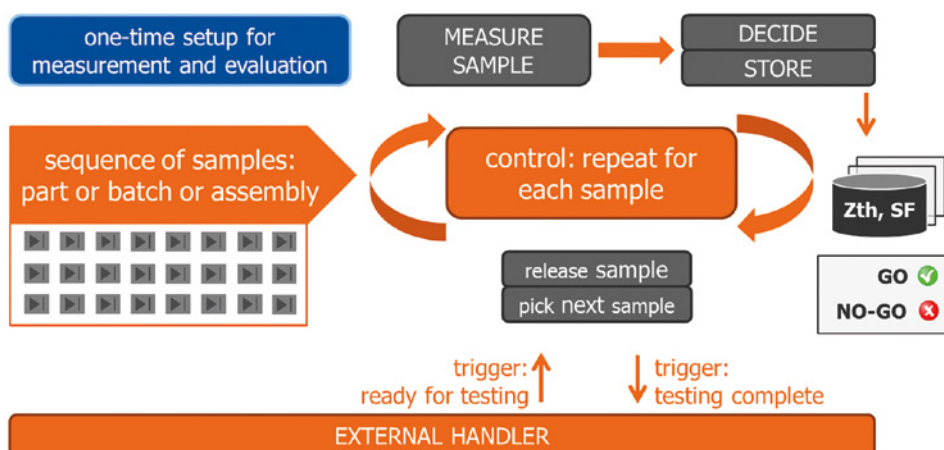


Figure 1. Schematic showing the operation of the volume tester and its interaction with an external handler

application of mass thermal characterization is binning components based on their thermal parameters, to allow segmentation for application or environment specific power consumption ranges.

Performing thermal transient analysis on a large number of samples requires a different way of setting up and controlling a T3Ster measurement, however it does not impact the fidelity of the technology at all. The volume tester set-up is shown in Figure 1, and it follows the main steps of:

Defining the measurement, done only once

- The measurement type is selected based on the device and the topology. For this, the set-ups are configured to serve a matching set of options.



Figure 2. Prototype Volume Tester

- The measurement is set up, including heating and sensing parameters and measurement times.
- Evaluation criteria is defined, which can be a simple go / no-go decision or binning, depending on either the thermal transient or the structure function.

Test sequence

A handler feeds the parts to be tested (sequentially one-by-one or as an assembled batch or as a module), and sends a trigger signal to the volume tester to start the test. In low volume applications this can even be a manual process, while in other cases the volume tester can be integrated with an automated handler.

The volume tester then tests the parts, and the measurement results are stored and displayed if required. An automatic evaluation can take place at this point with the results and decision stored, interfaced to an adjacent system and displayed if needed.

Once the volume tester has finished testing, it signals that it is ready to test the next part or set of parts.

The next testing round starts, while the previous test results can be evaluated to determine how the tested parts are to be handled in the supply chain.

Mentor has developed two working prototypes of such a system.

One of them performs concurrent testing on two batches of 8 LEDs, shown in Figure 2. These are mounted onto a board, but as components tested at the end of a production would be tested unmounted, for example in a test socket.

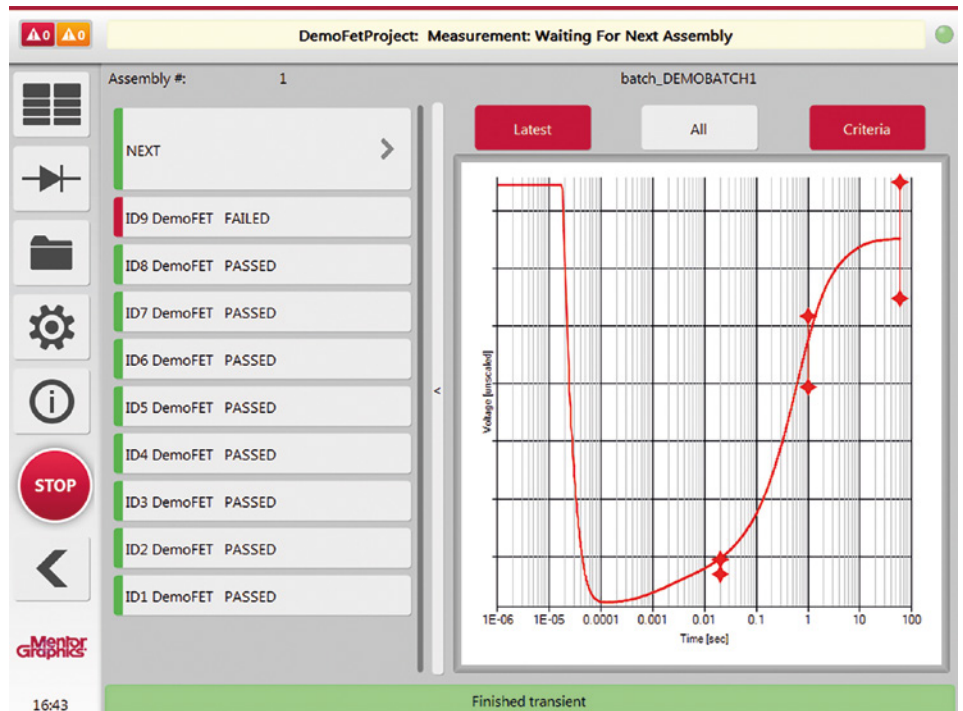


Figure 3. User Interface showing Test Results for FET Failing Test.

The system utilizes multiple T3Ster measurement channels to capture the temperature vs. time response of the LEDs as they are powered.

In another test set-up, a power electronic board with multiple power FETs is tested to make sure that all these devices have their junction to heatsink heat paths within the limits defined based on their application profile and the corresponding thermal simulation of the assembly. The captured response is compared at key points in time to check that critical parts of the package structure such as the die attach are within acceptable limits, as displayed in the prototype user interface shown in Figure 3. Both the sequential testing and the evaluation are fully automatic in this prototype, and start on a single trigger signal.

A Volume Tester set-up is highly modular in architecture, allowing multiple powering channels, including powering for power electronics components into the thousands of Amps, and multiple sensing channels. Flexibility is also present in control and interfacing to allow integration to various systems or adjacent measurements, so the system is configurable as well as scalable. In a volume tester project, the components added to the core modules are determined based on specific customer needs.

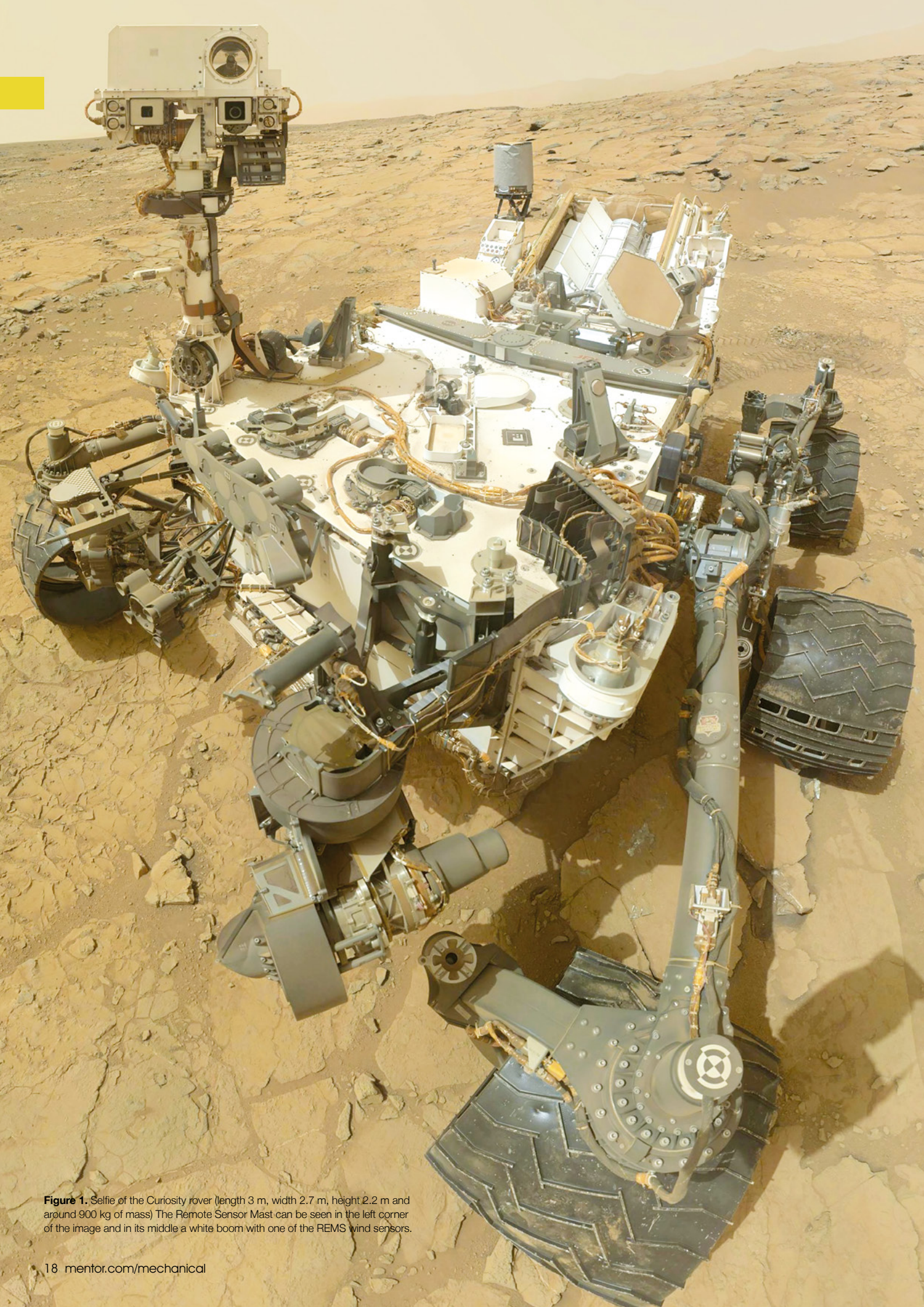


Figure 1. Selfie of the Curiosity rover (length 3 m, width 2.7 m, height 2.2 m and around 900 kg of mass) The Remote Sensor Mast can be seen in the left corner of the image and in its middle a white boom with one of the REMS wind sensors.

Curiosity: **Life** **on Mars**

Modeling the wind flow around the REMS instrument on board the Curiosity rover on Mars

By Dr. Josefina Torres; Dr. J. Gomez Elvira.; S. Navarro; M. Marin; and S. Carretero, Centro de Astrobiologia (INTA-CSIC), Edited by Mike Croegaert

The Rover Environmental Monitoring Station (REMS) is part of the payload of the Mars Science Laboratory (MSL) rover, better known as the Curiosity rover, which landed on Mars in August 2012. REMS is composed of a suite of sensors, including two wind sensors. These sensors are based on hot film anemometry and are installed in two small booms which are located in the rover's Remote Sensor Mast. Measuring winds on a complex structure like a rover requires to know as best as possible the influence of the rover on the wind fluid stream.

Venus, Earth and Mars are the only inner solar planets with significant atmospheres. Venus has a hotter and denser atmosphere than Earth, whilst Mars' is colder and less dense than our planet. Pressure on Mars goes from 5 to 9 mbar, and temperatures depend on geographical location, but at the Gale crater, where the Curiosity is running, temperatures range from -80°C to 5°C. Nevertheless, the atmospheric phenomena on Mars are similar to that which occur on Earth. The duration of the Martian day is several minutes longer than an Earth day and the time that takes to give a complete revolution around the sun is equivalent to two Earth years. Similar to Earth, it has four seasons, and the windy period is the second half of the Martian year, when dust storms are common.

In August 2012, MSL rover reached the surface of Mars. It is the size of a small

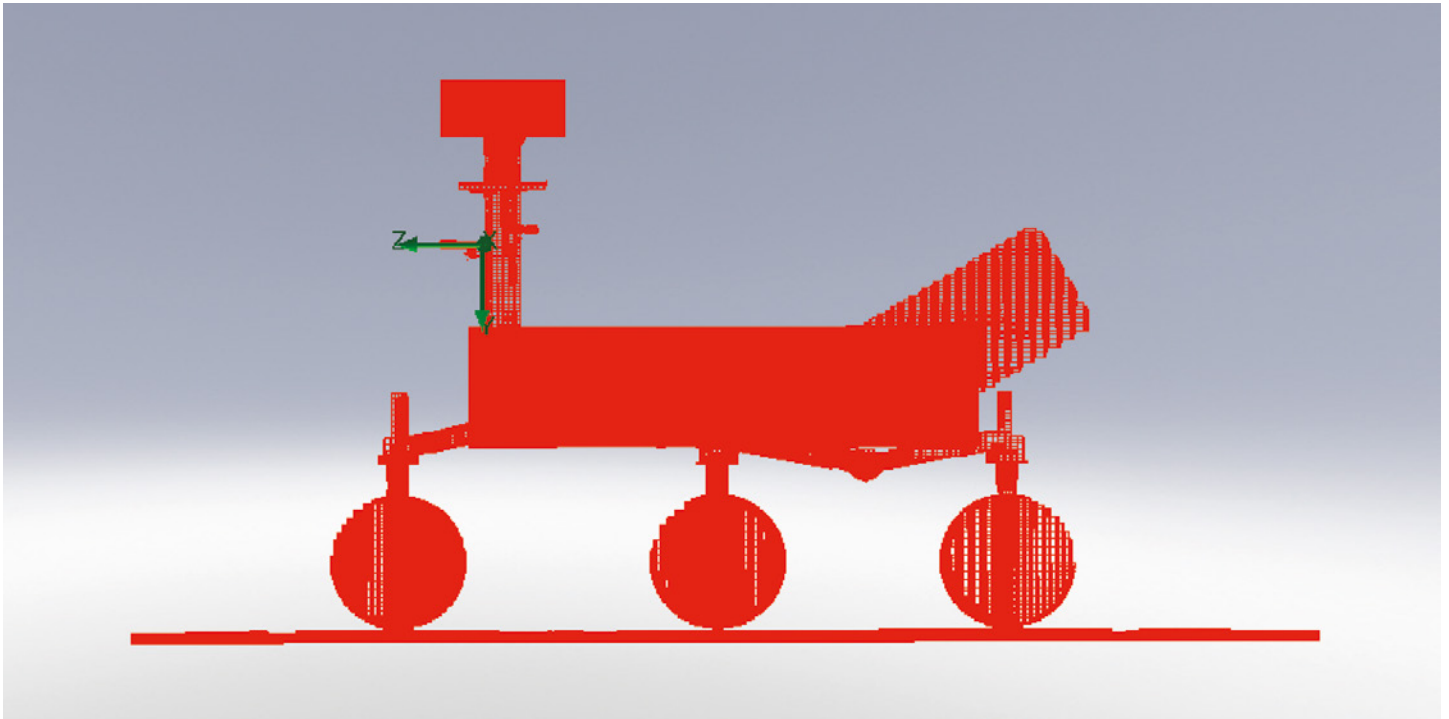


Figure 2. Rover solid cells inside FloEFD

car, and it is equipped with a payload composed of geological, geochemical and atmospheric instruments. It has a robotic arm that can dig and recover soil samples which can later be analyzed in situ. It has a number of cameras for navigation and scientific purposes. Its original mission was for one Martian year but 2017 will end its second full year on Mars. Its main goal is to determine the past habitability of the red planet, through the study of the water markers, mineral characteristics and also throughout the sediments of the Gale mount.

The MSL rover's central body contains most of the rover and instrument electronics. Its propulsion system is based on six motorized wheels and a suspension system to traverse the rough Martian terrain. It is powered by a Radioisotope Thermal Generator (RTG) and can communicate directly with one of the Deep Space Network of NASA antennas or using MRO or Mars Odyssey satellites to relay data to Earth. The Remote Sensing Mast supports some cameras for navigation and science, the ChemCam instrument and most of the REMS sensors.

Due to the general constraints of the rover design, the length of the two REMS booms are not long enough to be out of the rover fluid volume and therefore the rover can affect the fluid flow the REMS experiences. This makes it necessary to identify which

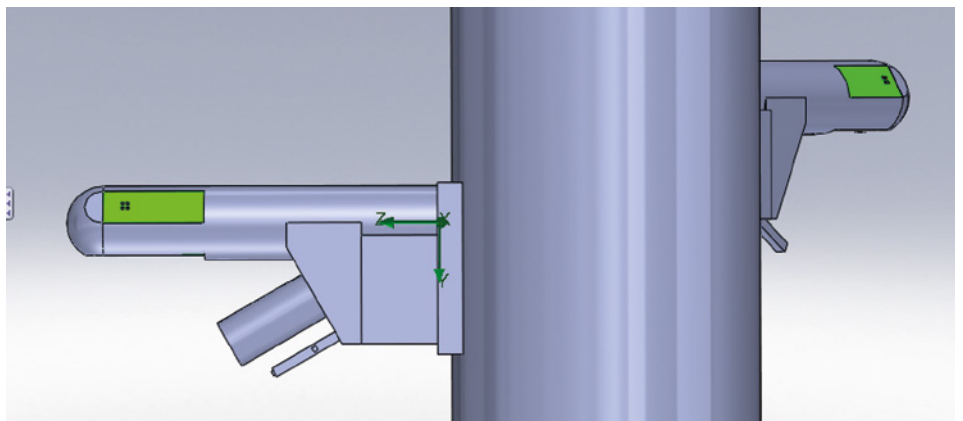
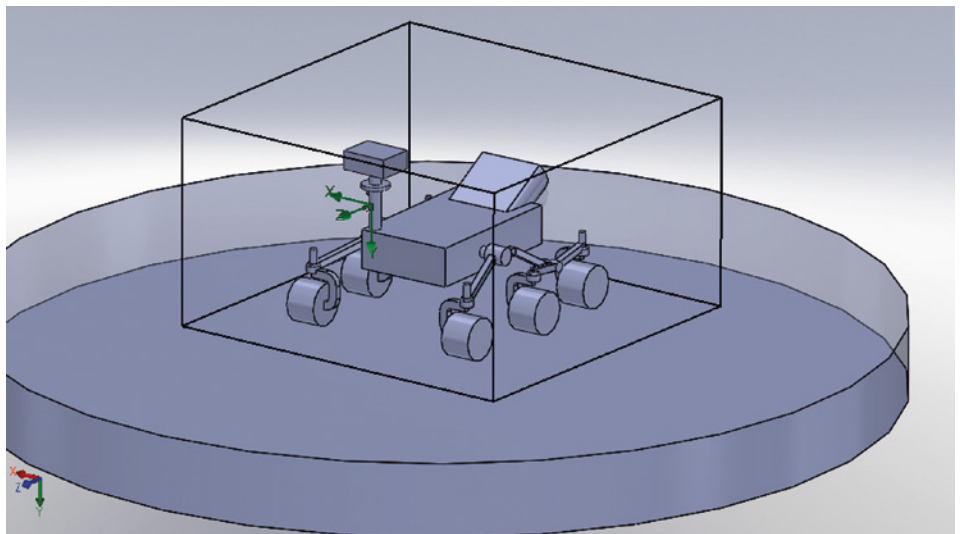


Figure 3. Top view of the Mars rover. 3D CAD model from jpl.mars.gov. Right side close up of both wind sensors on the mast, Boom 2 (left) Boom 1 (bottom)

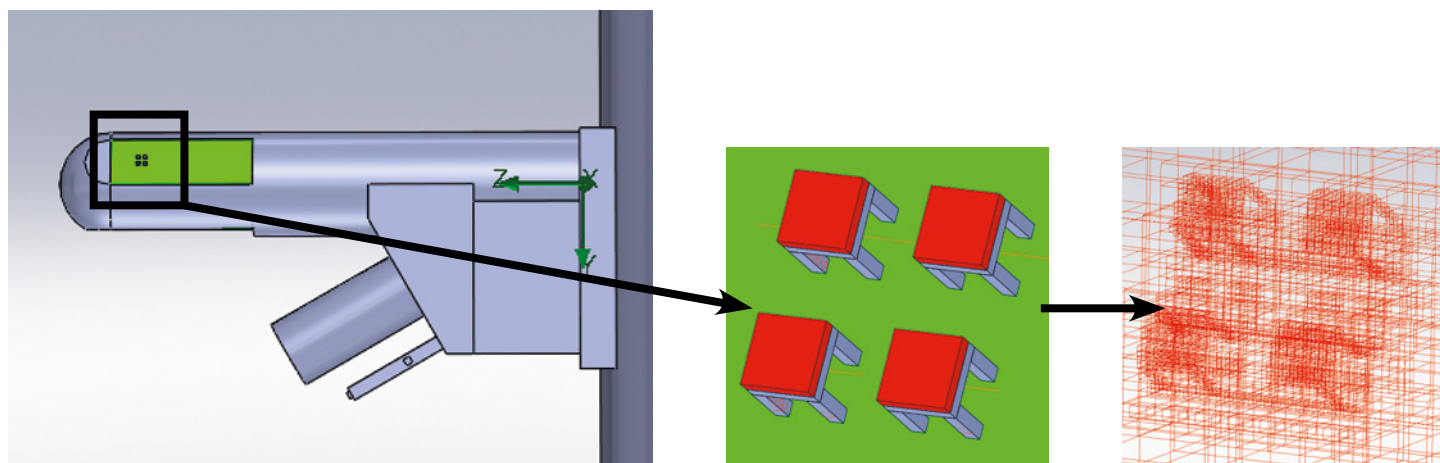


Figure 4. Detail of the wind sensor Boom 2 dice refined mesh

are the wind directions in which the impact of the rover is maximized and how it affects REMS measurement. Wind tunnel tests are not feasible due to time and facilities restrictions and therefore CFD simulation is the tool of choice. Understanding how the wind stream is perturbed by the rover, is the simulation goal for the REMS team.

The CFD simulation software used was FloEFD™ from Mentor, a Siemens Business. Utilizing FloEFD, an external boundary condition domain recreating Mars atmospheric conditions was generated with laminar and turbulent flow features activated. The simulations were also modeled with heat conduction in solids as well as free and forced convection.

The fluid computational domain size set for the simulations is 4x4x2 m. A true reproduction of the rover geometry was achieved using a fine mesh. The basic mesh dimensions $N_x = 123$, $N_y = 123$, $N_z = 123$ creates an initial mesh in the domain of 3cm mesh size. In addition, local meshes have been used to refine the solid cells in the rover: “wheels”, “mast and camera”, “deck”, “WS1” and “WS2”. Also a solid ground has been added to simulate the effect of the rover on the terrain.

The resulting Cartesian mesh consists of 3.2 million cells, which include 2.3 million fluid cells, 590,000 solid cells and 300,000 partial cells. Figure 2 corresponds to the rover solid cells.

The general settings for the simulations are set as follows: pressure of 713 Pa, temperature of 243 K, Fluid Air and Analysis Type “External”. Wind speed and direction are set in the velocity parameters box using the three components of wind speed V_x , V_y , and V_z .

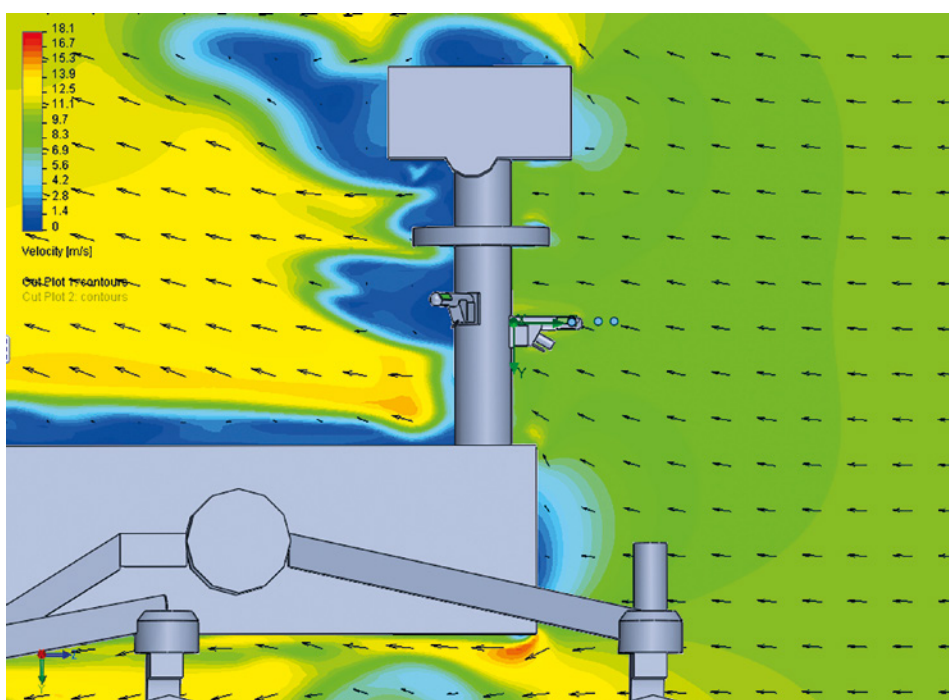


Figure 5. Detail of the point velocity around sensors

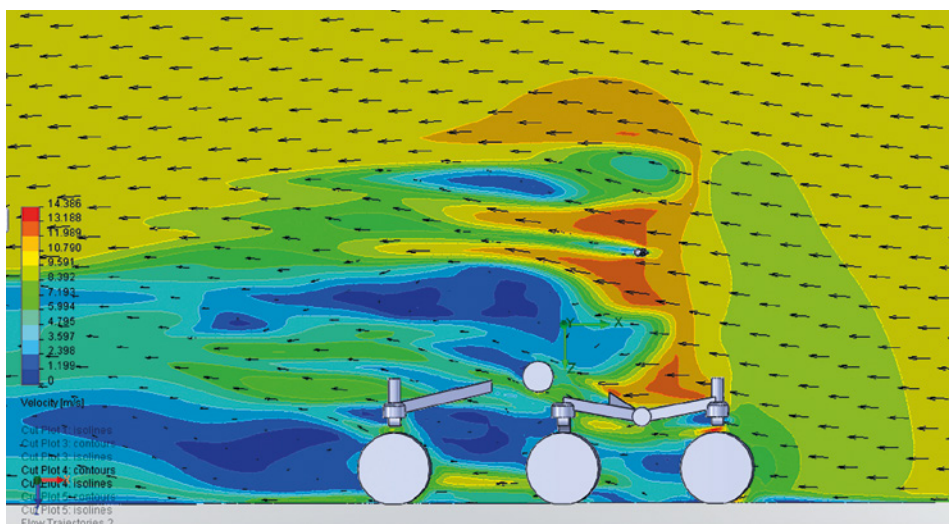


Figure 6. 10m/s Front winds ($\beta = 0$). Cut plot section at Boom 2

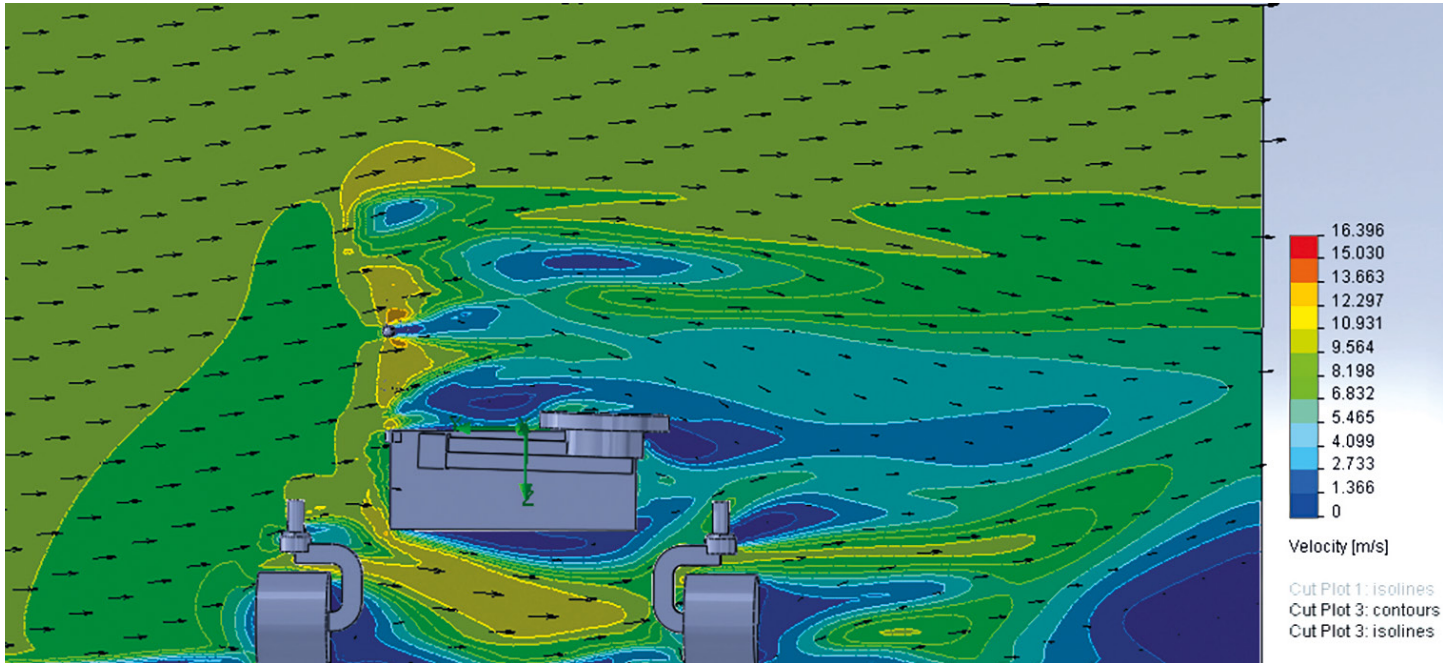


Figure 7. 10m/s side winds ($\beta = 90$). Cut plot section at Boom 1

With heat conduction in solids enabled, the team was able to simulate more realistic conditions of how the rover is heated and the interference with the atmosphere and wind stream.

CPU time of computation varies from 10 to 15 hours, depending on the wind velocity or direction chosen for the simulation in a 24 CPU machine.

The wind direction and speeds simulated have been: 5, 10 and 20 m/s of speed, yaw angles over range 0, 30...330° and pitch = 0°, 30°.

The 24 wind sensors are based on hot film anemometry, they are 1.5 mm x 1.5 mm x 1.5 mm in size and are located in the front end of both Boom 1 and Boom 2. Local fine meshes have been used for each sensor to mesh the solid area correctly, an example of the detail of the refined mesh is shown in Figure 4.

From the simulation results, the perturbation of the rover on the wind sensor for different directions and speeds can be determined. For this purpose, an extended number of simulations was required but once the model was prepared, a batch run of simulations can be sent by modifying the initial parameters.

The X,Y, and Z velocity detail information can be extracted from the set point parameters. These parameters have been created near each of the wind sensors and around both of the booms.

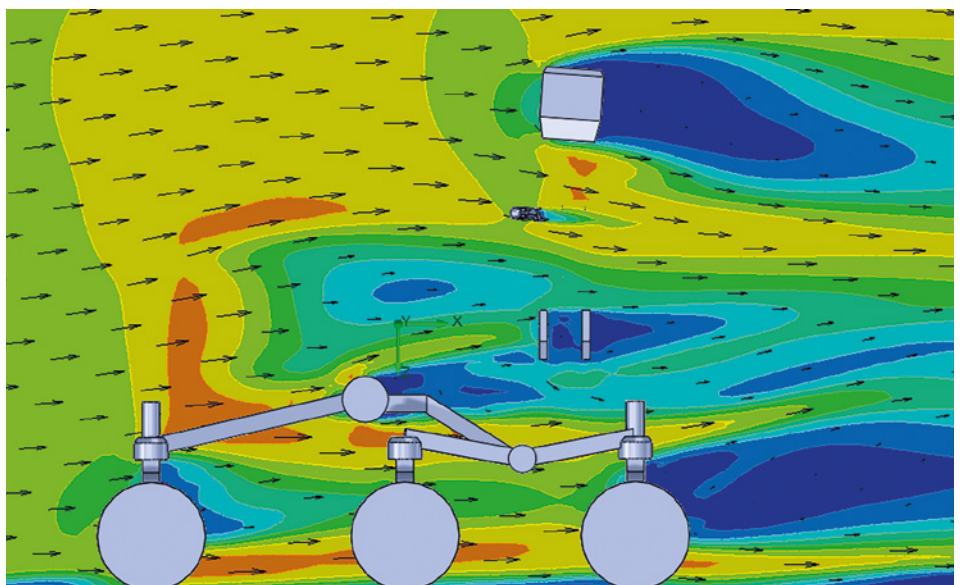


Figure 8. Rear winds ($\beta = 180$). Cut plot section Boom 2 level

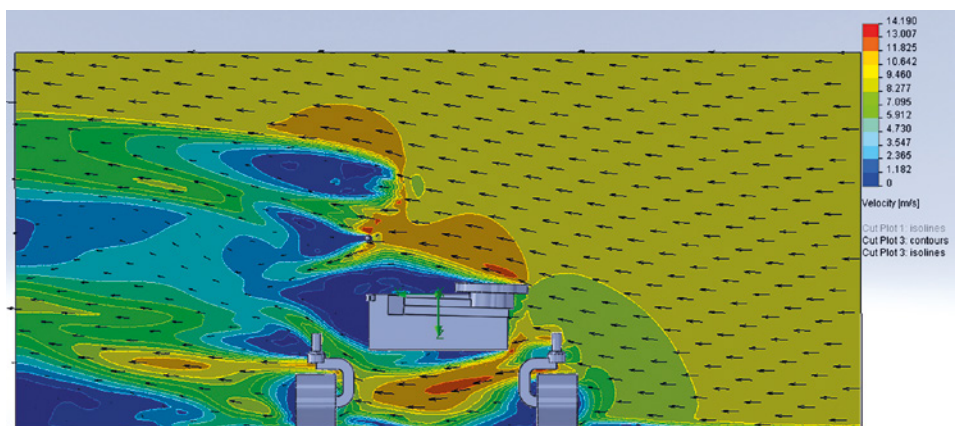


Figure 9. Front winds ($\beta = 270$). Cut plot section at Boom 1 level

The REMS team was able to determine, through FloEFD simulations, how incident wind on the rover from different directions disturbs the reading on the wind sensors.

Figures 6, 7 and 8 detail cut plots of the perturbation of the freestream wind speed profile at 10m/s for the wind directions 0°, 90°, 180° and 270°. The perturbation that the rover creates around the wind sensor area can easily be seen.

The simulations were also modeled with conduction in solids and convection, both free and forced. This enables the simulation to heat different parts of the rover, providing a more realistic perturbation of the free stream velocity. Figure 10 shows the effect of the heat plume with no wind and with 5m/s rear wind.

The REMS team was able to determine, through FloEFD simulations, how incident wind on the rover from different directions disturbs the reading on the wind sensors. With the output of these simulations the team gained a better understanding of which wind sensor is experiencing the closest result to the freestream velocity and understand the different wind directions and speeds that could disrupt both sensors due to the geometry of the rover.

References

- [1] Grotzinger, J.P., Crisp, J., Vasavada, A.R. et al. Space Sci Rev (2012) 170: 5. doi:10.1007/s11214-012-9892-2
- [2] Gómez-Elvira, J., Armiens, C., Castañer, L. et al. Space Sci Rev (2012) 170: 583. doi:10.1007/s11214-012-9921-1
- [3] Domínguez, M., Jiménez, V., Ricart, J., Kowalski, L., Torres, J., Navarro, S., Romeral, J., Castañer, L., A hot film anemometer for the Martian atmosphere. Planetary and space science, (2008) 1169:1179. Doi: 10.1016/j.pss.2008.02.013

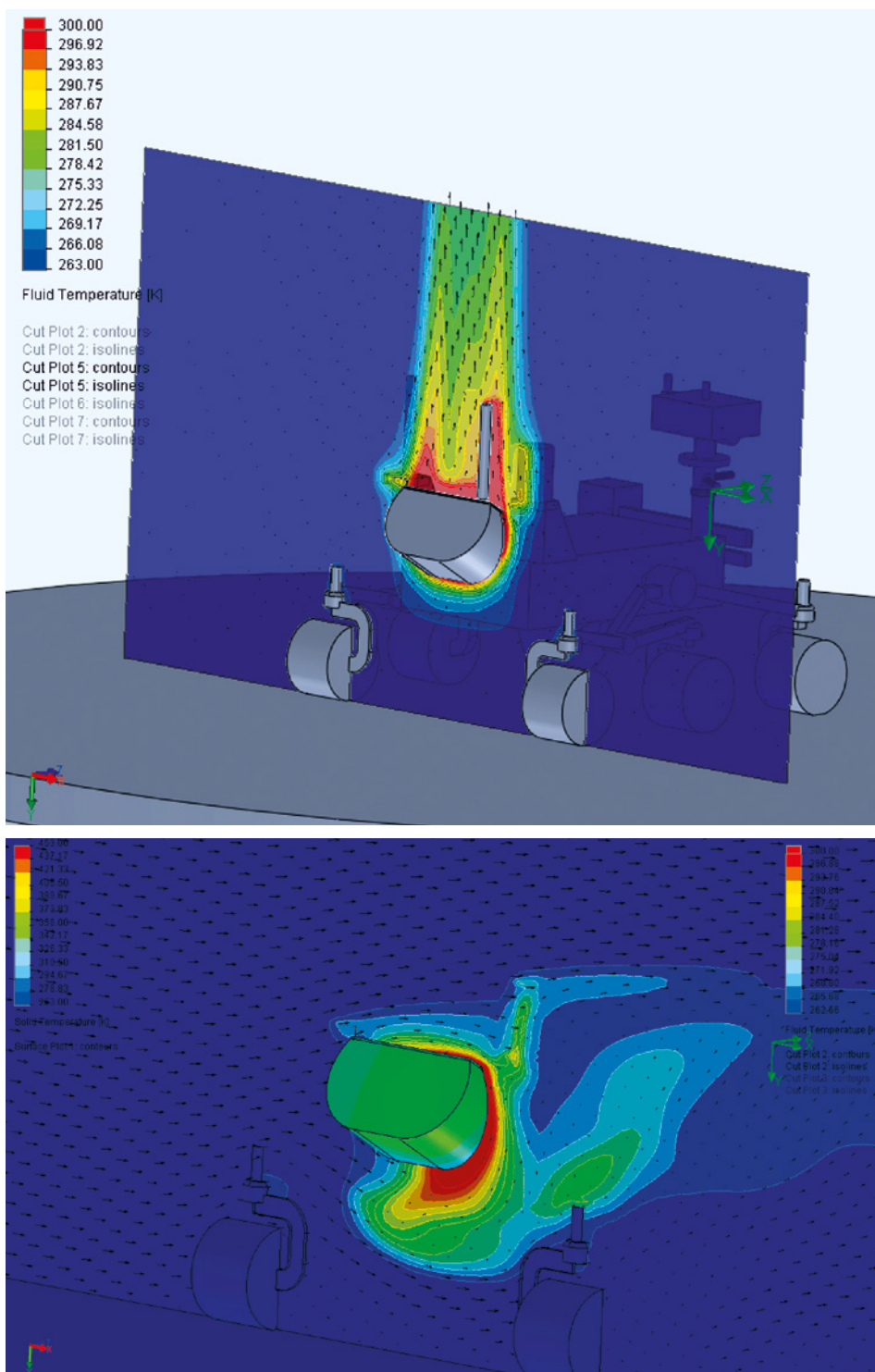
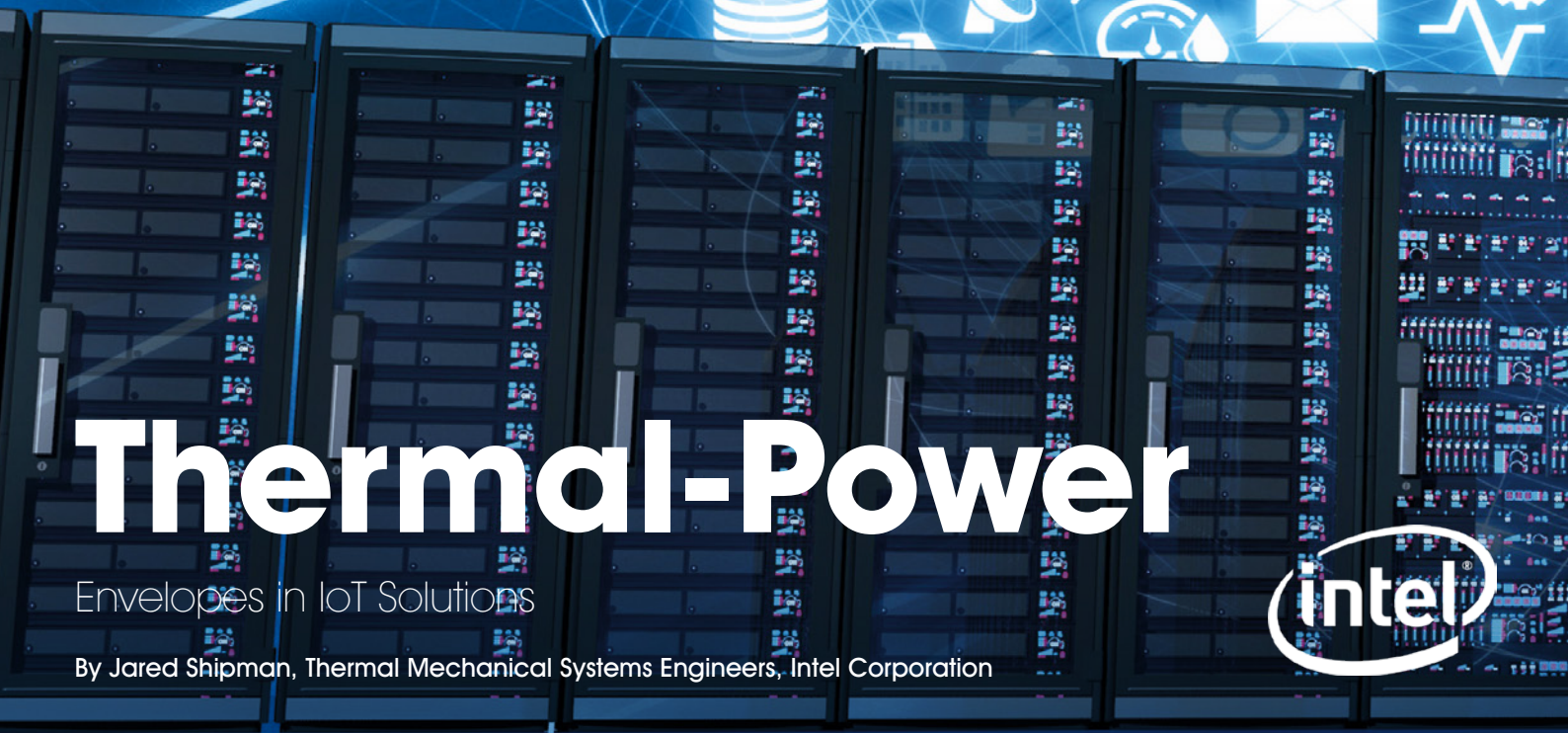


Figure 10. Rear winds ($\beta = 180$). Thermal plume of the RTG for rear winds



Thermal-Power

Envelopes in IoT Solutions

By Jared Shipman, Thermal Mechanical Systems Engineers, Intel Corporation

Intel's Internet of Things Group (IOTG) comprises a variety of divisions Retail Solutions, Smart Home/Building, Industrial Solutions and Transportation to name a few. Each division has its own challenges when it comes to designing solutions for their customers. The Thermal/Mechanical Systems Engineering team within IOTG is there to ensure that the solutions are designed with adequate thermal capabilities for the Intel processor within them.



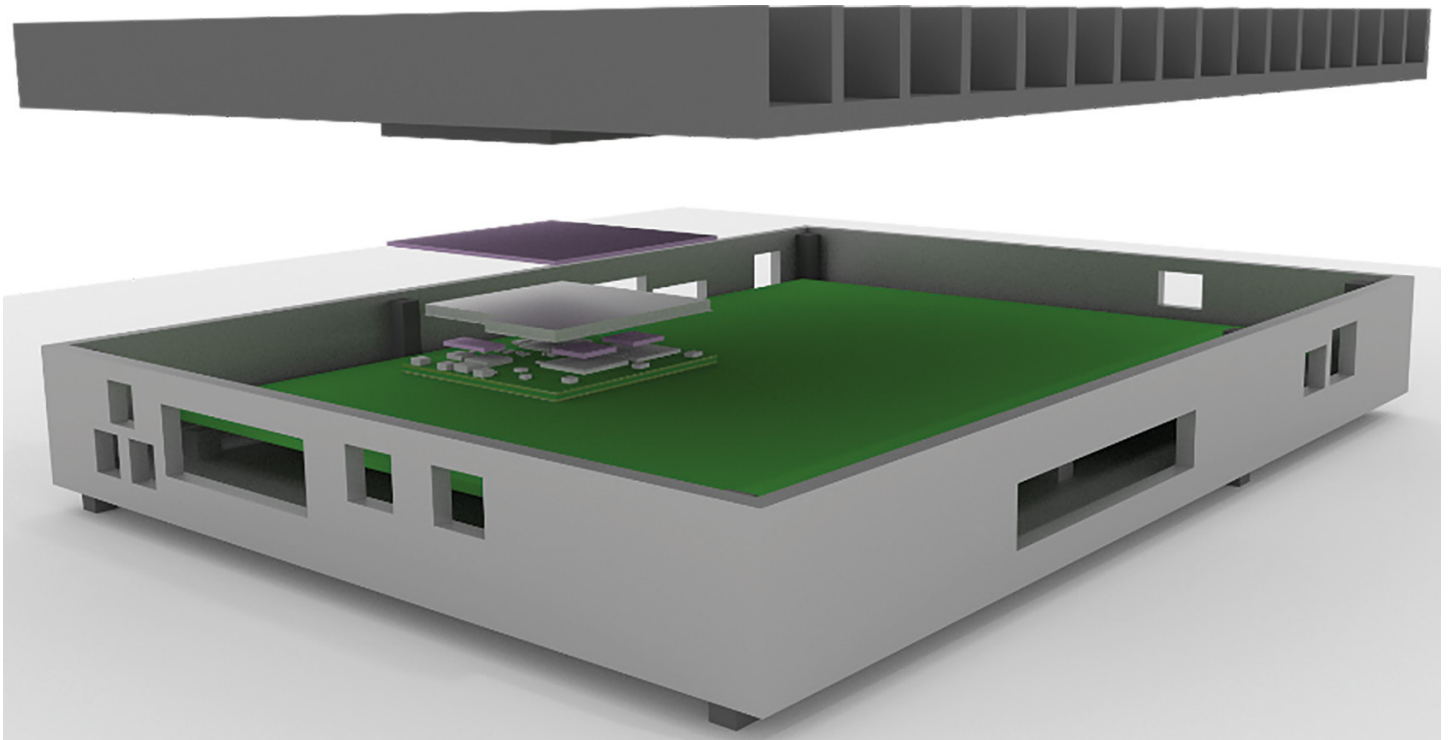


Figure 1. Rendering of a reference solution for an IoT module

Challenge:

As the Internet of Things continues to expand with more and more devices being connected to the Cloud the demand for smaller form factor devices with higher compute power is increasing. Not only do customers want better computing, the devices also need to be able to communicate via cellular or WiFi to send the data back to the customers' servers. With higher compute power comes an increase in junction temperature which creates a challenge for the thermal engineer. Adding to the small form factors is the spectrum of end customer use cases and operating environments. For example, a device in a storage container could be placed in the scorching Arizona sun or the frigid cold of Alaska and these devices need to operate flawlessly in both conditions. One of the tasks as a thermal engineer within the Internet Of Things Group at Intel is to aid our customers in their thermal solution by designing and validating a reference design.

Solution:

With so many end customer use cases it is impossible to validate them all so one way we have decided to solve this is by classifying the use cases into two broad categories of Application Only Processing

and Application plus Communication Processing. This allows us to focus in on the most thermally significant use cases for each category and design and validate to those. We also want to give our customers a method for understanding the thermal capabilities of our reference design, without it being too confusing, to the point that someone not in the thermal field could understand. This inevitably led us to the creation of the Thermal-Power Envelopes for each classification of use case.

Benefits:

With FloTHERM's simulation environment we were able to create and optimize the reference design with a high level of confidence that the design will perform as it did in the simulations. To verify this we built a prototype of the design shown in Figure 1 and tested it in an environmental chamber at different temperatures.

The test results showed that the simulations were accurate within two degrees. This is expected given the current limitations of measuring technology today. Validating the simulation results means that our model is now correlated to real world data which opens the door for our customers to use these models as a first step in their own

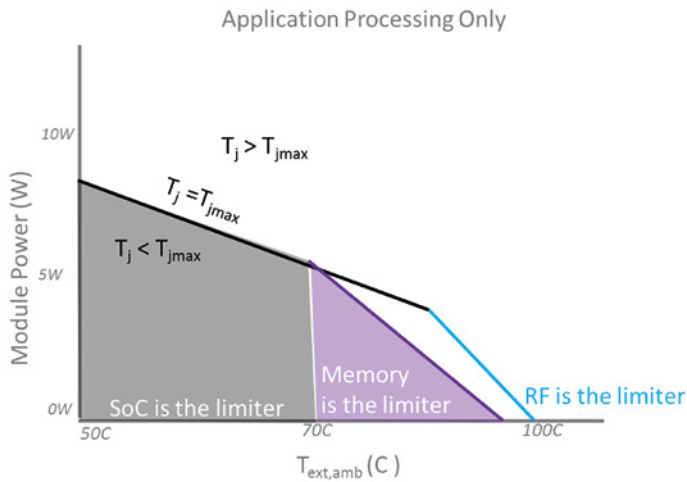


Figure 2. Thermal Cooling Capability Envelope for AP only work load.

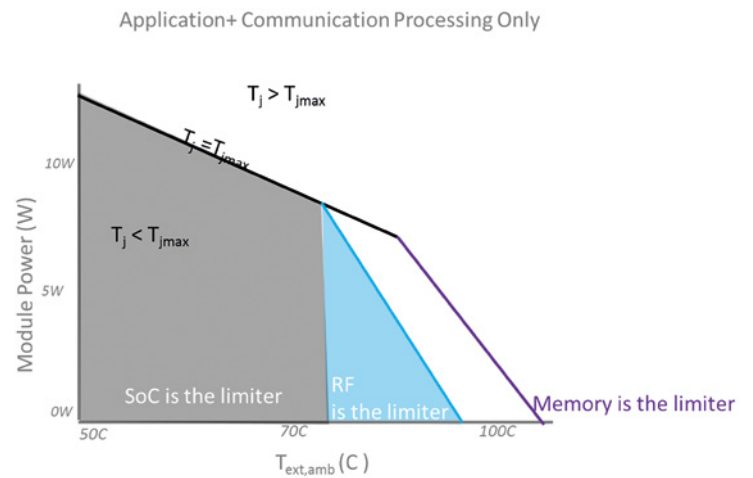


Figure 3. Thermal Cooling Capability Envelope for AP+CP work load.

thermal solutions saving them prototyping and testing costs. The correlated models are now used to generate the Thermal-Power Envelopes for this system. These Thermal-Power Envelopes are system dependent which means that a change in the thermal solution whether that be heatsink size, TIM selection, or some other variable will result in a shift in the curve.

These curves provide the customers with a fast and simple way to analyze and compare the thermal solution of a system. The charts also help the customers to understand the power and performance limitations of the system by outlining how much power the system can consume before reaching a component's specification limit at a given external ambient air temperature.

Conclusion:

The challenges that lay before today's engineers in a world that demands instant and accurate analysis of complex computations at the edge and in the palm of their hands are far from solved. None of which is more important than ensuring these devices can operate in the harshest environments. This means a properly designed thermal solution. With FloTHERM's simulations environment we are able to create, optimize, verify and validate a reference solution with minimum impact to prototyping and testing costs. FloTHERM's results were within two degrees of accuracy leading to the creation of the system's Thermal-Power Envelopes that provide our customers with a tool that they can evaluate and compare the performance of a system's thermal solution in a fast and simple way.

The challenges that lay before today's engineers in a world that demands instant and accurate analysis of complex computations at the edge and in the palm of their hands are far from solved. None of which is more important than ensuring these devices can operate in the harshest environments.

IR-Camera Thermal Management

By Atsushi Ishii, Director Sensor and System Functions, FLIR Systems
and Hugo Ljunggren Falk, KTH Royal Institute of Technology



F LIR Systems develops thermal imaging cameras and components for a wide variety of commercial and government applications. Depending on the end use, a product design might be driven by economical or dimensional factors while other applications are constrained by extreme environmental operating conditions. Whether the product is designed for firefighting purposes or to monitor a datacenter, FLIR continually explores opportunities to shorten their product development cycle.

Many development cycles are shortened by integrating simulation early in the design process. In addition to the time saved, the cost of developing a product can decrease substantially by reducing the number of prototypes built and tested. In terms of sustainable energy engineering, by “streamlining” the development cycle by adding simulation, less physical resources are used to create prototypes which means a reduction in environmental footprint.

To explore the benefits of introducing simulation early in the design process, the FLIR AX8 stationary camera was used in a case study with FloTHERM™ XT. The AX8 camera has been developed to monitor apparatus in industrial sensor networks, such as telecom electrical boxes or refrigeration units in supermarkets. A rendering of the camera is provided in Figure 1.

The case study was considered in two phases, Alpha and Beta. Alpha represents the earliest part of the design process, where decisions such as board layout are considered, and Beta represents the fully detailed analysis.

The simulation during the Alpha phase only includes the PCB and is shown in Figure 2. With FloTHERM XT, when the PCB design changes, the board can simply be swapped out through the FloEDA Bridge. The initial conditions and values set will be kept for the new board. Also, parametric studies can be used to set different configurations which can range from initial conditions to changes in geometry and is useful when comparing different solutions against each other.

The Beta phase, which represents the detailed analysis, is then considered. Simulation during

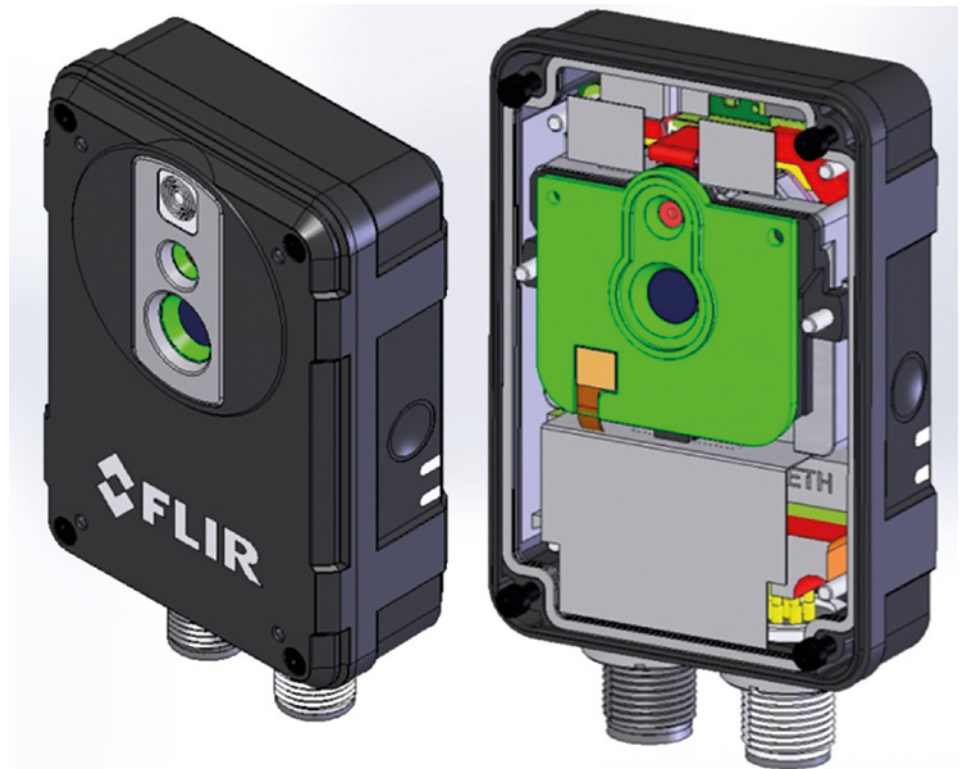


Figure 1. FLIR AX8 with and without cover

the Beta phase would include any thermal relevant components including the mechanical assemblies and enclosure. The simulation setup for the Beta phase is shown in Figure 3.

To assess the integrity of the simulations they were compared to temperature measurements of the camera in a loaded condition. Measurements during the Alpha phase were conducted using a FLIR T640 thermal imaging camera mounted on a tripod. Thermocouples were used to measure temperatures during the Beta phase.

Results Comparison: Alpha phase

The Alpha phase was used to determine if correlation between measurement and analysis could be achieved with only the PCB, in a lab environment. With correlation the analysis could be used to explore PCB design choices with respect to layout and overall PCB footprint. Figures 4 and 5 show the IR images captured with the FLIR T640 for the FLIR AX8 printed circuit board. Figures 6 and 7 show the FloTHERM XT results of the PCB in a natural convection environment. Table 1 shows a component temperature comparison of the IR image and simulation results.

The Alpha phase simulation results compare well with the bench top IR camera measurement. Any proposed board level design changes could be explored with confidence without building and testing numerous prototypes.

Result Comparison: Beta phase

The Beta phase was used to determine if correlation between measurement and analysis could be achieved when considering the full assembly. With correlation, the analysis could be used to explore thermal design choices such as materials, thermally conductive gap fillers, and venting. In addition the analysis could be used to predict performance under any environmental or usage condition. Figure 8 shows a solid temperature cross section of the simulation results and identifies the dominant heat transfer paths.

The Beta phase simulation results compare well with the bench top thermocouple measurements. This simulation model would allow a thermal design team to explore design alternatives and consider operating environments that would be too expensive or time consuming to otherwise consider.

Summary

Whether a product design is constrained by extreme operating environments, cost, or form factor, introducing simulation early in the process will shorten their product development cycle. Validated simulation processes reduce the cost of design through time savings and number of prototypes.

This article is summarized from the Master of Science Thesis: Thermal Management in An IR-Camera. Hugo Ljunggren Falk, KTH School of Industrial Engineering and Management, Stockholm

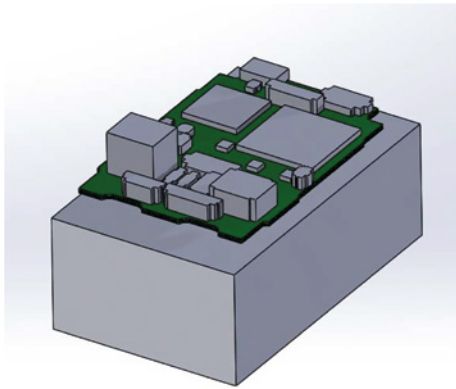


Figure 2. Alpha simulation setup

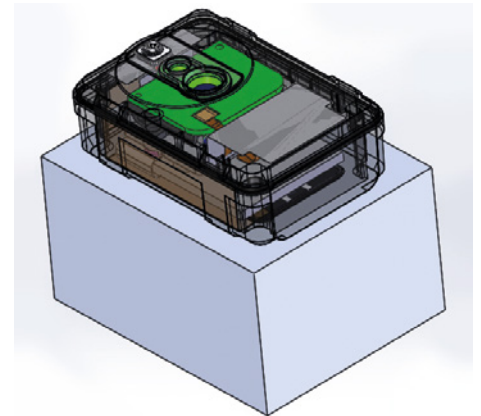


Figure 3. Beta simulation setup

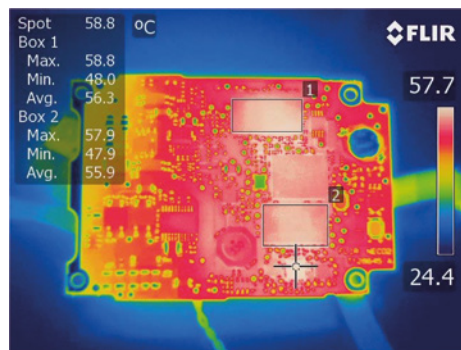


Figure 4. Alpha phase PCB top surface IR image

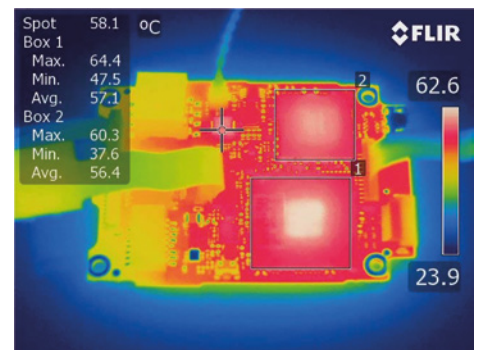


Figure 5. Alpha phase PCB bottom surface IR image



Figure 6. Alpha phase top view simulation results

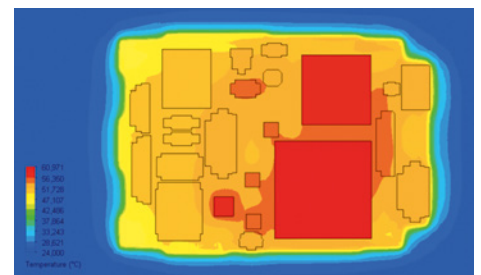


Figure 7. Alpha phase bottom view simulation results

Probe	Temperature [°C]		
	Measurement	Simulation	+/-
CPU	57.1	61.0	3.9
FPGA	56.4	57.7	1.3
Rectifier for PoE	58.1	55.8	-2.3
FPGA memory	55.9	55.5	-0.4
CPU memory	56.3	55.7	-0.6
Power mgmt. unit	58.8	57.0	-1.8

Table 1. Alpha phase results comparison

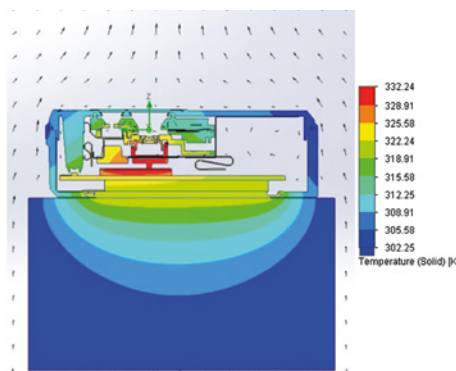


Figure 8. Beta solid temperature distribution simulation results

Probe	Temperature [°C]		
	Measurement	Simulation	+/-
Aluminum back plate	52.5	49.1	-3.4
CPU	58.9	58.7	-0.2
FPGA memory	55.4	49.1	-6.3
FPGA	57.1	58.1	1.0
Visual Cam	48.5	52.4	3.9
IR Sensor	47.2	48.2	1.0

Table 2. Beta phase results comparison

How to.....

Optimize an IGBT Cold Plate

By Anton Saratov, Application Engineer, DATADVANCE and Mike Gruetzmacher, Technical Marketing Engineer, Mentor, a Siemens Business

Insulated Gate Bipolar Transistor (IGBT) modules, are used in a wide range of industries. In electronics, IGBTs are used for Variable-Frequency Drives (VFD), for electric vehicle induction furnaces, in wind power applications and also in refrigerators, to give just a few examples.

An increase of the cooling fluid velocity increases the heat transfer coefficient. This leads to a higher heat flow rate, which leads to lower IGBT chip temperatures. However, at the same time, higher velocities also cause an increased pressure drop. The heat exchanging surface area, in this case, the cold plate surface, can be modified by pins or fins in several variants and arrangements (Figure 1). A shifted arrangement for example, usually leads to a higher heat flow rate compared to an aligned arrangement, but it leads to an increasing pressure drop, which increases the energy consumption for pumps.

The factors Size, Weight, Power, and Cost (SWaP-C) play an important role for the product competitiveness. Figures 2a and 2b show an overview of the example model.

Parametric Studies

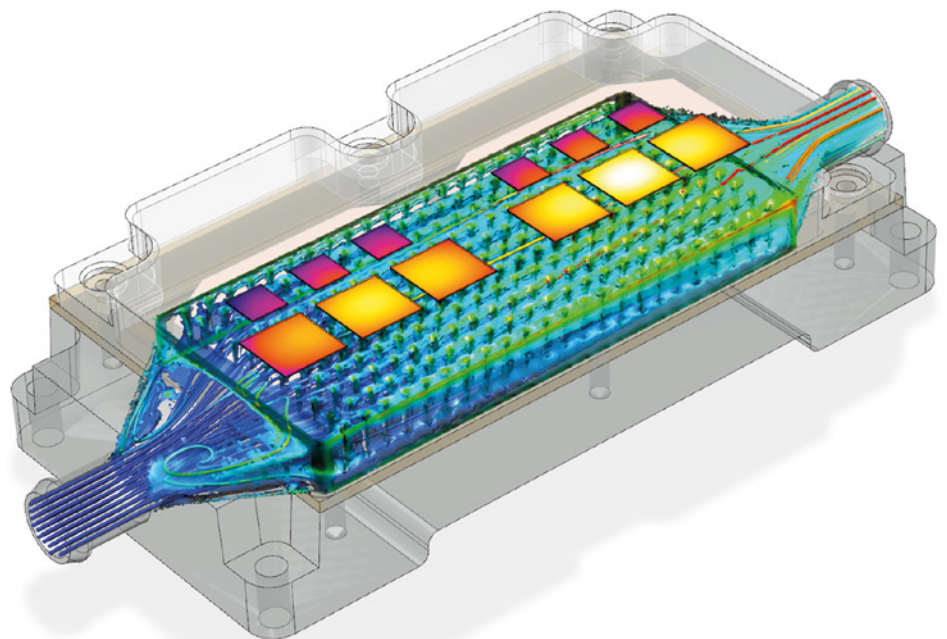
Parametric studies in FloEFD can lead to the following results:

Figure 3 depicts the results of five variants. On the x-axis is the pressure drop, the y-axis the maximum IGBT temperature and the bubble size illustrates the weight. The larger the bubble the heavier the cold plate. The smooth cold plate has the lowest pressure drop while also being the lightest in size, but the IGBT temperatures are the highest of the group. The cold plate with the shifted fins ensures the lowest temperatures but it results in the highest pressure drop and is the heaviest variant.

The operating curve in Figure 4 shows the results of a parametric study in which the volume flow rate is varied from 0.1 to 5 liters per minute.

DoE Study in FloEFD

A DoE study can be conducted in FloEFD with the settings shown in Figure 7:



The number of experiments is defined automatically according to the previously defined variations and simulated. The results and the response surface are shown in Figure 8. The response surface illustrates the CAD volume of the cold plate, the maximum IGBT temperatures and the pressure drop, with the varied parameters on the x and y axis as well as the corresponding result parameter on the z-axis.

Additional objective functions for the “Find Optimum” function are defined. For this example a maximum pressure drop and a maximum IGBT temperature are applied, which might be defined by a customer’s project specifications (Figure 9).

The optimal design point is now searched on the response surfaces and created as an

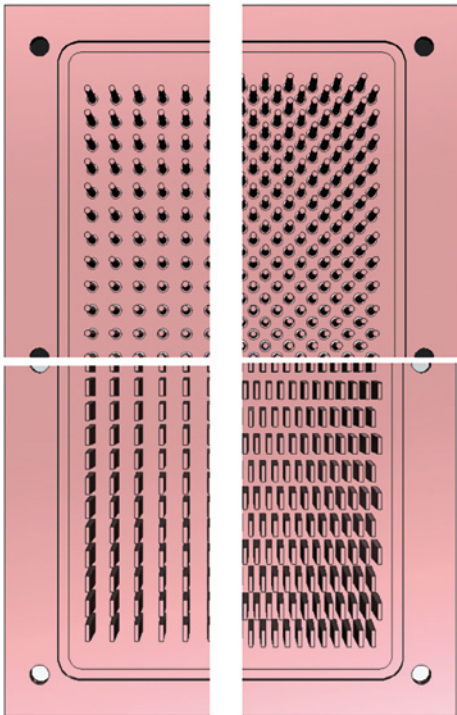


Figure 1. Various versions of the cold plate

optimum design point in this scenario. Figure 10 shows the optimized cold plate variant resulting from the DOE.

pSeven and FloEFD

Built-in tools for design exploration like Parametric Study are very useful for a better understanding of the model and preliminary optimization studies. However, in many cases, the problem is too complicated to be solved with such tools and that is where external tools come to play.

pSeven by DATADVANCE is such a platform for the automation of the simulation process and design space exploration. A graphical interface allows users to create workflows with different CAE tools and sophisticated optimization algorithms enable efficient solving times for high-dimensional multi-objective constrained problems. Additional tools for dependencies and correlation studies and approximation building can also be useful for a deeper understanding of the model.

How to control FloEFD

To perform the optimization study in an external tool, one needs a way to control the FloEFD project. There are two possible solutions – a dedicated Parametric Study mode, and via FloEFD API.

Parametric Study in FloEFD has an External Optimizer mode that allows the user to pass

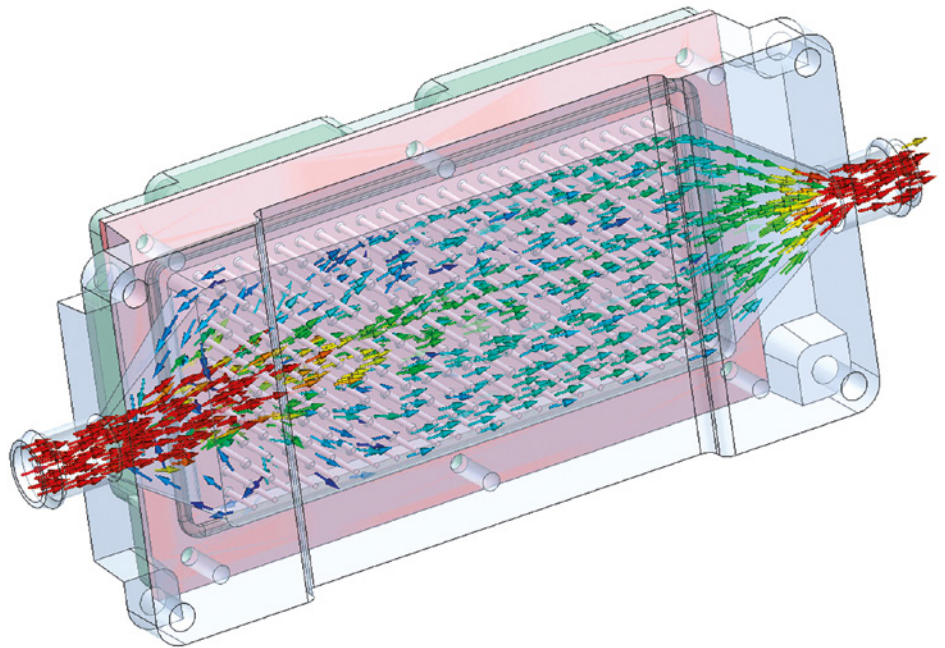


Figure 2a. Overview

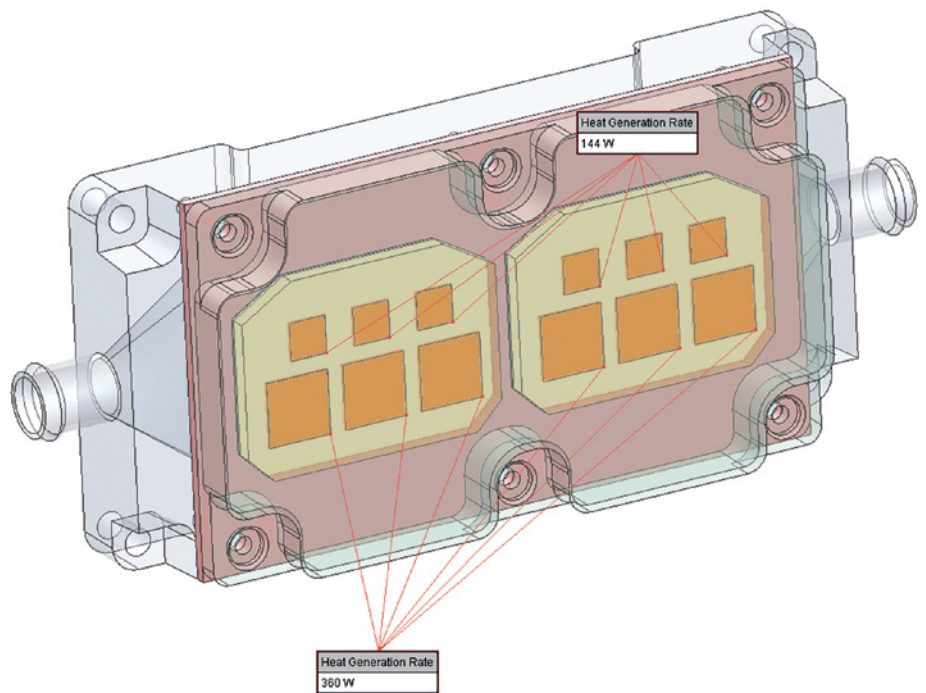


Figure 2b. Overview

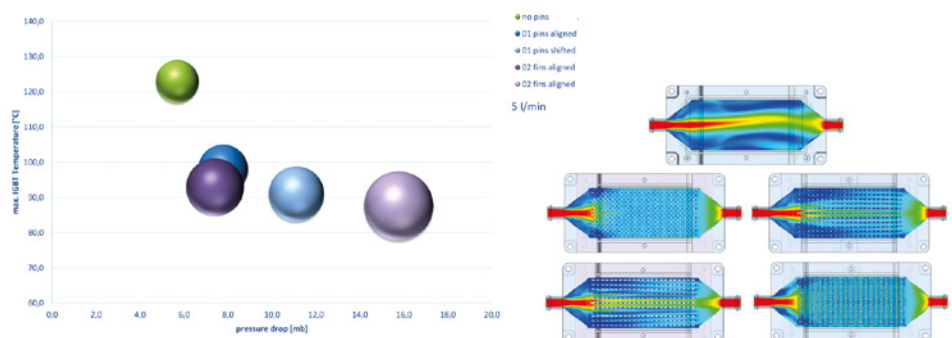


Figure 3. Comparison of the five variants

the project parameters in xml files and run a simulation from a command line.

Once the parametric study is created, an input xml file needs to be prepared, then placed in the proper place in FloEFD project, run a starter from command line, wait until the simulation ends and then grab the output file and extract results.

API interface is another option. It allows users to change the project inputs and boundary conditions, simulation settings, rebuild and run simulations and retrieve results.

pSeven has a special direct integration block for FloEFD versions for major CAD systems. It combines the flexibility of the API-based approach and an easy-to-use graphical interface. Once the model is specified, the user can select geometrical and simulation inputs and outputs from a dependencies tree as variables for optimization or other studies.

FloEFD block can be connected to an Optimizer or DoE block to act as a simulation driver in the study.

Two-objective optimization problems are considered in order to minimize the temperature of electronic modules and decrease the pressure drop in the system. Moreover, a maximal temperature difference is constrained by 10% to provide equal aging of the electronics.

Six geometry parameters are varied: pin elliptic cross section widths, the distance in a row and between rows, shift between rows and conic angle of the pins. Optimizer settings are shown in Figure 15.

pSeven has SmartSelection heuristics to select the proper algorithm and its settings from a long list.

In this case, a surrogate-based optimization algorithm is used. It allows for setting an explicit budget of evaluations. Number of model runs is set to 120 for this problem.

The result of two-objective optimization is Pareto-frontier. The optimization history in drag versus maximum temperature axis is shown in Figure 16.

Pareto-frontier is useful for trade-off studies but the final decision as to which of the configurations is best is up to the expert.

Automated simulation also allows the user to perform DoE study and create

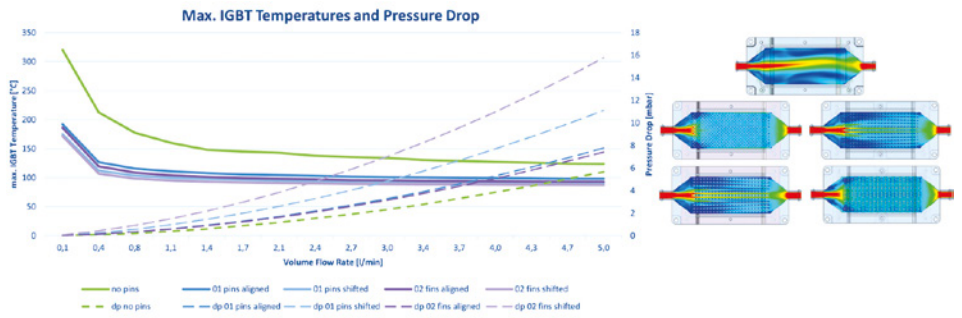


Figure 4. Operating curve

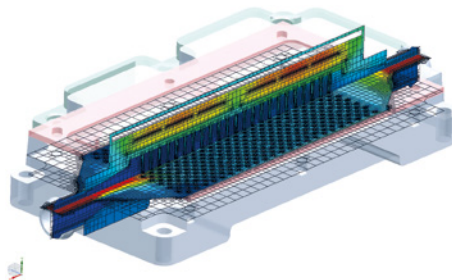


Figure 5. FloEFD simulation

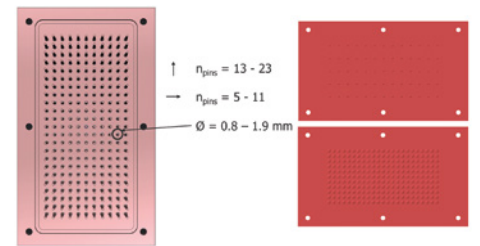


Figure 6. Variation parameters and limits

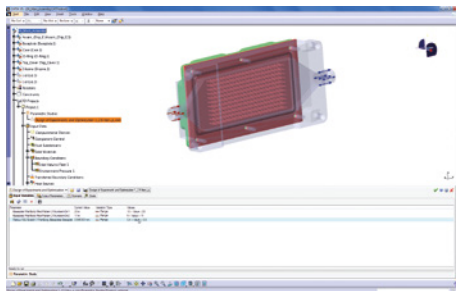


Figure 7. Settings DoE study

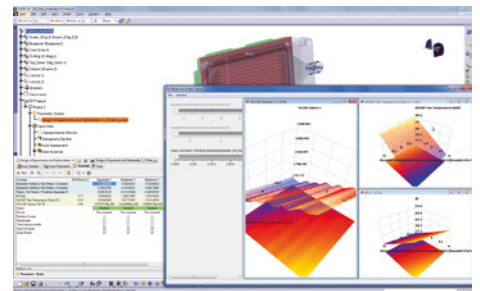


Figure 8. Results and response surface

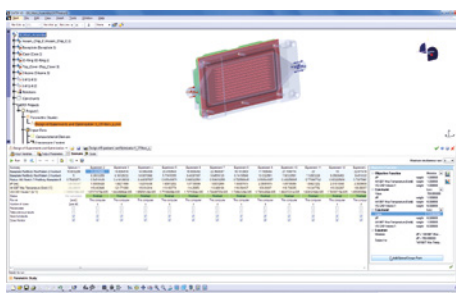


Figure 9. Find optimum function

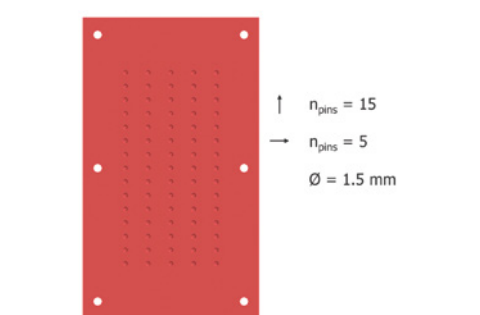


Figure 10. Optimized variant

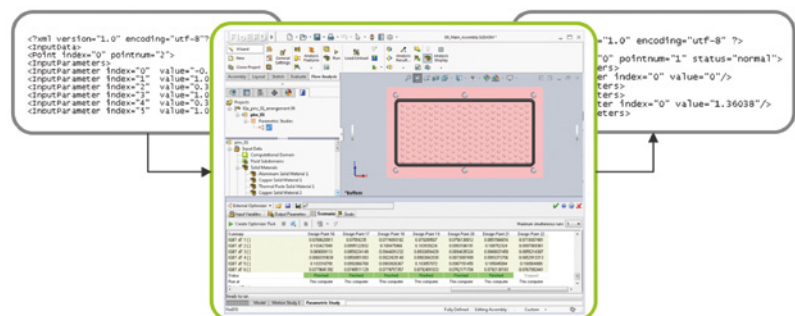


Figure 11. Parametric Study run with xml files

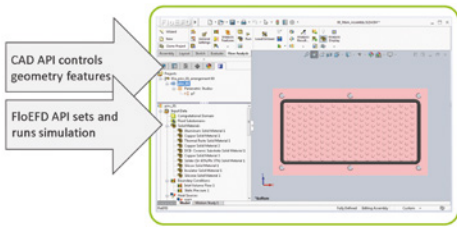
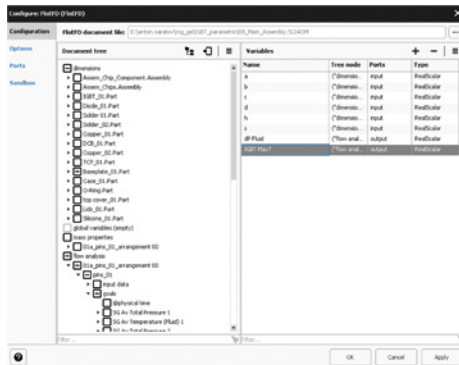


Figure 12. Simulation run by API



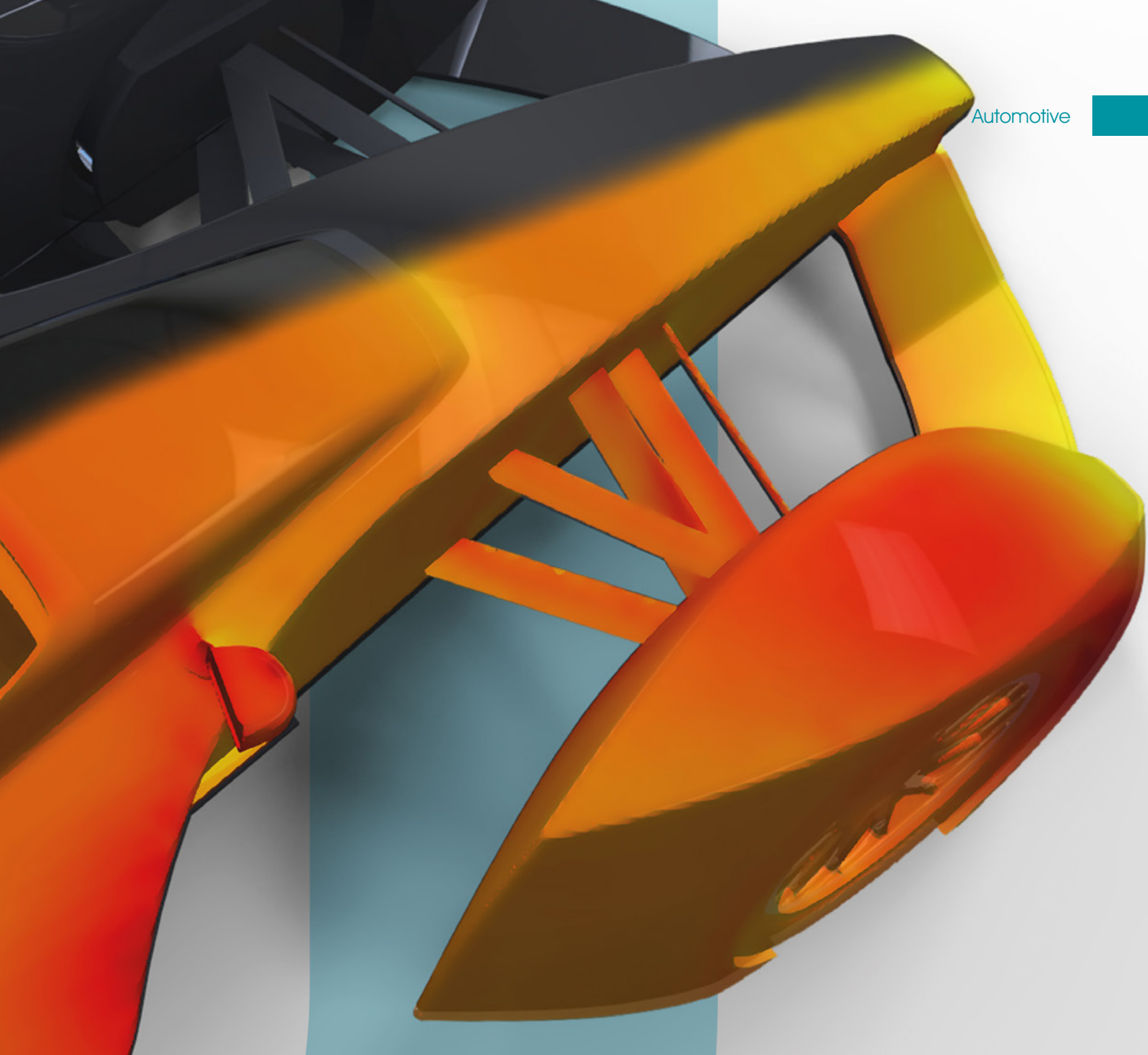
Up in the Cloud

Turbo Charging FloEFD Usage

By Koen Beyers, CEO, Voxdale Bvba



Figure 2b. Formula E, Season 5 Racing Car



In 1965, Gordon Moore claimed that the number of transistors in integrated circuits would double approximately every two years.

CFD and FEA simulations prove that he could not get closer to reality. With increasing RAM and faster CPUs, more and more simulation models are being calculated, more cells are generated and faster computing speeds are expected. On the one hand, the available computing power is used to make innovations more complex and shorten development cycles simultaneously. On the other hand, of course, it's simply because engineers can. Engineering hours are often the highest cost factor, which means that it can be more economical to use the available computational capacities rather than cost-intensive manual preparation work which could save computation time.

To be always up-to-date and to provide the best available technology to customers, "Monster Hardware" has been invested in for years. Every second year, an investment was made in new computers, with double speed, and twice as much capacity, which amounted to about €3,000 per workstation. Even at the end of the millennium it was quite possible that heavy hardware and even tube displays were transported to on-site presentations and customer visits, as affordable and high-performance laptops and projectors with sufficient resolutions were, at that time, future dreams.

Figure 1 shows a state-of-the-art computer from the year 2010. The processor (four

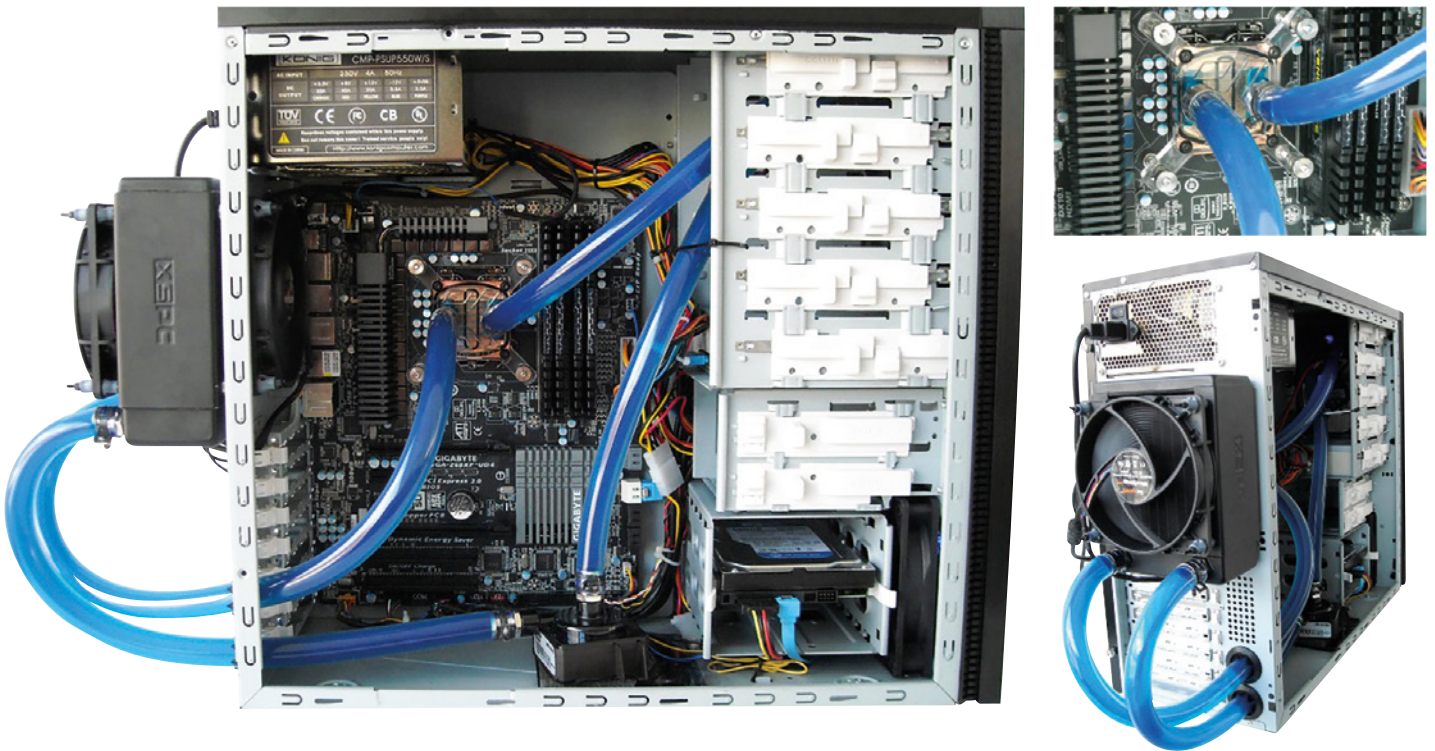


Figure 1. State-of-the-Art Computer from 2010

cores / eight threads) was overclocked up to 4.7 GHz instead of 3.4 GHz and the memory to 1600 MHz instead of 1333 MHz. The computation time for one of Voxdale's Mentor FloEFD example models was reduced to five hours from nine, which were needed before the overclocking. The result was great, the sense of empowerment for the engineers involved was wonderful.

Simulation in the Cloud

Cloud computing is not a revolutionary concept these days. We're all working together through Amazon Cloud, Google Drive, Dropbox, Trello, iCloud, and SharePoint, but the growth potential it brings is "more than exponential", higher, and faster than Moore's Law.

As a design, engineering and simulation company, Voxdale is working with confidential CAD data, with legal and rare software licenses, and with limited resources, it was quite a leap to take. But it was successful. Voxdale's own licenses can be used on virtual machines in the cloud and virtual high performance machines can be configured in just a couple of minutes. Simulation models with, for example, 40 million cells and a study with ten variants are now feasible without any problems. An example configuration consist of a 20 core hardware, at 3.1GHz, with 140GB RAM.

Realization

In this specific example, the Microsoft Azure cloud environment is used. The cloud computing platform, was put into operation in 2010 and is available in 34 regions around the world (status March 2017). [1]

The Azure environment is just like a Windows computer that is accessed by using the "Remote Desktop Connection". Hence, the installation and way of working is just like working on a familiar Windows based system. As a result, the exact same surfaces appear, so the engineering work is done in the usual familiar environment, including the FloEFD GUI and no additional introduction time is required. The simulation process remains the same, only the files are uploaded to the cloud.

Generally, the calculation of CFD simulations requires sufficient CPU power and RAM capacities, but the post processing, which means the results display on the complex CAD model, requires high level graphics card power in addition to RAM.

Therefore, it may be advisable to set up two cloud configurations, with both having the same amount of RAM. The system for the calculation has more CPU capacity, the configuration for the following post processing has less CPU capacity but high-level graphics power instead. The simulation

I now have the power at hand to run multiple variants of Formula 3 and Formula E cars without the former fear for hardware capacity.

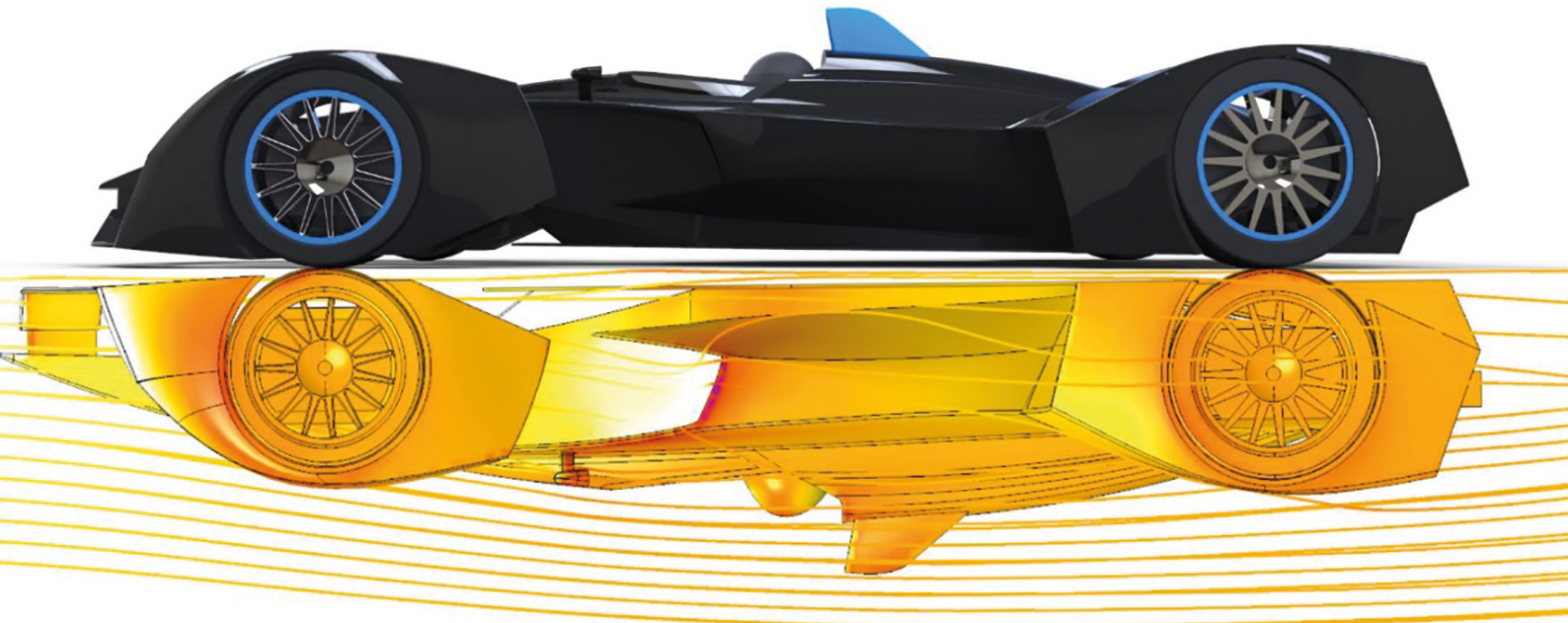


Figure 2a. Formula E, Season 5 Racing Car, approximately 33 million cells

results can be transferred from the virtual machine for the calculations to the virtual machine for the visualization.

The licensing of the software products can be implemented very easily. The Azure environment can be integrated into the domain so that the company's license server can be accessed. Alternatively, if, for example, no corresponding domain is available, the license server can be connected via a VPN connection.

One particular example Voxdale solved on the Azure cloud, had around 35 million cells. For comparison: even on the already well-equipped workstation, it was only possible to run 9 million cells. The FloEFD adapted grid refinement was applied, which automatically refines the grid in high flow gradient regions during the calculation [2]. The calculation time was around 6 days for 1,500 iterations.

The main benefits of working in the cloud in the daily simulation process are:

- The results are stored in the cloud in a safe environment,
- There is no need to continuously invest in workstations,
- Costs are flexible only the actual time on the virtual machine has to be paid, and
- The system stays on stand-by, all software and configurations remain installed for the next use.

Examples

Some impressive benchmarking projects have already been conducted on a cloud basis, including validations for the Bike Valley Full Scale wind tunnel [3]. This technology will reduce the risks of challenging prospective

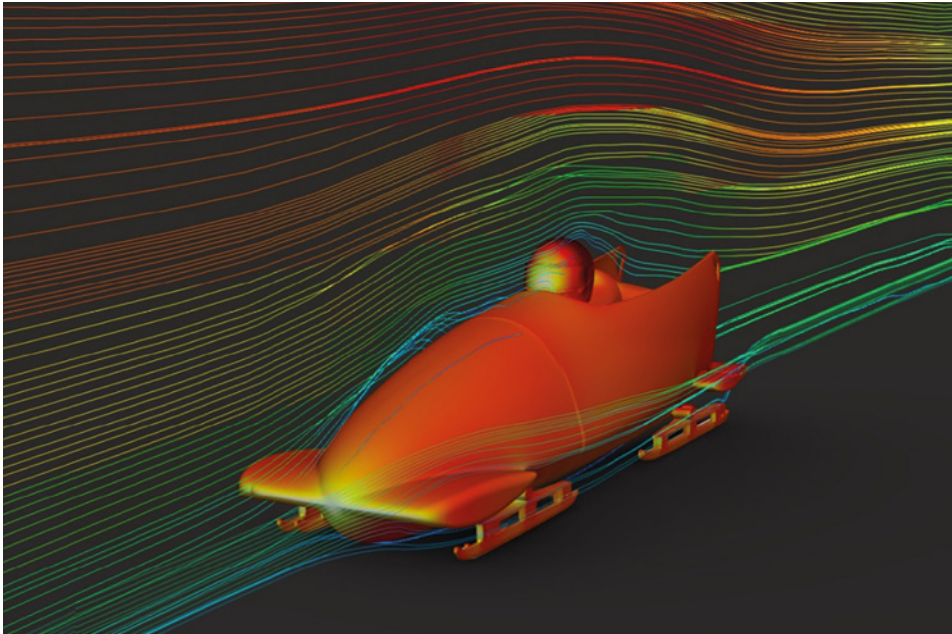


Figure 3. Designing of a super bobsleigh for the 2018 Winter Olympics, using approximately 9 million cells

projects while at the same time increasing innovation. We are expecting exciting times for applications in the automotive, aerospace, electronics, performance, process and medical industries.

A Glance into the future

Let us return once more to the situation a few years back described in the introduction above. At that time one would not have thought that large amounts of data, such as complex three-dimensional CAD models and simulations, could be transmitted via mobile phones. Today, on the road, we can transfer technical models, even with large amounts of data, over the mobile network and view them (with a sufficiently large display) on mobile devices, such as smartphones and tablets.

Perhaps fixed desktop workstations will also lose their importance in the next few years, and complex technical simulations can be carried out in the cloud from anywhere.

References

[1] <https://azure.microsoft.com>
 [2] SmartCells – Enabling Fast & Accurate CFD <http://go.mentor.com/4Pppz>
 [3] Calibration of Low Speed Cycling Wind Tunnel – Part 1 <http://www.flandersbikevalley.be/wp-content/uploads/2016/02/White-paper-calibration-part-1-final.pdf>

Rocket Science and FloMASTER



Korean Aerospace Research Institute Validates
NARO Spacecraft Fueling Scenarios with FloMASTER



Edited by Mike Croegart, Aerospace Industry Manager, Mentor, a Siemens Business

Like most space launch vehicles, the Korean Aerospace Research Institutes (KARI), NARO spacecraft uses liquid oxygen (LOX) and Kerosene as propellants. The two liquids are piped to the rocket motors separately and when they are ignited, they react and produce an enormous amount of thrust that can propel these heavy crafts through the earth's atmosphere. This is not new technology and is relatively straight forward for rocket science. The real challenge of these systems, is fueling the vehicle. The volatility of the LOX and the need to fuel all three stages of the rocket at the same time makes optimizing and validating the fuel scenario vital.

Since LOX is a cryogenic liquid it has to be maintained at a very low temperature and there is always a certain amount of the fuel that boils off to a gaseous state while the rocket is being fueled. Therefore, the system must be capable of expelling the gaseous oxygen as well as maintaining a balanced fueling strategy. Additionally, cryogenic liquid LOX may suddenly be injected into the projectile tank and LOX feed line, which is initially kept at normal room temperature, resulting in thermal shock damage. Therefore, in order to prevent such a thermal shock phenomenon, it is essential to carry out an operation procedure for pre-cooling the projectile tank and the LOX supply line.

KARI took advantage of FloMASTER's ability to run both steady state and transient simulations to verify the piping system and the filling scenarios would perform as expected.

Figure 1 is a schematic of the LOX system. The LOX filling system stores and supplies the LOX required for the launch vehicle and safely discharges the LOX from the vehicle during the cancellation of a launch. It is also used to sample the LOX for quality control. The LOX filling system consists of a storage tank located in a central facility, a cryogenic valve and a transfer pump. After the supply line has cooled down, the LOX supply operation mode to the full projectile

tank begins. At this time, the filling mode to the LOX tank is divided into large flow filling, small flow filling, supplementary large flow filling, and supplementary small flow filling. The supplemental filling mode is performed to compensate for the amount of cryogenic fluid in the tank that is absorbed and vaporized from the tank wall and hot pressurized gas. Each filling mode is changed by adjusting the opening of the cryogenic valve. The supply operation mode is then terminated when the projectile tank is completely filled.

Figure 2 represents a schematic diagram of the kerosene filling system. Unlike the LOX filling system, in the case of the kerosene filling system, no separate cooling operation procedure is required since the temperature of the supplied fluid is not in a cryogenic state. In addition, kerosene is less sensitive to temperature than LOX, so a boil-off phenomenon occurs less frequently. Thus, the kerosene filling system has a relatively simple system operating mode compared to the LOX filling system. There are a total of four filling modes for the LOX filling system, but there are only two filling modes for the kerosene filling system: large flow filling and small flow filling.

In this study, the filling scenarios in the LOX and kerosene filling system required for the stable filling mode of the three-stage NARO

KARI took advantage of FloMASTER's ability to run both steady state and transient simulations to verify the piping system and the filling scenarios would perform as expected.

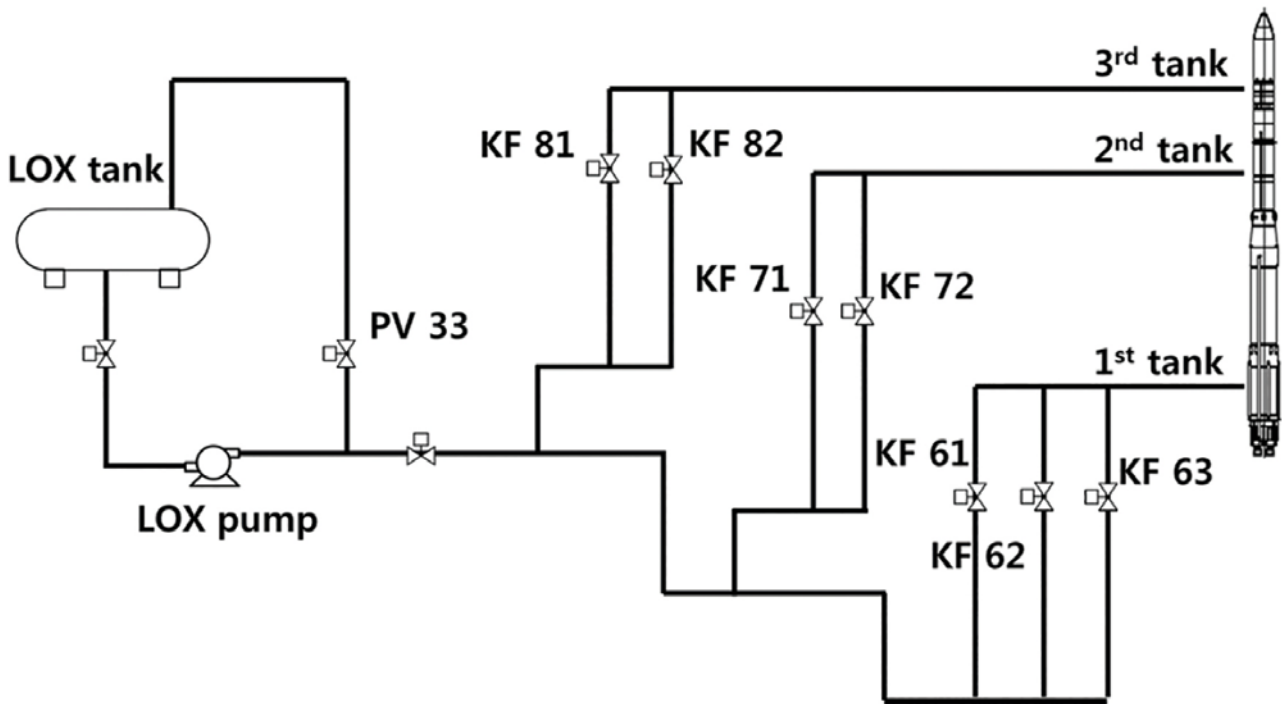


Figure 1. Schematic diagram of liquid oxygen filling system.

rocket were selected and the filling flow rate was selected accordingly. FloMASTER was used to construct a filling system satisfying the selected filling flow rate. The representative system for the LOX filling is shown in Figure 3.

The capacity of the cryogenic flow control valve was determined through steady state analysis. Then, the transient analysis was performed based on the steady state analysis result. This allowed the overall filling flow rate and amount supplied through each filling line to the tanks on a time varying basis to be calculated to confirm they met the design operating conditions.

The LOX filling system of NARO consists of a total of three feed lines. For the first tank feed line, three flow control valves are used to control the flow rate. Two flow control valves are used to control the flow rate for the second and third tanks. Finally, there is also a recovery line that recovers the remaining LOX back to the LOX storage tank. Liquid oxygen stored in the LOX storage tank is fed to the projectile tank at each stage using an LOX pump. Table 1 shows the capacity of the LOX tank located at each end of the KSLV and the height of the planned installation.

The filling flow rate in each mode that satisfied the LOX full charge time condition is chosen (about 90 minutes). The LOX filling to the projectile tank is mostly through the small flow filling and large flow filling modes.

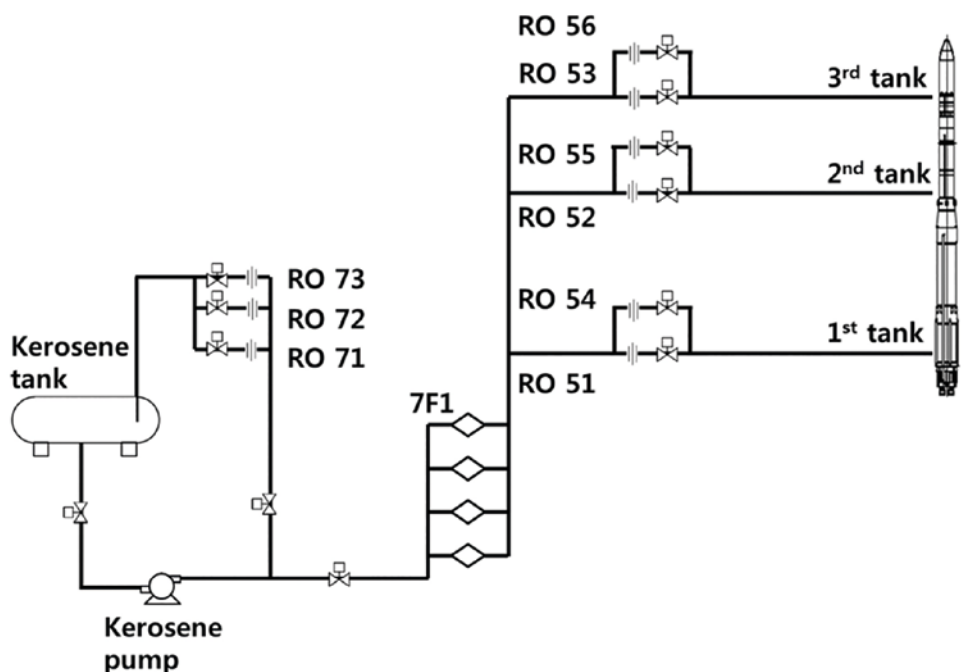


Figure 2. Schematic diagram of kerosene filling system

The projectile tank is first filled up to 30% capacity with a small flow feed and then up to 95% with the large flow filling mode. Finally, the remaining 5% with the small flow filling mode. Assuming that the filling of each projectile tank is completed at the same time, the supply flow rate according to the filling mode at each stage is calculated as shown in Table 2.

The process of filling the LOX tank was analyzed by transient analysis by applying the calculated capacity value of the flow control valve, the filling mode and the filling time. Figure 4 represents the LOX flow rate supplied in the first stage and the liquid level (%) of the first stage LOX tank when the LOX filling mode is performed. Figures 5 and 6 represent the LOX flow rate supplied to the second and third stage LOX tanks and the liquid level (%) of each LOX tank, respectively.

As a result of the transient analysis, it was confirmed that the filling completion time of the single-stage LOX tank was about 98 minutes, which was about 9% higher than the LOX full charge time condition (90 minutes). This is within the allowable range of design error of 10%. The second and third stage LOX tanks are filled in 97 minutes and 95 minutes, respectively. Therefore, it was confirmed that the full charge time difference of each LOX tank was within five minutes.

The kerosene supply system also determines the supply flow rate using the kerosene tank capacity and full charge time conditions (70 minutes). Table 1 shows the capacity and installation height of the kerosene tank. The kerosene tank has an installation height similar to that of the LOX tank. Unlike the LOX filling system, the kerosene filling system feeds for five minutes with the initial filling, up to 95% with the large flow filling, and the remaining 5% with the small flow filling mode.

Figure 7 represents the 1D FloMASTER model of the kerosene feed system for the kerosene filling system, two orifices are used to control the flow rate for each of the stages. In addition, kerosene is supplied to the projectile using a vane pump that supplies a constant flow rate, and the remaining kerosene is recovered back to the kerosene storage tank. A 1D steady state flow analysis was performed to determine the orifice size satisfying the calculated filling flow condition.

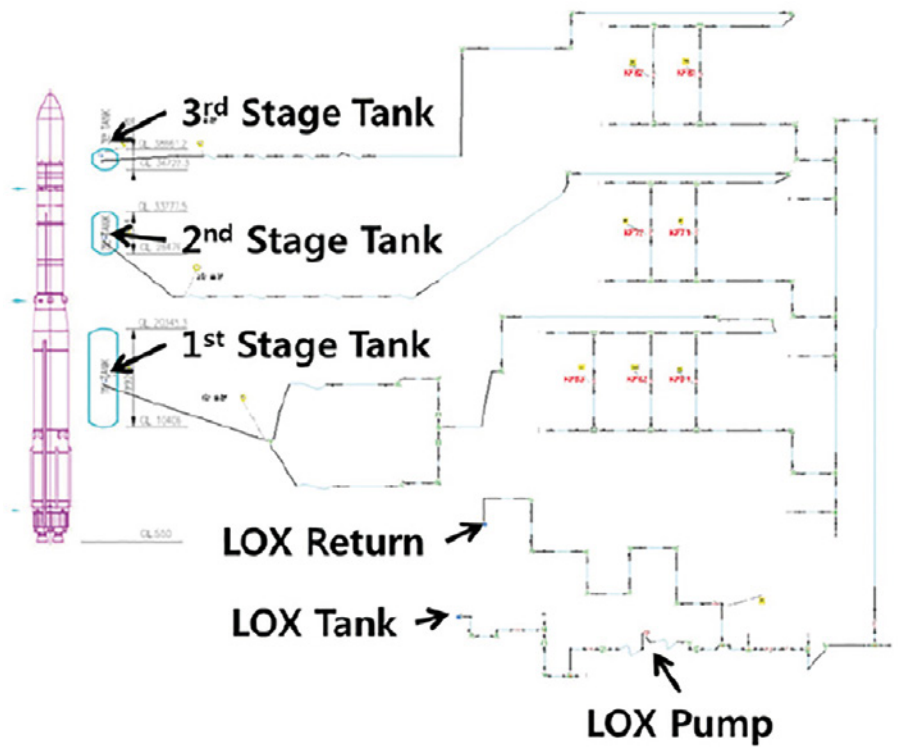


Figure 3. 1D analysis model of LOX filling system

Tank	Volume [%]	Height [m]
1st Stage	100 (Ref.)	0 (Ref.)
2nd Stage	29	21.3
3rd Stage	6.6	32.8

Table 1. LOX tank specifications

Mode	Small flow filling	Large flow filling
	Flow Rate [l/ min]	
1st	618.1	1450
2nd	180	422.3
3rd	40.8	95.8

Table 2. Flow rate calculation result with LOX filling scenarios.

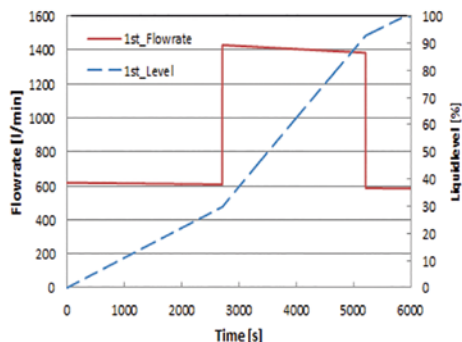


Figure 4. Volumetric flow rate and liquid level profile for 1st stage LOX storage tank.

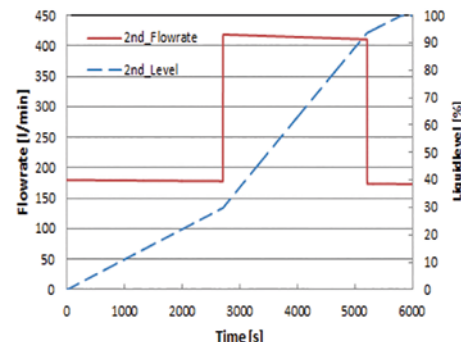


Figure 5. Volumetric flow rate and liquid level profile for 2nd stage LOX storage tank.

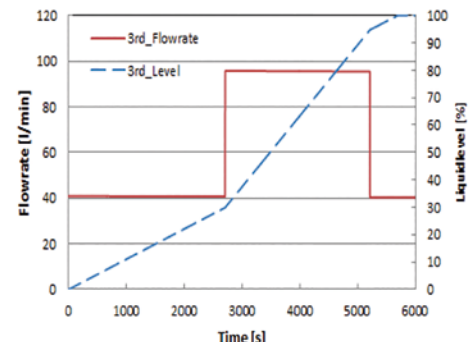


Figure 6. Volumetric flow rate and liquid level profile for 3rd stage LOX storage tank.

The transient analysis was performed using the orifice diameters calculated from the steady state analysis. The filling flow rate and the kerosene tank liquid level (%) change characteristics obtained from the transient analysis are shown in Figures 8, 9, and 10 for the three tanks, respectively. After the kerosene filling mode was changed from the small flow filling mode to the large flow rate filling mode, the flow rate of the first stage tank gradually decreased as the fill progressed. Conversely, the flow rate of the stage two tank gradually increased. It was confirmed that the flow rate of the Stage 3 tank also gradually increased. This is because the head value of the first stage kerosene tank increases significantly compared to other tanks. As a result, the reduced first-stage kerosene feed flow is distributed to the second and third stage feed lines. It was confirmed that the filling was completed in 66 minutes for the first tank, 64 minutes for the second, and 63 minutes for the third. This satisfies the kerosene filling time condition (70 minutes). It was also confirmed that the filling time difference of each kerosene tank was under five minutes.

The engineers at KARI were able to utilize FloMASTER's flexibility and accuracy to predict the correct control valve settings and orifice sizes to achieve the flow rate of LOX and kerosene flowing to each stage and demonstrate that the system design and filling scenarios provide a stable filling operation mode of NARO propellant filling system.

Summarized from original paper: Analysis on the Filling Mode of Propellant Supply System for the Korea Space Launch Vehicle. Jaejun Leea . Sangmin Parka . Sunil Kangb . Hwayoung Ohb . Eun Sang Jungc, *a Advanced Technology Institute, Hyundai Heavy Industries Co, Korea. b Launch Complex Team, Korea Aerospace Research Institute, Korea. c Department of Bioenvironmental Energy, Pusan National University, Korea

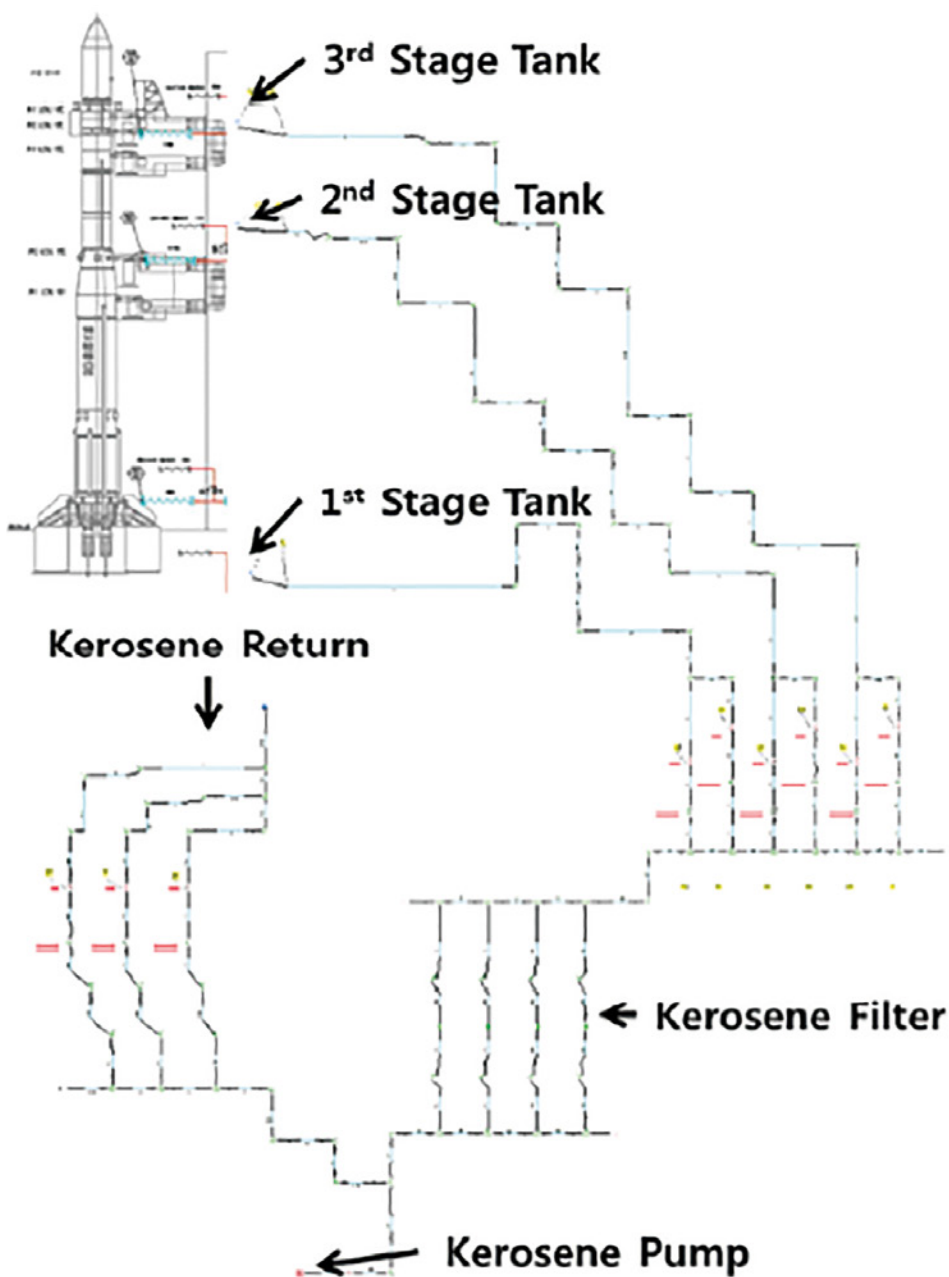


Figure 7. 1D analysis model of kerosene filling system

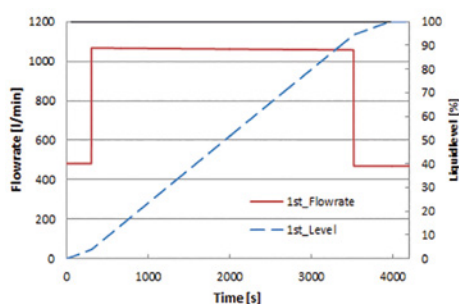


Figure 8. Volumetric flow rate and liquid level profile for 1st stage kerosene storage tank

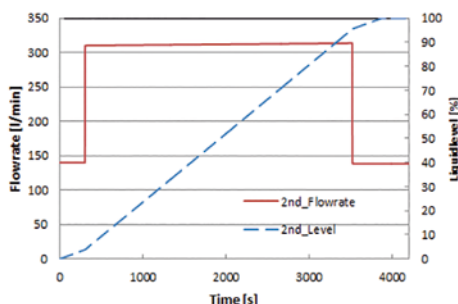


Figure 9. Volumetric flow rate and liquid level profile for 2nd stage kerosene storage tank

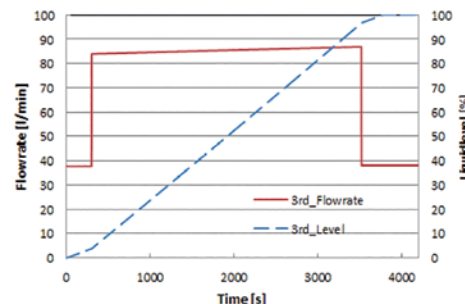


Figure 10. Volumetric flow rate and liquid level profile for 2nd stage kerosene storage tank



INTERVIEW

Wendy Luiten

Q. You have been in the electronics cooling field for over 20 years. How has electronics cooling changed over that time?

A. If we are really counting, I guess it is closer to over 25 years, although I remember way back in the early nineties that my then boss thought it was not worthwhile for me to learn flotherm – famous last words. I think the main change by far is the use of CFD and especially the GUI. I remember having to number my own nodes and integration points in the FEM code I used when I first started my career, and colouring in the printed number fields that were delivered on huge reams of folded paper – unimaginable in these days.

Q. What is your background in thermal design?

A. Worked in Lighting, TV, and Healthcare. I actually majored in heat and fluid flow, and started at Phillips Manufacturing Technology lab – the applied split-off of Phillips Research- as a thermal and thermo-mechanical specialist so when I moved to the division of consumer electronics, getting started at electronics cooling was a natural progression. I started out in TVs and that grew to consumer electronics products in general. After a couple of restructurings and the sell-off of the CE divisions I found myself back at Phillips Research and working on Lighting and Personal Health products.

Q. What are the common electronics cooling challenges, and what are the differences?

A. I have predominantly worked in consumer goods – so end-customer focus, speed of development, cost and manufacturability are very major drivers common to all three fields of Consumer electronics, Lighting and healthcare. The big differences I saw were in development speed and in platform use – the art of developing a set of common parts to cover not one product but a whole range of products. In general, the markets with more competition tend to be more challenging – but that is part of the fun.

Q. Can you tell us about Wendy Luiten Consulting and what your company does?

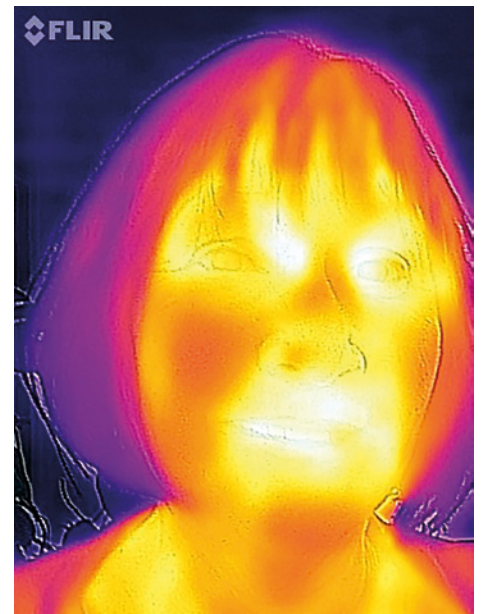
A. I do thermal design and simulations for clients and I provide training. Wendy Luiten Consulting is my next big adventure- I took voluntary leave from Philips research to get back in touch with the business again. In the past few years I have also branched out in Design for Six Sigma – I am an Innovation Master-BlackBelt-in-progress. What that actually means is that I look into the entire chain from discovering to designing-in and delivering value in electronics products. WLC develops and delivers training and advises in the combined field of thermal design and design for six sigma, which are surprisingly interlinked if you look into it.

Q. What are the challenges your customers are facing today?

A. For most people, thermal design is the ultimate performance limiter, and it is hard to do really well because so many different disciplines and so many system levels are involved and, in the end, you are working with invisible entities. The majority of electronics products are air cooled- which means the main component is not even on the bill of materials, and all kinds of enabling design features tend to get overlooked or not documented, and then people tend to re-invent the same wheel many many times.

Q. Which project have you done that you are most proud of and why?

A. I have to answer with two projects here – THE most exciting thermal project by far was the thermal design and architecture of the world's first ever fan less flat TV monitor. I wrote up that story in the paper 'Cooling of a Flat Tv monitor', which won the Semitherm Best paper award in 2002. More recently I am very proud of the work that I did on the Philips DfSS Green Belt and Black Belt training curriculum, expanding, re-writing and re-structuring the material to deliver present day product development skills.



Q. When you teach electronics cooling, what key points you want people to get?

A. Oh, there are so many key points! I think the most important one is that your thermal design is made or broken in a few vital early architecture choices – it is absolutely essential to figure out what they are – and then guard these choices through the entire design flow. And these can easily be choices that the EEs and MEs overlook as non-thermal related, surface sizes, gap sizes, material choices – that sort of thing.

Q. What do companies get wrong when it comes to thermal design?

A. There are still a lot of companies out there to which thermal malfunction just happens. They are unaware that there is such a thing as thermal design. One step up are the companies that use thermal design, and even CFD, but with a way of working that is straight from the hardware dominated nineties – they make an electrical design and a mechanical design, and when these are fully finished and detailed they submit the CAD and CAE files to CFD calculations. That really is just substituting the hardware prototype with a CFD run, and not profiting from the vastly larger possibilities that using CFD in concurrent architecture brings you. It is like when the car was replacing the horse – you have the engine outside of the vehicle like a horse was. But since then we have found out that integrating the engine into the vehicle has big advantages.

Q. How have simulation tools changed the way thermal design is done?

A. I would say the impact is vast, and on two points. The first is of course the speed of development – you do not have to wait for hardware prototyping and repeated hardware measurements. The second is related to the speed: insight in how your design functions. Computer simulations enable a thorough investigation of your solution space that would be inaccurate with analytical models and just impossible with traditional hardware and in addition they can calculate the effects of limit cases that would be impossible to build. This enables to really find the optimal thermal design in terms of total system desirability. Of course, there is also a risk – a CFD code in the hands of an unskilled user can make lots of untrue predictions, but that is really the risk of any tool at all in the hands of an unskilled user.

Q. What is your philosophy about how simulation tools should be used across the product creation process?

A. My philosophy is that they should be

used from the earliest phases of concept design to discover the main parameters and guide the vital choices. I typically do the first CFD right after the back-of-the-envelope hand calculations – and this has the advantage of having like a double check both on the hand calculations and the earliest CFD model – just to be sure that I did not forget to model an important effect. Then, as the design grows, the CFD model evolves in complexity as well and can be used to monitor the effect of changes in the subsequent steps.

Q. What would you like electronics CFD be able to do that it can't do today.

- A) In general: Maybe make the whole process more fool-proof from a thermal concept point of view. Like I said, a CFD tool in the hands of an unskilled user is a dangerous thing. Maybe with warning messages like 'I see that you have switched off radiation but there is no fan or external flow involved – are you aware that radiation is very significant in natural convection cooling?' or 'I detected a significant heat flow over an interface between two parts modelled as ideally conducting – are you sure?' or even 'I detect a significant temperature difference across an interface that you modelled as non-conducting – are you sure?'. I can imagine you could use Robins B and Sc numbers for something like this.
- B) For me personally: Adapt the command center so I can run my DOEs more easily. The ability to switch groups of variables would already be a HUGE help, as well as (in flotherm XT) the ability to switch geometry on or off. The fact that the geometry is in a different scenario table in flotherm XT makes it very complicated to do a DOE in architecture phase. In addition, calculating the effect would be comparatively easy to do in flotherm itself.
- C) In design and optimize phase making the transfer function and doing the montecarlo and the tolerance analysis would also be mathematically easy to do from my point of view. Obviously, you already have a random generator on board for the monte carlo because you do ray tracing, and I can imagine that the capability of doing the thermal tolerance analysis would be a feature that could be unique to flotherm and also add considerable value to the end user.

Fast Design of Medical Ultrasound Probes with FloTHERM

By Kazuya Motoki, Hitachi, Ltd., Japan

HITACHI
Inspire the Next



Ultrasound systems (Figure 1.a) for diagnostic images have been around for several decades. They have advanced in the last twenty years to include much more sophisticated electronics that deals with high quality scan images on much larger screens than ever before but in smaller, more compact systems that draw much higher power consumptions to manage.

Hitachi supplies ultrasound scanner systems and a wide range of probes (Figure 1.b). Each probe includes piezoelectric transducers, as an imaging sensor, which generates heat during scan. Recently, more of the electronics associated with the probe have been used inside the probe to improve image quality. As the performance of probes increase, heat generation is becoming a bigger issue compared to our previous designs.

International safety standards (IEC 60601-2-37) exist that manufacturers must comply with in terms of the thermal limits for ultrasound probes (Table 1). These temperature limits must not be exceeded while the equipment is powered continuously for up to 30 minutes so as to prevent burns. As well as this we need to allow for real world probe situations like on and off usage, variations in ambient conditions, and body temperature variations in patients. Prediction of the transient surface temperature rise, rather than the equilibrium temperature, is a key measure we use for assessing probes and hence any CFD code must be able to do a transient thermal simulation correctly. We chose the FloTHERM thermal analysis tool a few years ago because it was faster at getting simulation results than our existing tool, easy to mesh, had a good interface with our MCAD software, and it was easy to pass our CFD predictions to our FEA tool.

We typically have two to three weeks to influence the design of a probe. Our typical workflow before we used FloTHERM is shown in Figure 2 (a). We tended to finalize on the product design after several rounds of prototyping but we found difficulties with our then CFD tool and it was difficult to know what the problems were in the final assembled product. Figure 2 (b) shows the process workflow we have iterated to over the last few years with FloTHERM, because of its capabilities, to shift design



(a)



(b)

Figure 1. (a) Typical Hitachi Ultrasound Scanning System and (b) a selection of Hitachi Ultrasound Probes

to the left and an earlier stage that has allowed us to have many fewer prototypes and a cost saving of X2. In this instance, the result achieved was because we were able to review the thermal analysis predictions versus actual measurements early on, identify and rectify problems for each assembly process, and then move to the next part of the process.

From a product design perspective, we also want a CFD tool that has high analysis precision and low prediction errors. To achieve this we first made sure our probe constituent material properties were correct – such as thermal conductivity, emissivity, specific heat and density. To ensure high precision, we carried out rigorous test measurements on all of our supplier materials (Table 2) and found that certain materials (for example, Materials B that was composites) had big variations (in red font) than those shown in manufacturer datasheets.

The next thing we did in this thermal simulation process was to improve our transient thermal analysis predictions by first simulating a simple probe inside FloTHERM (Figure 3) at steady state and then we did a more detailed probe model (with each component part accurately modeled) reviewing each process transiently. Here, the temperature dependence of the ceramic heater should be taken into account via measurement of its resistance at a fixed voltage (Figure 4) when the heater was used in the simple mock-up in experiment. These heater temperature characteristics needed to be input into FloTHERM and controlled to maintain a constant power during the simulation process, otherwise the CFD simulation would overestimate or underestimate the actual measurement results. Through these processes, we found that using Cartesian meshes inside FloTHERM gave the most accurate CFD predictions (Figure 5) for the probe assembly when compared with actual measurements, especially when we used measured material properties in the detailed probe model (Figure 6). We also used FloTHERM's excellent Command Center capability for multiple early Design of Experiment analysis. In summary, we found that our simulations are very accurate, ten times faster than before, and we have a design process that fits our manufacturing needs and we use FloTHERM 100% of the time on our four core machine. Indeed, FloTHERM has helped us to invent several patents for our probes.

Test state	Body surface applications	Invasive applications
Tissue-mimicking material	Initial temperature: 33°C or more T < 43°C	Initial temperature: 37°C or more T < 43°C
Left in air	Initial temperature: 23°C ± 3°C T < 50°C	

Table 1. Temperature standards for ultrasound probes

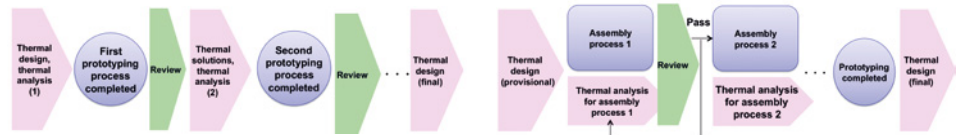


Figure 2. Hitachi CFD simulation workflow before FloTHERM (a) and today (b)

Material	Thermal conductivity [W/mK]	
	Manufacturer Catalog value	Measured value
Material A	0.3	0.3
Material B	15	5
Plastic A	0.2	0.2
Adhesive A	0.2	0.2

Material	Emissivity	
	Manufacturer catalog value	Measured value
Material A	0.86	0.96
Material B	0.8	0.15 (Gold-plated surface)
Material C	0.9	0.96

Material	Specific heat [J/kg]	
	Manufacturer catalog value	Measured value
Material 1	900	850
Material 2	1,900	1,500
Material 3	1,000	650

Table 2. Ultrasound probe constituent material thermal property measurement results

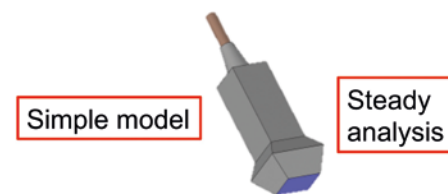


Figure 3. Simple FloTHERM model geometry of a Hitachi probe

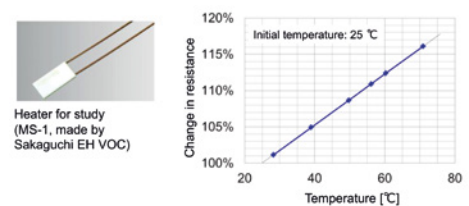


Figure 4. Ceramic heater characteristics

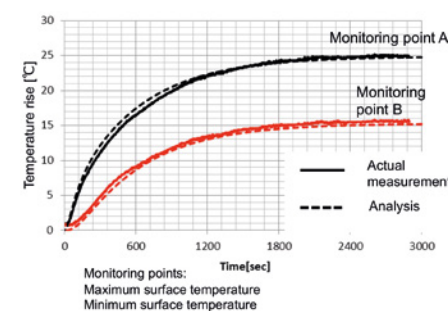


Figure 5. Transient thermal measurements versus FloTHERM predictions of a simple probe

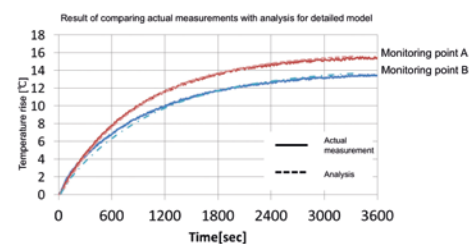


Figure 6. Transient thermal measurements versus FloTHERM predictions of a detailed model probe

Evaluation of Characterization Methods for Solid Thermal Interface Materials

Pushing DynTIM's Accuracy and Range

By Fabian Streb, Dirk Schweitzer, Infineon Technologies AG; Thomas Lampke, Technische Universität Chemnitz; and Manfred Mengel.

Future packaging technologies require increasing package-level thermal management and improved heatsinking, which then demands improved heat transfer from the package to the heatsink. Thermal Interface Materials (TIMs) play an important role, both between the package and the heatsink, and also integrated into the package to provide thermal contact between the die and the lid for example, where electrically isolating materials are used.

Including a TIM appears simple, but is deceptively so. The performance of a TIM depends on temperature, pressure, surface roughness (of device and heatsink), to name just a few factors. [1,2] Consequently, characterizing their thermal performance experimentally is not straight-forward, but is important, if the thermal design is to be robust. One further complicating factor is the fact that several measurement methods for thermal conductivity exist, but are not necessarily comparable because the different methods use different boundary conditions. Across the industry there is no standard method in use today by TIM vendors, and so it is not possible to compare similar products from different vendors as different TIM vendors use different measurement systems.

Given this situation, it is essential we gain a better understanding of how different measurement systems result in different thermal conductivity values to be able to compare vendor datasheet values, with a particular focus on TIMs where both thermal performance and electrical resistivity are important.

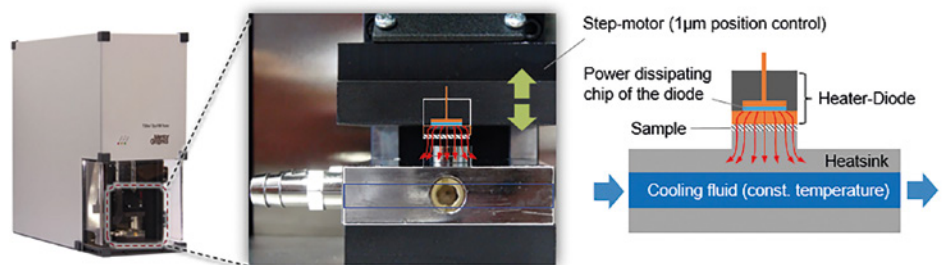


Figure 1. DynTIM Showing Operating Principle

To study this topic we selected TIM measurement techniques that are commonly-used within the industry:

- Transient plane source method (TPS) Hot Disk TPS3500 (by Hot Disk AB, Sweden), and
- DynTIM from Mentor, a Siemens business.

These were complemented by measurements done by our partners using:

- LaserFlash (by Netzsch) courtesy of Plansee SE (AT); and
- TIMA measurements (by Nanotest GmbH) courtesy of Berliner Nanotest Institute.

Material	A	B	C	D
Material Type	CDIM	Laminate	CDIM	Laminate
Matrix	Epoxy resin	Epoxy resin	Silicone	Silicone
Filler Material	SiO ₂	Al ₂ O ₃ , BN	Al ₂ O ₃ , ZnO, SiO ₂	Al ₂ O ₃ , glass fibre
Filler Vol. %	80	70-80	90	Unknown
Vendor Data	≈ 1	7 - 8	1 - 3.5	3.0
DynTIM	1.21 ± 0.01	(13.38 ± 2.65)*	4.26 ± 0.5	2.47 ± 0.039
TPS	1.06 ± 0.02	11.0 ± 0.53	3.91 ± 1.28	3.26 ± 0.2
Laser Flash	0.98 ± 0.09	5.37 ± 0.85	4.18 ± 1.62	2.15 ± 0.3
TIMA	1.30 ± 0.09	(10.41 ± 3.9)	4.24 ± 1.37	2.51 ± 0.09

Table 1. Comparison of Measurement Results Obtained with Different Methods.

The TIMA measurement system conforms to standard ASTM-D5470, as does DynTIM. Of these, DynTIM can be used for all kinds of materials provided that the required sample geometry can be prepared, and is available at Infineon's thermal lab in Munich. Its primary use in Infineon is to provide thermal conductivity measurements to provide data to increase the dependability of Infineon's thermal simulations.

During DynTIM's operation, the heater diode is heated with a constant heating current I_H until thermal equilibrium is established. This is then switched to a much lower sensing current I_S and the temperature response of the diode junction T_j monitored during the cooling down process, as heat passes through the sample into the cold plate below.

The temperature change ΔT_j from hot to cool state is measured for samples of the same material and cross-sectional area (A) but varying thickness (t). For each sample thickness the thermal resistance is determined and plotted vs. sample thickness:

$$\theta_{total} = \frac{\Delta T_j}{\Delta P}$$

The measured thermal resistance θ_{total} contains contributions from sample, tester, and thermal contact resistance:

$$\theta_{total} = \theta_{sample} + \theta_{tester} + \theta_{contact}$$

When measuring samples of different thickness (t) the thermal resistances of tester itself and the contact interfaces resistances remain constant, so:

$$\Delta \theta_{total} = \Delta \theta_{sample} \text{ as } \Delta \theta_{tester} = \theta_{contact} = 0$$

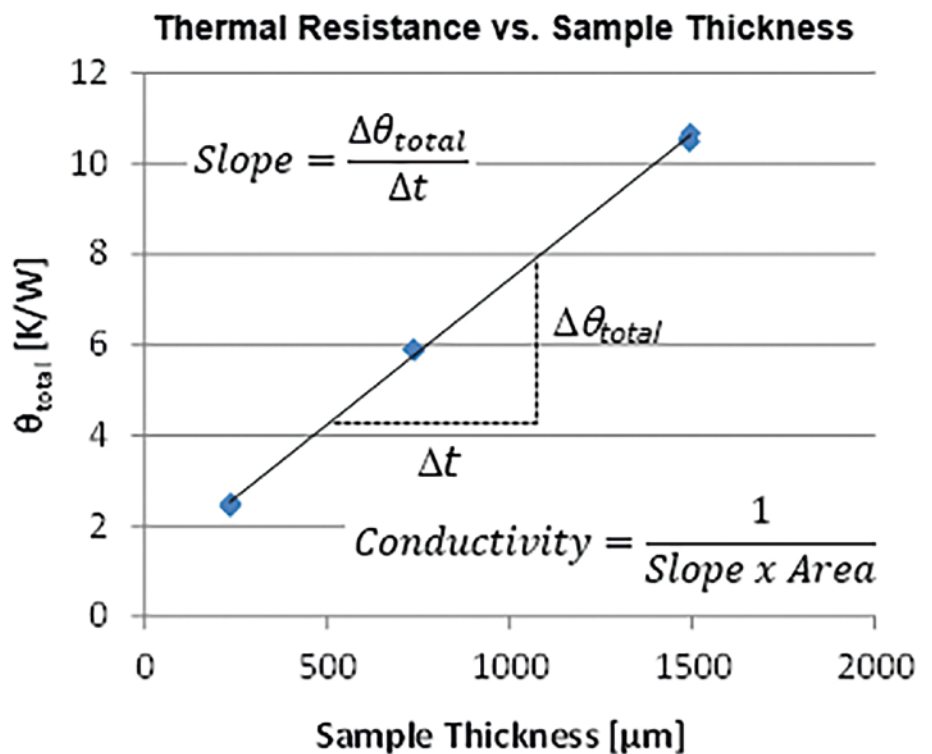


Figure 2. Thermal Resistance vs. Sample Thickness

The sample's thermal conductivity is directly related to the slope(s) of the line. (Figure 2)

In the study, four different materials were investigated. The selection includes two laminates and two cavity direct injection molding materials (CDIM), two with epoxy resin and two with silicone matrix and a wide variety of fillers (SiO₂, Al₂O₃, BN, ZnO and glass fibers). The more flexible TIMs on silicone basis (Materials C & D) can be used without additional thermal grease whereas the harder materials (Materials A & B) require thermal grease to decrease the thermal contact resistance towards device and heatsink.

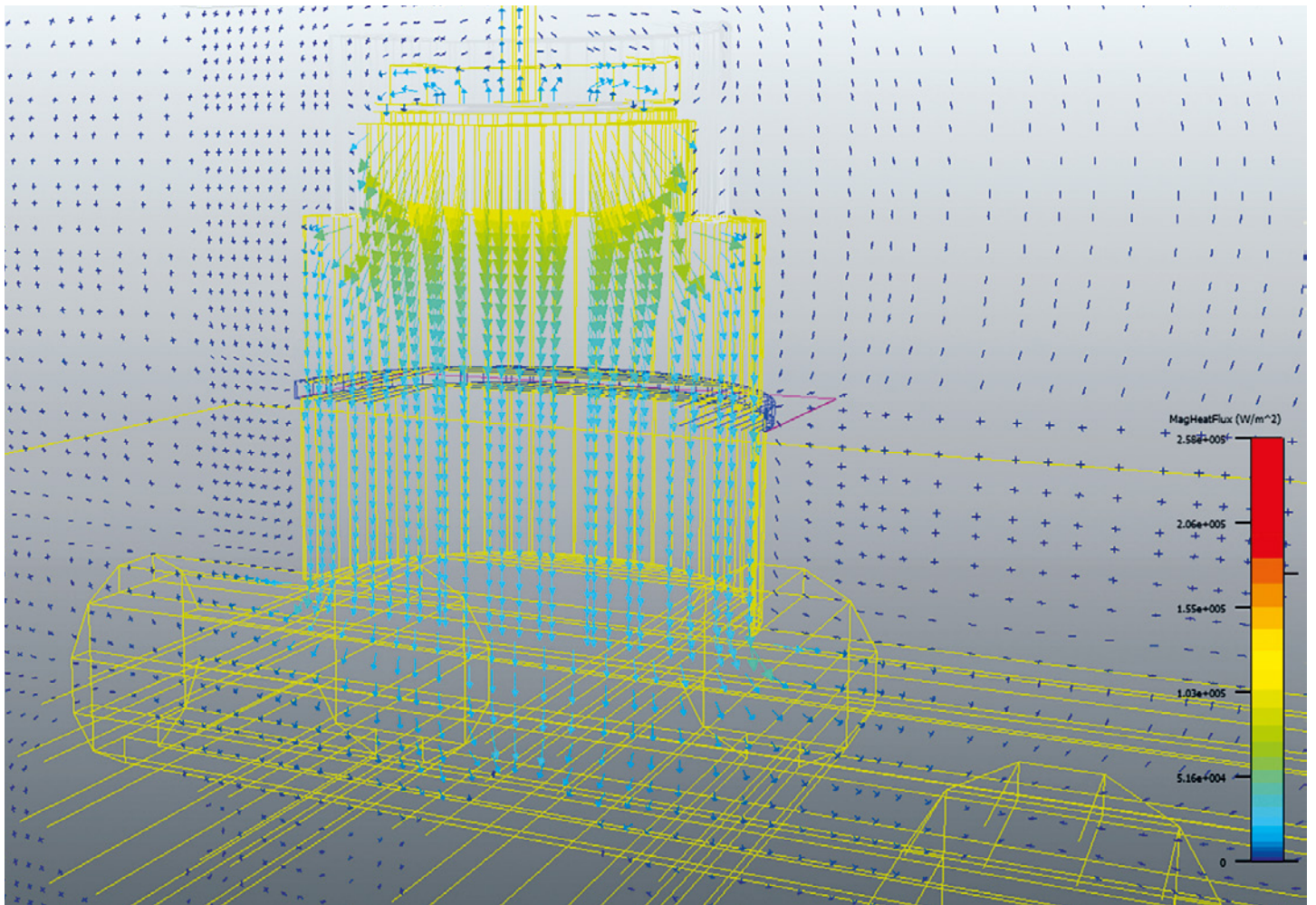


Figure 3. Heat Flux Vectors through DynTIM Sample and into Cold Plate

For some materials big deviations are seen between thermal conductivity values obtained by different methods, producing results that differ by >100%. The different methods show different levels of uncertainty. With the exception of Material B, for which only two thicknesses were available, DynTIM has the smallest error bands (shown in green in Table 1) while either the TIMA system or the Laser Flash exhibited the highest uncertainty (shown in red in Table 1). The DynTIM results agree very well with results obtained with the TIMA instrument, which like DynTIM conforms to ASTM-D5470 measurement standard. On the other hand the measurement results using TPS and Laser Flash in some cases did not even overlap with the DynTIM/TIMA results within their respective error bounds.

The evaluation of the DynTIM measurements assumes that the total power P generated in the diode actually flows through the TIM sample. To ensure this, the diode is embedded in a block of hard plastic material with low thermal conductivity. However, since there are no perfect thermal

The DynTIM tester has proven a valuable add-on to our T3Ster, enabling us to measure not only the thermal conductivity of TIMs but also of other semiconductor packaging materials like mold compound and die attach adhesives.

**Dirk Schweitzer, Senior Staff Engineer
Simulation, Infineon Technologies AG**

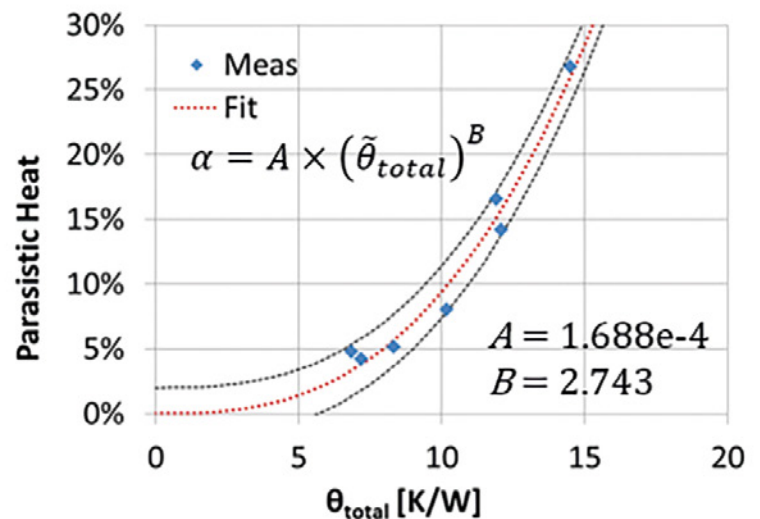
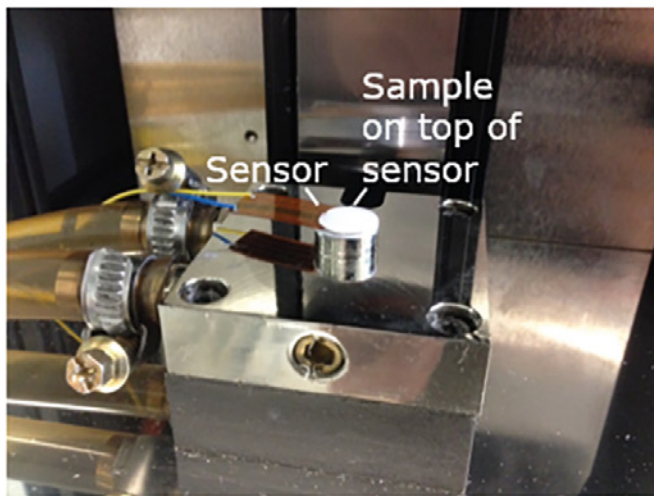


Figure 4. Sample on top of Sensor (left), and % Parastic Heat vs Total Thermal Resistance (right)

insulators we have to assume that at least a small portion α of the heat will not pass through the sample but flow through other structures of the tester. We call this portion the parasitic heat flow. Calibrating for the parasitic heat loss can further increase the accuracy of the DynTIM measurements, and so is of significant interest to Infineon. To determine the amount of parasitic heat we performed a series of measurements with a heat-flux sensor positioned with the sample in the heat-flow path of the DynTIM-tester.

The commercially available sensor internally consists of a large number of PN-junctions connected in series to create a thermopile, embedded in an epoxy matrix between two copper sheets. If heat flows through the sensor the thermopile generates a voltage (Seebeck effect) which is directly proportional to the heat flow density. This allows the proportion of the total heat flow $(1-\alpha)$ that passes through the sample to be measured directly. This is shown visually using a FloTHERM simulation in Figure 3.

The experimental setup showing the lower liquid-cooled cold plate and heat flux column are shown in Figure 4 (left). By increasing the thermal resistance of the sample under test it is possible to increase the parasitic heat losses as a proportion of the total heat dissipated by the diode heater, and detect what these heat losses are by measuring the remaining heat that passes through the sample. The inferred parasitic heat loss is found to increase exponentially with increasing total resistance as shown in Figure 4 (right).

Given how good the fit is, not only can we eliminate the error due to the parasitic

heat loss in this way, at the same time we can extend the measurement range of the DynTIM tester beyond the recommended limit of 10 K/W. Our aim is to redo the error analysis for DynTIM taking into account additional influences not considered so far, and to explore the method further by means of simulation to better understand the impact of all details of the measurement setup on the results.

Understanding the nature of the parasitic losses, coupled with the ability to correct for them will make DynTIM a far more accurate system and extend the range of materials it can be applied to. This accuracy, combined with versatility make it one of the most useful pieces of thermal conductivity measurement equipment available for TIMs.

References:

- [1] Evaluation of Characterization Methods for Solid Thermal Interface Materials, Fabian Streb, Dirk Schweitzer, Infineon Technologies AG; Thomas Lampke, Technische Universitat Chemnitz and Manfred Mengel. 10.1109/SEMI-THERM.2017.7896940
- [2] Characterization Methods for Solid Thermal Interface Materials, Fabian Streb, Dirk Schweitzer, Infineon Technologies AG; Thomas Lampke, Technische Universitat Chemnitz and Manfred Mengel. DOI (identifier) 10.1109/TCPMT.2017.274823 (To be published later in 2017)

Peristaltic Pump Electronics Thermal Design with FloTHERM XT



Fluid Technology Group

By Michael Clements, CEng MIET, Electronics Engineer, Watson-Marlow Fluid Technology Group

Watson-Marlow Fluid Technology Group produce a range of chemical metering pumps. Their Qdos pumps are specified to replace diaphragm and other designs of metering pump as a result of their precision flow rates and significantly lower maintenance costs when handling abrasive or corrosive fluids. The success of these pumps and their technology makes them the ideal choice for rugged applications.

One such application for Qdos pumps is metering chemical coatings on to seeds, with the pump mounted on the seed planter towed behind a tractor. Seed treatment is now common practice for agriculture and horticulture industries, where the thick fluid coating may contain growth promoters, inert carriers or fertilizers, as well as antimicrobial or antifungal treatments.

The requirement to deploy Qdos pumps externally has introduced some new design complexity. As all Watson-Marlow pumps are mains powered, the mains powered 48V 200W internal Switched Mode Power Supply Unit (SMPSU) had to be replaced by a 12/24V DC input power supply.

The original power supply was constrained by the footprint of the mains SMPSU, with an initial heatsink design intended to ensure that the power supply components would be kept cool enough at the output power and input currents required for a target 90% efficiency, giving a thermal load of 20W. The pump housing is non-optimal for cooling due to its construction of glass-loaded plastic and also contains a brushless DC motor that can vary between 70°C and 90°C surface temperature at a maximum ambient of 40°C. The initial heatsink design looked reasonable, but could not be evaluated without an expensive machined prototype being manufactured.

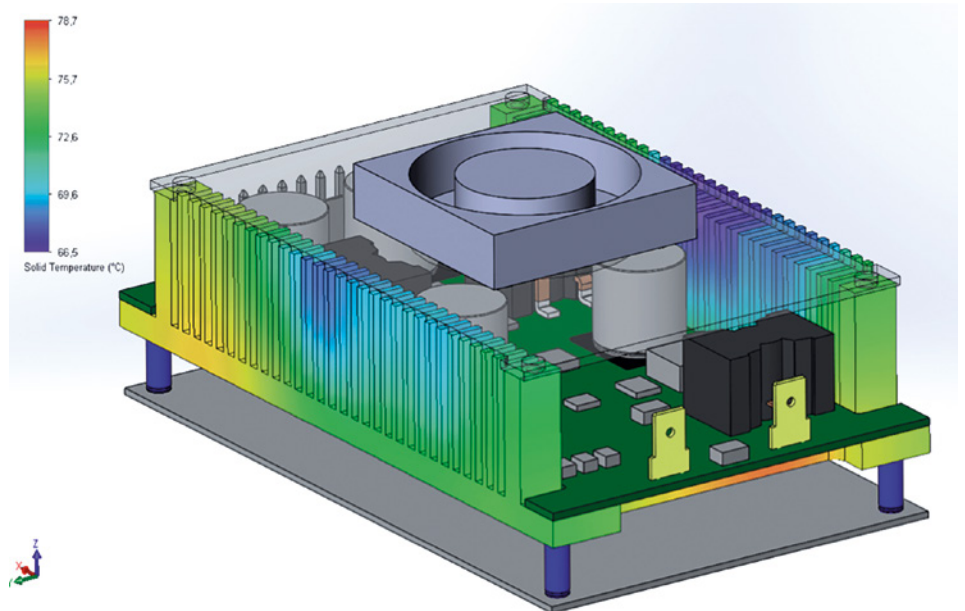


Figure 1. Original Watson-Marlow design as evaluated by IC Blue

Previous experience of FloTHERM, coupled with use of PADS PCB design software suggested that FloTHERM XT for PADS would be the best tool for evaluating heatsink designs.

Working with the Mentor business partner, IC Blue, Watson-Marlow evaluated the original design using FloTHERM XT for

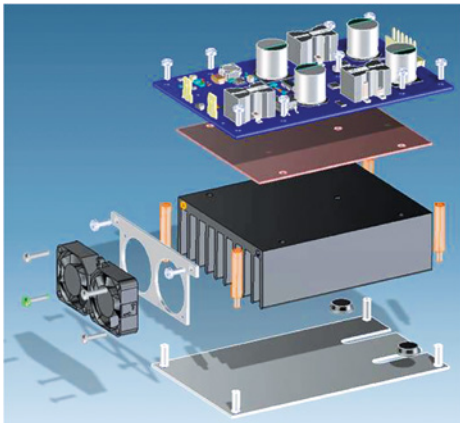


Figure 2. Dual Fan Extruded Heatsink Design showing Complexity of PCB Imported from PADS

PADS, discovering that the heatsink did not work well, with excessive temperatures shown on the components, as well as being prohibitively expensive to machine, requiring a large number of fins.

Based on the success of the evaluation work by IC Blue, Watson-Marlow were able to make a business case to purchase FloTHERM XT for PADS to be used by their own development team. The purchasing decision was used to great effect, enabling a completely redesigned heatsink utilising dual 30mm fans and a standard heatsink extrusion, with the DC power supply meeting the cost and size target, as well as matching the original mains SMPSU, shown in Figure 2.

Throughout this development work, Watson-Marlow were able to take component placement, board design and power data, directly from PADS (Figure 3) into FloTHERM XT in a smooth and efficient manner. As a result, FloTHERM XT simulations were fully synchronized with the PCB layout and circuit design, without thermal risks. Watson-Marlow also use PTC Creo for their mechanical design, and were able to read native Creo geometry directly into FloTHERM XT for PADS, allowing other designs of heatsink to be incorporated directly and used without modification or further simplification.

With this workflow, Watson-Marlow used FloTHERM XT for PADS to undertake many further investigations, re-designing the heatsink to a form that can be cast to save costs over the extruded part. They were also able to optimize air flow paths through the cast heatsink to achieve the equivalent cooling performance of the above dual fan design, but using a single 30mm fan resulting in further cost savings. Two of the many variants studied are shown in Figure

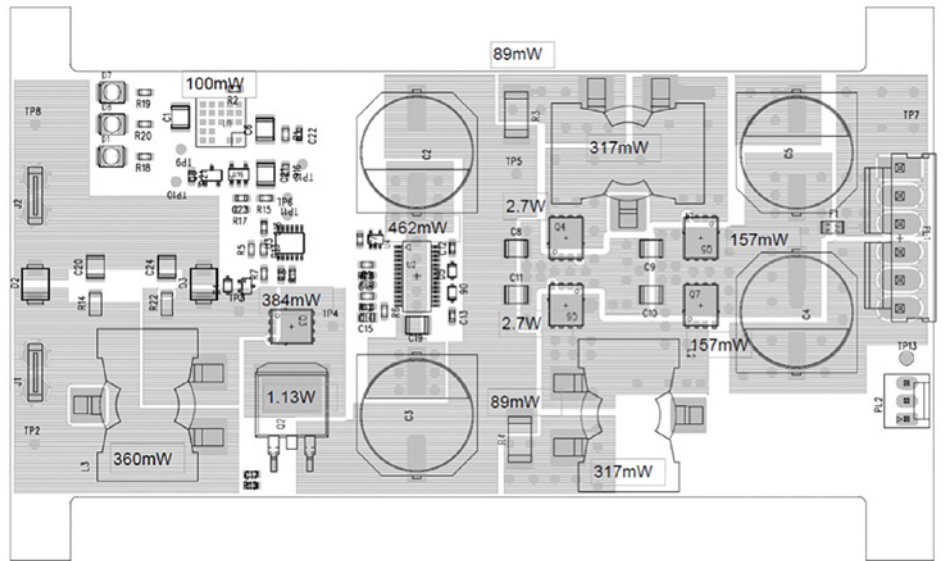


Figure 3. PCB component layout drawing from PADS

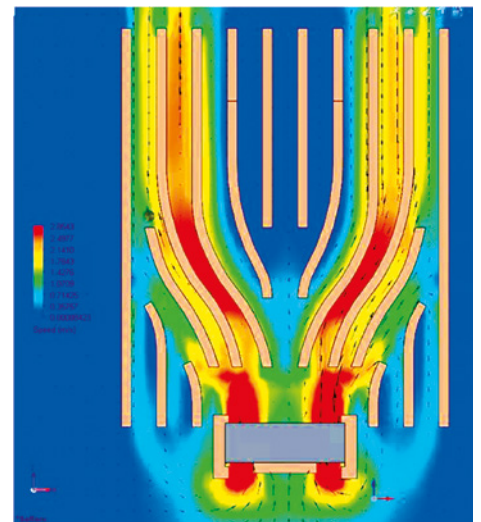
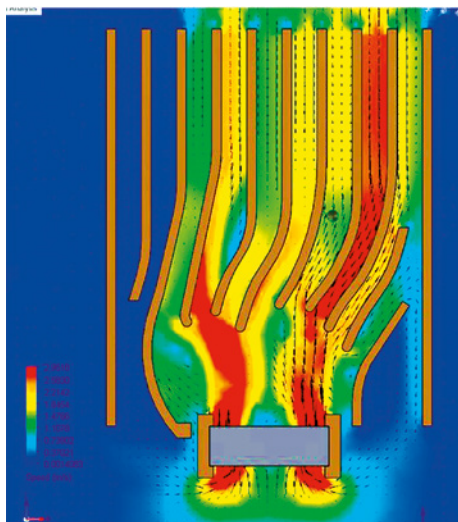


Figure 4. Preliminary Designs of Cast Heatsink Evaluated by Watson Marlow

4, indicating how complex the interaction is between the flow exhausting the fan and passing along the heatsink fins.

The success of this project, which has enabled Watson-Marlow to produce an efficient and effectively powered DC dosing pump, has also opened up new markets, for example, in solar powered pumps for remote applications where mains power is not available. Examples of this application are for waste water treatment plants in remote locations or deployed directly into the PLC-BUS for use in factory automation applications.



Team Bath Racing Takes to the Track

with Improved Thermal Performance

By Marios Mouzouras, Team Bath Racing

At Team Bath Racing, we are a group of undergraduate engineers at the University of Bath who, each year design and build our own single-seat open wheeled race car to enter into Formula Student competitions around the world.

We started working on the project as 3rd year students. Working as a team to design a race car from scratch as part of a design and business project which contributes to our degrees. We then take these designs to compete in the Class 2 design event at Silverstone in the United Kingdom where lessons are learnt and are used to develop the design further. As we enter our final year of engineering study, manufacture of the car begins and we watch our designs become a reality.

In the final year of the project we design the thermal management system for the car, after some research we decided to use FloMASTER as part of the design process. The ultimate goal was to use FloMASTER to create a representative transient thermal model of the vehicle's cooling and lubrication system. This would include the engine, turbocharger, radiators, pumps, piping, header tanks, oil cooler, and fans. To begin the process of the design, maximum temperature boundary conditions were set and then several experiments were conducted to obtain the necessary inputs for the transient model.

Tests were performed including in-house dynamometer to quantify the heat transfers taking place at each engine RPM and torque. Then an outdoor air flow test was performed to determine the relationship between the air flow through the radiators and the vehicle's speed with fans on or off. Finally, a coast down test conducted to determine the vehicle rolling and drag resistance coefficients to develop an engine torque model to match the engine heat transfer against torque during vehicle operation. How these tests fit into the creation of the thermal model is shown Figure 1.

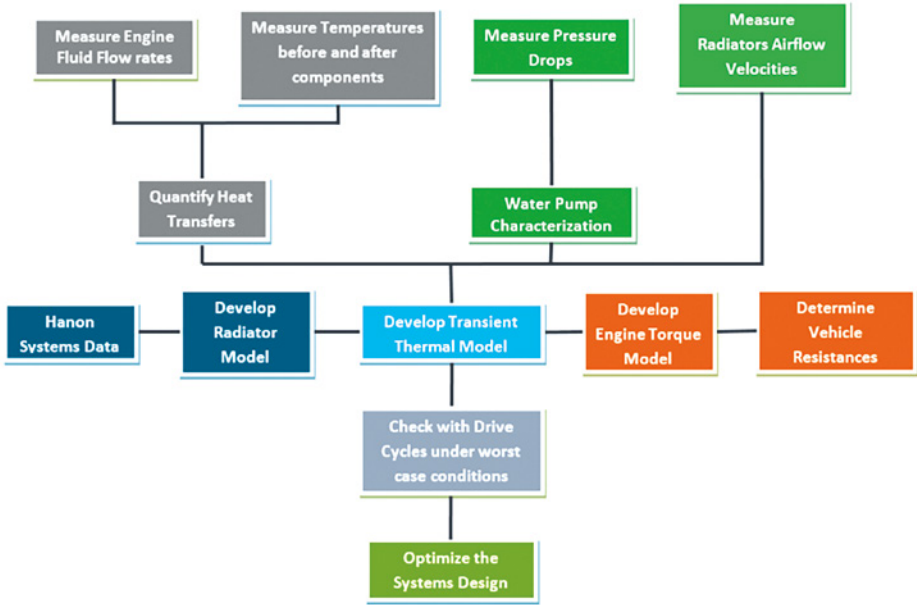


Figure 1. TBR Transient Model Design Workflow

With the data collected, the next step was to create a radiator model using both the fin and tube geometry of the radiator and the manufacturer's performance data. The learning curve was easy, and a model was easily produced compared to the pre-existing methods (MATLAB). The results showed a good response with a change in coolant flow rate, but had an increasing discrepancy with an increase in air flow velocity. This issue was mostly likely caused by error with the longitudinal and transverse pitch of the tubes stating that the values are very small. The values for different pitches were tested and a relationship was identified that as the values decreased, the heat rejections increased. Experiments were made by switching from

Status	Air Flow Face Velocity [m/s]	Air Mass Flow [kg/s] $\rho \cdot V \cdot A$	Heat Rejection [kW]					Maximum% Error
			Coolant Flow Rate [l/min]					
			5	10	15	20	30	
Actual	2	0.175	7.739	8.772	9.168	9.376	9.593	1.12561
Model			7.709365	8.870739	9.118235	9.362359	9.609325	
Actual	4	0.35	11.54	14.33	15.52	16.18	16.88	0.27477
Model			11.54212	14.32238	15.50826	16.22446	16.87317	
Actual	6	0.52	13.62	18	20.02	21.18	22.46	0.80299
Model			13.7137	18.03974	20.1389	21.35007	22.5902	
Actual	8	0.699	15.01	20.82	23.69	25.38	27.28	0.26864
Model			15.05032	20.79624	23.7308	25.40707	27.32277	
Actual	10	0.873	15.91	22.85	26.45	28.62	31.12	0.21858
Model			15.89765	22.87429	26.50781	28.56353	31.12781	

Table 1. Heat Rejection Versus Coolant and Air Flow Rates

Status	Air Flow Face Velocity [m/s]	Air Mass Flow [kg/s]	Coolant side dP [kPa]					Maximum% Error
			Coolant Flow Rate [l/min]					
			5	10	15	20	30	
Actual	2	0.175	0.4739	1.502	3.172	5.409	11.53	6.66578
Model			0.46938	1.60212	3.3472	5.70391	12.2398	
Actual	4	0.35	0.4851	1.507	3.177	5.414	11.53	5.94536
Model			0.467095	1.59578	3.33611	5.68809	12.2155	
Actual	6	0.52	0.4927	1.512	3.182	5.42	11.54	5.69237
Model			0.465929	1.59173	3.32845	5.67672	12.1969	
Actual	8	0.699	0.4985	1.516	3.188	5.425	11.54	6.668205
Model			0.465259	1.58887	3.32274	5.66799	12.1818	
Actual	10	0.873	0.5026	1.516	3.192	5.43	11.55	7.509948
Model			0.464855	1.58681	3.31848	5.66138	12.1699	

Table 2. Coolant Pressure Drops Versus Coolant Flow Rates

cross flow heat exchangers to other heat exchanger models in FloMASTER. It was then determined that the best results were obtained using the thermal heat exchanger which had a 1.13% error compared to actual data. In addition, the trends when increasing coolant flow rate or air flow rates were both as expected. There were small differences at the 6 to 10 m/s air flow velocities, because the fixed time step for the air mass flow gave a maximum of 0.005 kg/s difference between modeled and actual which is shown in Table 1.

It was also important to test the pressure losses as shown in Table 2. There was an anomalous change in pressure drop observed from the experimental data. In the experimental case of 2 m/s of air flow, the pressure drops from 54.91kPa to 52.33kPa with an increase in coolant flow rate and then starts increasing with high air flow rates. This was not captured by the model which instead predicted a constant increase as flow rates increased which followed the rest of the data sets as expected.

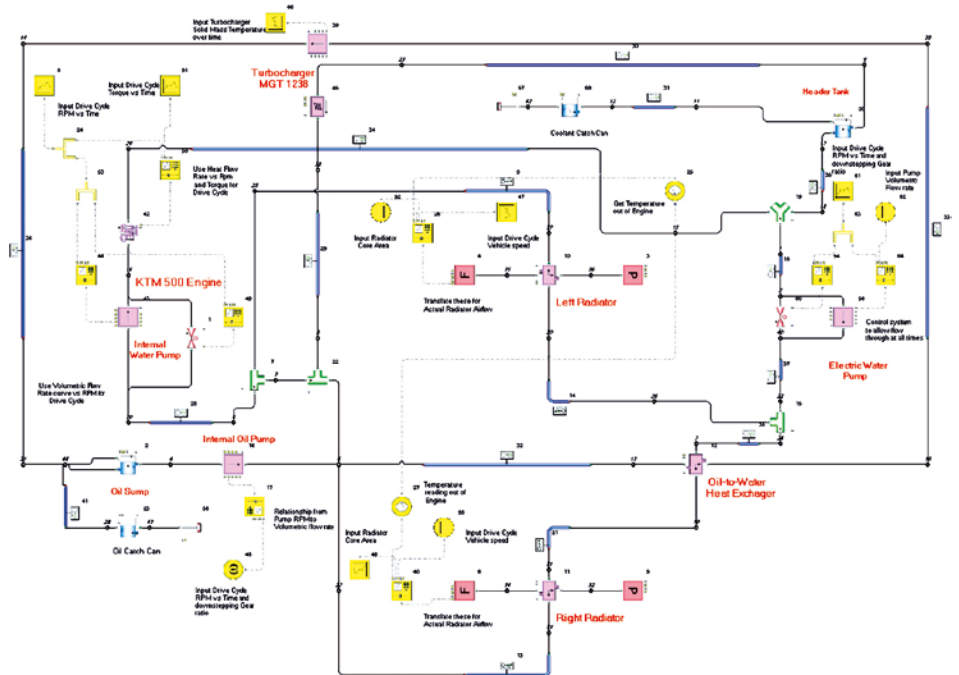


Figure 2. Team Bath Racing Transient Model Schematic in FloMASTER

A similar accuracy was observed on the coolant side, with an increase in pressure drop with an increase in coolant flow rates. For constant coolant flow rates the pressure drop for the actual data increased with an increase in air flow velocity, whereas for the model, the opposite was happening but at a much smaller rate.

Overall though, the heat duties and pressure drops had a very small error between the modeled and actual data. The heat duty's maximum error was 1.12% while for the pressure drops, the maximum error was 7.6%.

With the radiator model completed, the rest of the components were then modeled using a combination of experimental data obtained through testing and logged data from last year's endurance event at Silverstone. This included crucial information such as engine RPM, vehicle speed, and time. The completed model is shown in Figure 2.

TBR16's car was first modeled and validated using the coolant temperatures logged from the event. The maximum coolant temperature was matched with the time needed for the coolant to reach a steady-state being very similar. One difference was the rate at which the coolant's temperature increases being slightly different. Although, half way through the endurance race, there is a compulsory engine shut-down period where there is a driver change. No coolant temperature data was logged during that period, but the model predicted a larger temperature drop. This proved that the model is reliable and can be used to model TBR17's cooling and lubrication system as shown in Figure 3.

In addition, a number of tests were completed to optimize the system such as testing various radiator core sizes at different ambient temperatures. Additionally, running with a single radiator at the event instead of two, having one unexpected broken radiator during the endurance race, checking different size oil coolers and their position in the cooling system, fan sizing, Electric water pump sizing, pipe diameter selection, and some control strategies.

With the help of FloMASTER we were able to reduce the cost, time and resources needed to physically test all these aspects and a model was set up for future years to benefit as well. This also saved some weight from the car and helped us to better understand how the cooling and lubrication system works.

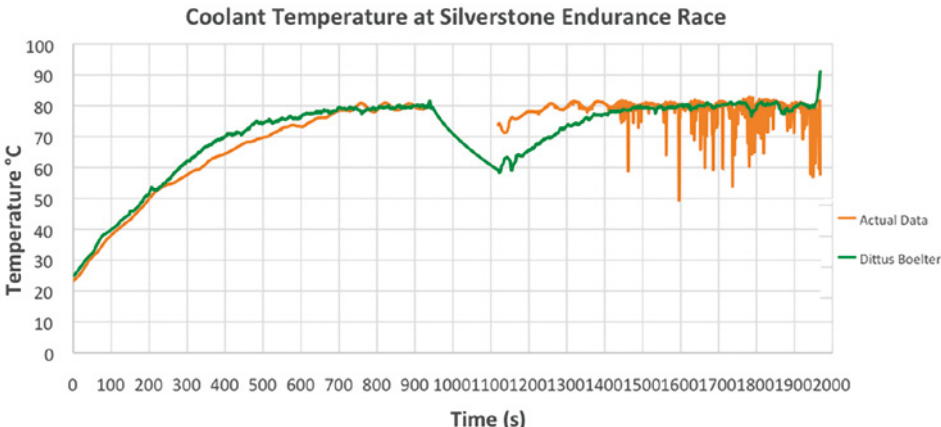


Figure 3. FloMASTER Predicted Coolant Temperature Versus Test Data



Technion Leverages FloEFD to **Validate Versatile Transonic Micro-turbine Test Rig**



By Beni Cukurel, Assistant Professor, Technion-Israel Institute Technology

The ability to experimentally investigate turbine profile performance has been an area of interest for both academia and industry for a long time. While there is a relatively large number of existing test rigs, Technion are using a unique closed loop continuous transonic turbine cascade design that offers potential benefits that existing rigs do not.

The goal of the planned rig is to create a platform for versatile test aided design of compressor stators and turbine nozzle guide vanes that will significantly reduce the turnaround time between different experimental set ups and provide researchers with a reliable tool that can simulate aero-thermal parameters relative to micro-turbomachinery. Over time, this will produce a large empirical database that can be used for CFD validation. Along these lines, the capabilities are geared towards convenient aerodynamic performance studies including improved transonic loss correlations, as well as evaluation of heat transfer characteristics under a broad range of thermal management (cooling) techniques.

The Technion Transonic Linear Cascade (TTLC) differs from the already existing facilities in several unique ways. The facility is designed to provide effortless modification of incidence and stagger angles (in the range of $\pm 20^\circ$), absent of any alterations to the test section. Furthermore, the considered vane geometry can be easily replaced allowing the quick swap design, which permits the cascade to be re-bladed without manufacturing or re-assembly of other components. At the exhaust, the cascade outlet can accommodate a large range of flow turning angles to address the needs of both compressor and turbine stators.

The test rig is also expected to operate continuously, providing periodic conditions over at least two passages surrounding an

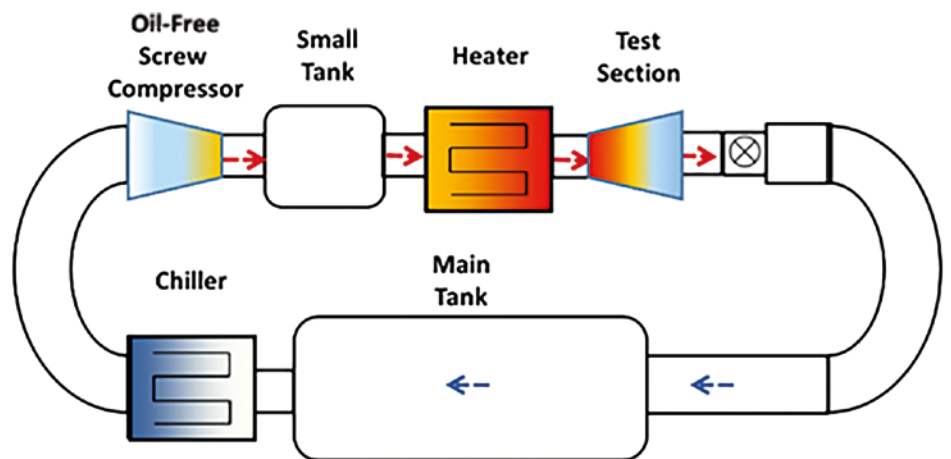


Figure 1. Closed-loop TTLC facility layout

airfoil. Due to mass flow limitations, TTLC has to implement a finite number of blades. Typical axial turbomachinery profiles can be effectively imitated by a set of individual blades.

Since it is near impossible to design a fixed-framed cascade for different sized vanes, similarity principles are used to scale the dimensions of the components through preservation of Re and M numbers. By independent control of these two non-dimensional quantities, different aerodynamic conditions can be simulated. Heat transfer characteristics of the hot gas section are also preserved to retain the gas to solid temperature ratio. Therefore, TTLC is required to maintain true $M-Re-T$ ratio independency.

FloEFD simulations give the researchers at Technion confidence that their test rig will perform as expected and when complete will be able to provide validation for future CFD simulations.

The cascade features a modular design that is able to accommodate a wide range of compressor stator and turbine vane configurations. The main test section sub-assemblies and the reference frame used are presented in Figure 2. The subsections include: an inlet (1), flow straightener and turbulence grid (2), controllable main frame frontboards (3), bladed test section (4), optical access window (5), rotating disks (6), controllable main frame tailboards (7) and an outlet (8). Technion utilized FloEFD to optimize the design of the inlet, frontboards and tailboards.

Inlet flow characteristics are crucial factor for the test section performance. The flow enters the test rig through a standard 6" diameter flange, and the cross-sectional area is reduced by 28% in a linear fashion to provide flow in a high aspect ratio rectangular slot. The inlet is designed to produce attached uniform flow with minimal boundary layer thickness. This is achieved by the bellmouth shape with zero gradient solid boundary conditions where the air is expanded in the XY plane, while contracting in the XZ plane.

In this configuration, the Bell-Mehta guidelines describe the contraction plane profile, while the expansion shape is dictated by the linear area change. The design was tested using FloEFD. It utilizes a modified k-ε two-equation turbulence model (where turbulence intensity (*i*) is 2% and turbulence length scale (*l*) is 2mm) in association with immersed boundary Cartesian meshing technique, coupled with a two-scale wall function treatment. The average dimensionless wall distance (*yy+*) was 125. Since the entry length of the input pipe is less than 5 diameters, the incoming flow was assumed to be uniform. The simulations results are presented in Figure 3, and no observable separation is present in the flow path.

Honeycomb is a typical component for most wind tunnel designs due to its ability to negate cross-flow vortices, which

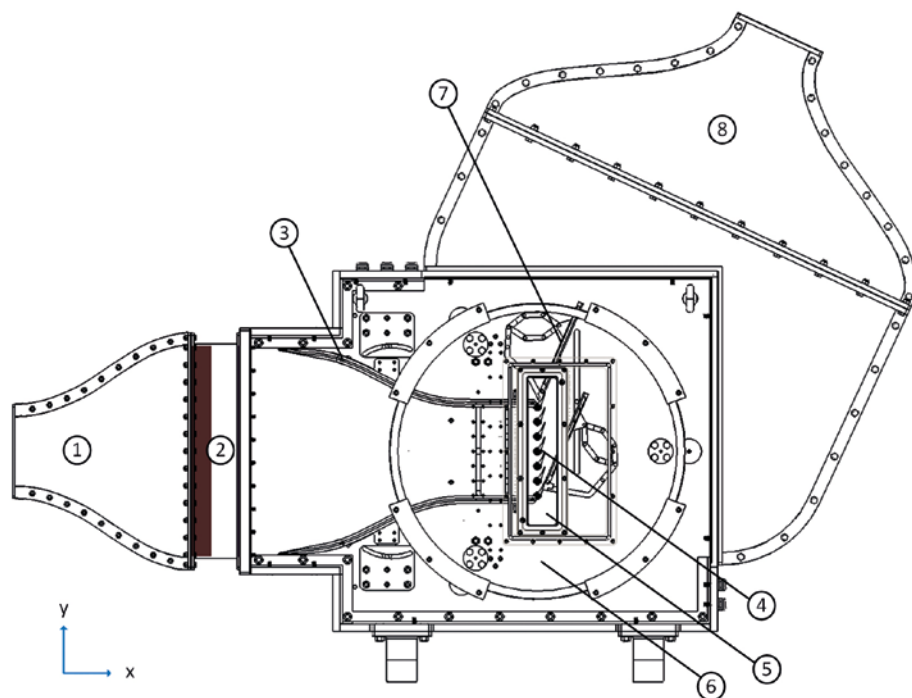


Figure 2. TTLC test section layout and reference frame

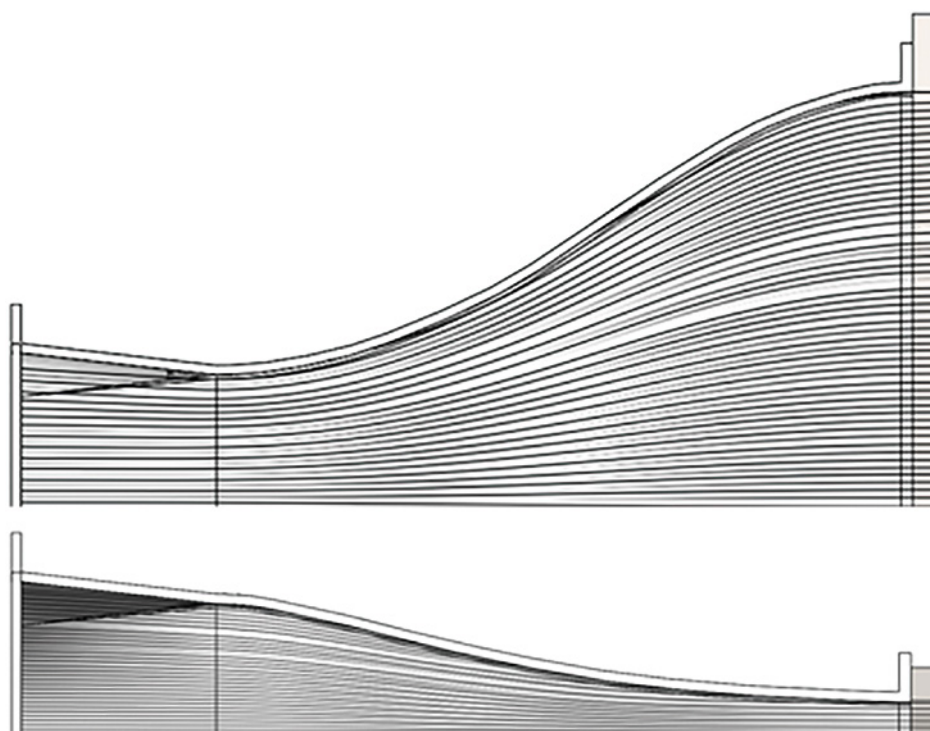


Figure 3. Flow lines across the inlet XY (top) and XZ (bottom) cross-sections

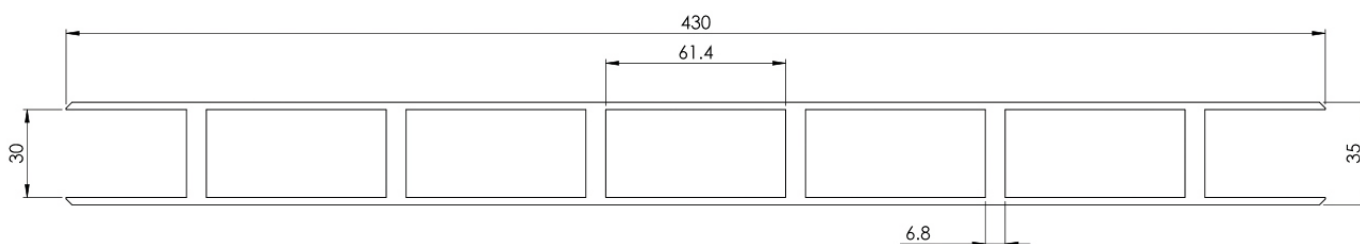


Figure 4. Turbulence grid design [mm]

are typically created due to upstream geometrical changes. Due to lateral turbulence inhabitation and pressure loss considerations, the implemented honeycomb design consists of 3.2 mm hexagonal aluminum cells with size to length ratio of 10. Lastly, in a typical turbomachine, different components have varying turbulence intensity levels. The first compressor stage usually has very little turbulence, whereas the last turbine stage experiences much higher levels due to the upstream combustor and stages. Therefore, in order to mimic the turbulence intensity of various engine relevant conditions, the cascade includes a modular turbulence grid, situated downstream of the honeycomb. A representative turbulence grid is depicted in Figure 4, simulating typical first turbine rotor vane's turbulence intensity of 5%.

The test section of the rig is mounted on a rotating disk to allow the blade positioning to have a variable incidence angle $\pm 20^\circ$ (Figure 5).

As a result of the disk rotation, the frontboards are to be maintained sealed and parallel for all incidence angles (Figure 6). Three modules keep the walls leak-proof and aligned for all conditions. Movable Teflon seals (A) keep the walls leak-proof, while the positioning mechanism (B) and leaf springs (C) translate the circular motion of the disks to parallel movement of the boards.

Two distinct configurations were considered during the frontboard design process - bellmouth curved and straight shaped. The simulation results are presented in Figure 7 for both shapes. Based on the reduced boundary layer development, the bellmouth configuration was selected as the frontboard design choice.

Nevertheless, the frontboards boundary layers may cause partial blockage of the far side test section passages, such that they no longer contribute to periodicity. An additional simulation was conducted to quantify the boundary layer thickness in the XY and XZ planes (Figure 8). At three chords upstream of the test section, the boundary layers in the XY plane cover 12% of the pitch in the two far most passages. In order to overcome this issue, a slanted boundary layer suction mechanism is implemented at the end of the frontboards before the test section at two chords upstream of the test section. The air is ingested (up to 4% of overall flow rate) through a thin slot, the mass flow of

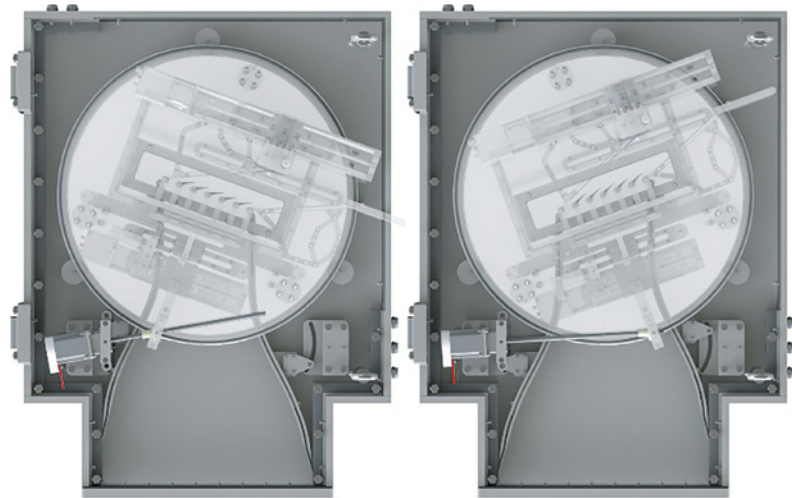


Figure 5. Disks rotation mechanism set to $\pm 20^\circ$

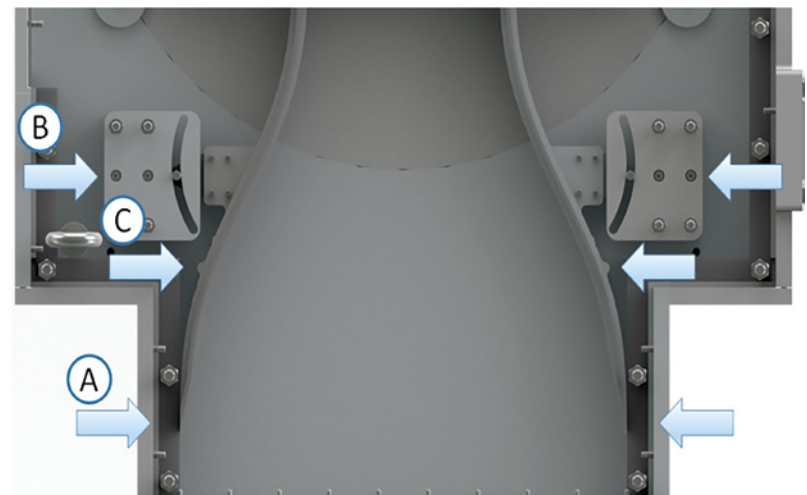


Figure 6. Frontboards sealing and support mechanisms

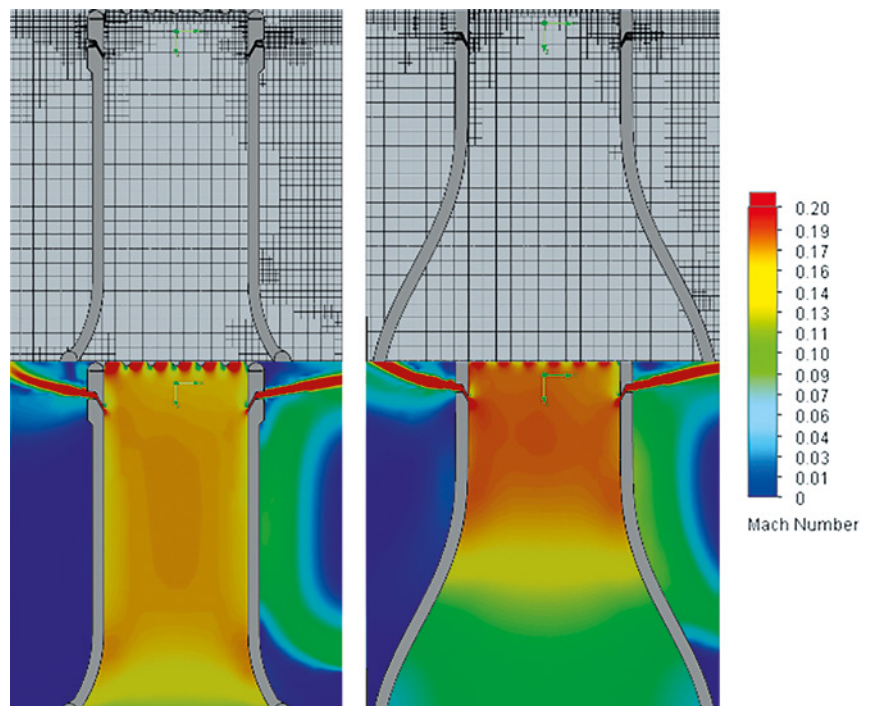


Figure 7. Frontboard XY flow simulation - mesh and results for straight frontboards (left) and bellmouth shaped frontboards (right)

which is regulated by an external valve. This mechanism can effectively purge the entire momentum deficit. However, it is challenging to suck the boundary layer in the XZ direction, while preserving the total air mass in the closed system. Nevertheless, at the immediate upstream of the test section, the top and bottom boundary layers cover 30% of the span in total, resulting in 2D flow in the remainder 70% of the blade height. Hence, the cascade is suitable towards aero-thermal investigation of various 2D airfoil profiles.

The flow behavior and the validity of the experimental data are heavily influenced by the span-wise flow characteristics upstream and downstream of the test section. The inlet boundary layer suction maintains relatively uniform 2-D pressure and velocity distributions across all six passages. Together with exit tailboard actuation, the final design can achieve downstream periodicity in all stagger and incidence angle configurations. According to FloEFD simulations under nominal design conditions, Figure 9 depicts stream-tubes colored by local Mach and total pressure distributions over the two middle passages. Periodicity is expected to be achieved within 5% in M distributions.

These FloEFD simulations give the researchers at Technion confidence that their test rig will perform as expected and when complete will be able to provide validation for future CFD simulations. This will in turn provide design engineers confidence in their simulations of evolutionary design changes in micro-turbomachinery.

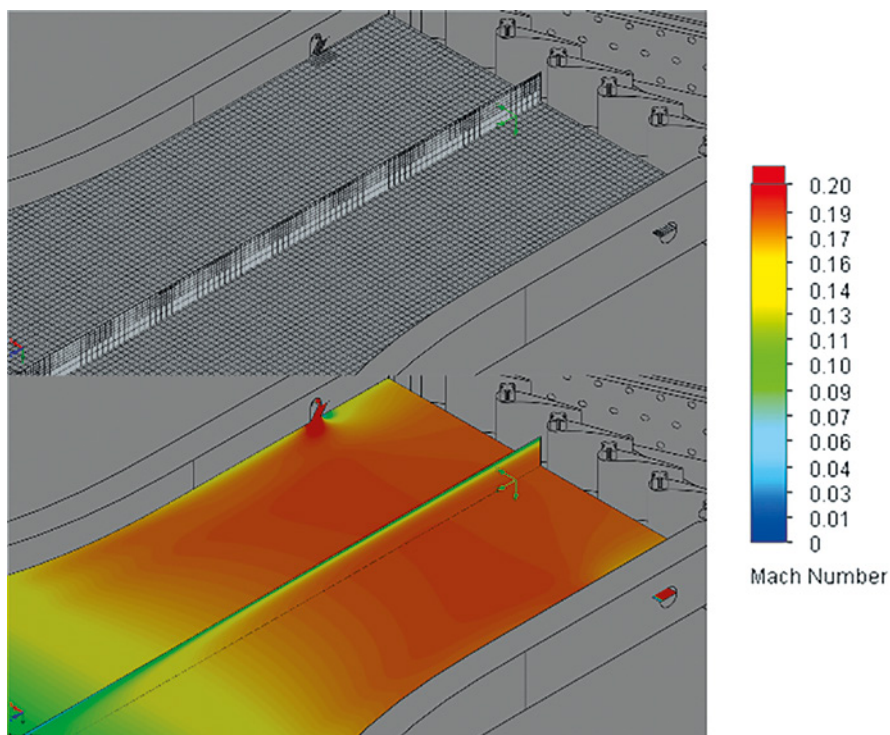


Figure 8. Frontboard 3D flow simulation - mesh and results for bellmouth shaped frontboards

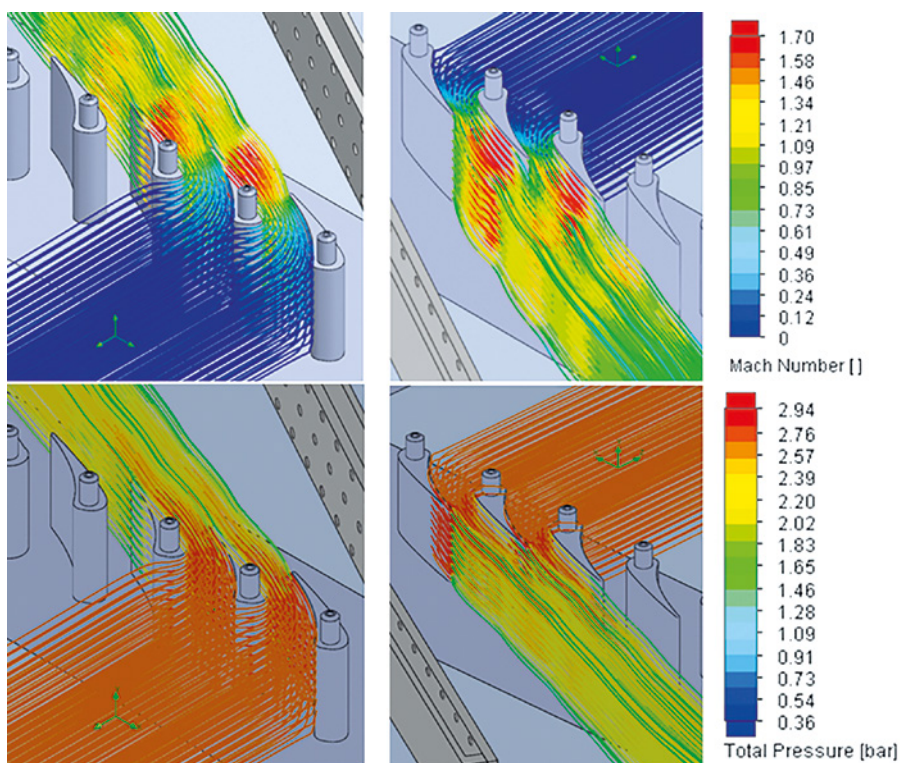


Figure 9. Mach No. (top) and total pressure (bottom) distribution in the streamlines

The Technion Turbo & Jet Engine Laboratory aims to conduct cutting-edge research and advanced development in the field of gas turbines for propulsion and power generation applications. The turbomachinery center mainly focuses its effort on the hot gas section, consisting of the combustor and the turbine. The scientific contributions are primarily applicable towards small scale engines, which are commonly used in distributed power generation, business jets, unmanned air vehicles, auxiliary power units, marine applications etc.

Keeping it Cool in Gas Turbines

By A.V. Rubekina, A.V. Ivanov, G.E. Dumnov, A.A. Sobachkin (Mentor Graphics Corp., Russia); K.V. Otryahina (PAO NPO Saturn, Russia).

One of the key problems in the design of advanced gas turbine engines is the development of effective cooling methods for the turbine vanes and blades. Due to competition and continuous improvement an increased complexity of cooling technology is required in the design of turbine engine parts. In view of the material and time costs for experimental research, CFD has been accepted by turbomachinery companies as one of the main methods for evaluating the performance of new designs. Industrial CFD applications range from classical single- and multi blade-row simulations in steady and transient mode to heat transfer and combustion chamber simulations.

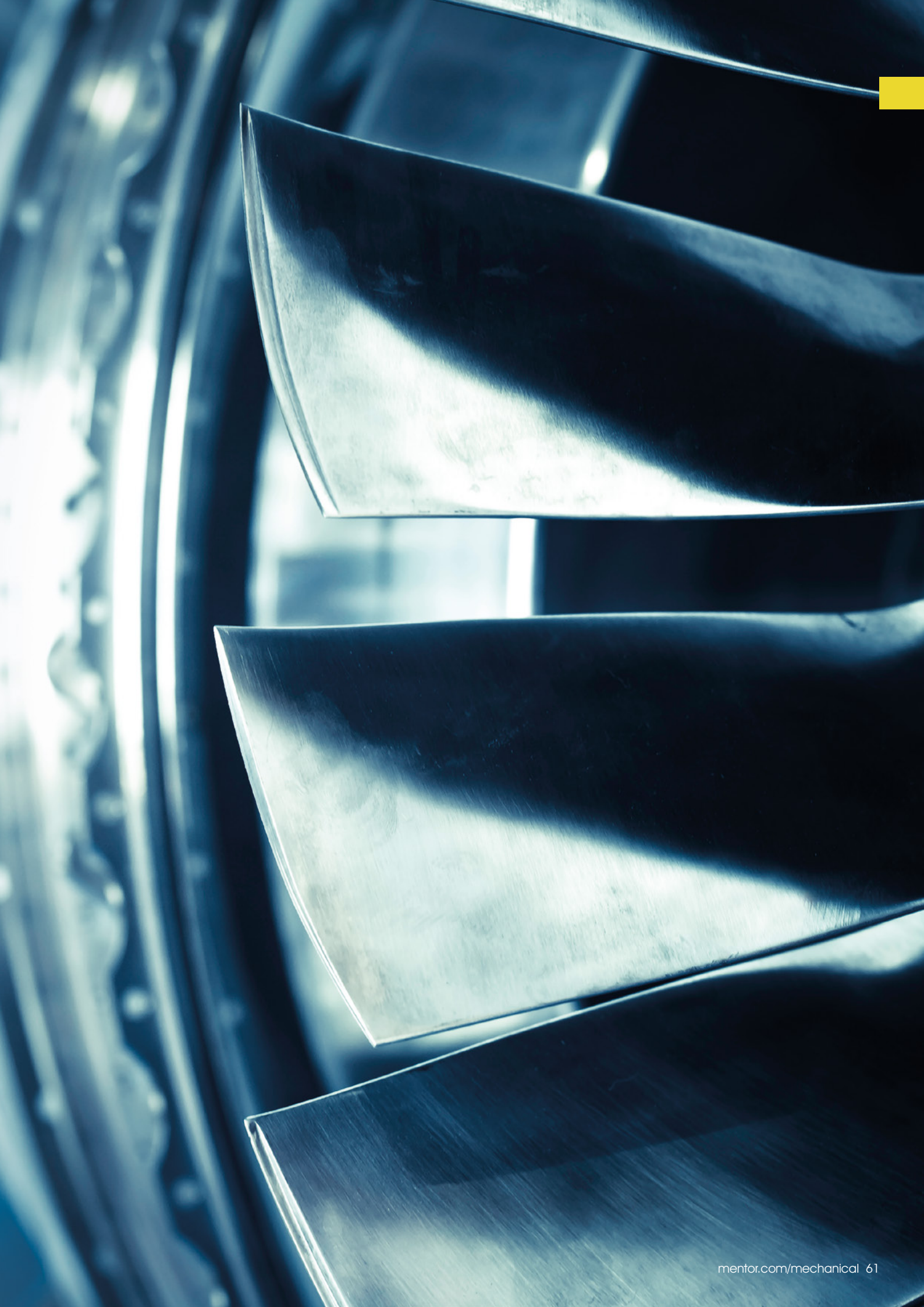
Depending on the type of machine, physical and geometrical effects have to be taken into account. A complicating factor is that it is necessary to carry out parametric studies considering several geometric options in the process of designing the cooling systems. This normally takes a lot of time to generate mesh models due to the mesh resolution required in the boundary layer. With this in mind, PAO NPO Saturn investigated FloEFD's accuracy for this application with the goal of taking advantage of its CAD embedded technology and automatic meshing to significantly reduce the overall simulation time and allow them to frontload their design process. The investigation looked at three different cases.

The first case is the NASA C3X Vane Experiment. This case consists of a 2D blade cascade consisting of three vanes characteristic of a first-stage turbine. Geometry parameters of vane and cooling channels were taken from Hylton et al (1983). Each of the vanes was cooled by an array of ten radial cooling holes. The vanes were fabricated of stainless steel, which has a relatively low thermal conductivity.

The cooling parameters such as average temperature and mass flow rate are presented in Table 1.

Three mesh configurations were analyzed. For coarse mesh M1 number of cells was about 25.500, for medium mesh M2~48.000, for fine mesh M4~121.400 cells. These meshes had the same topology, but basic mesh density was varied. Around the central vane all cells were additionally refined by two levels and into cooled channels by three levels.

The calculation results for each mesh are presented in Figure 2. Figures 3-4 show temperature and heat transfer coefficient distributions along surface of vane. Negative distances indicate the probe positions on the pressure side. Positive values indicate the suction side locations of temperature measurements. The peak in heat transfer coefficient distribution is observed on the suction side of the vane. This is due to the more rapid laminar-turbulent transition in boundary layer as compared to experiment where this transition was also observed but was smoother.



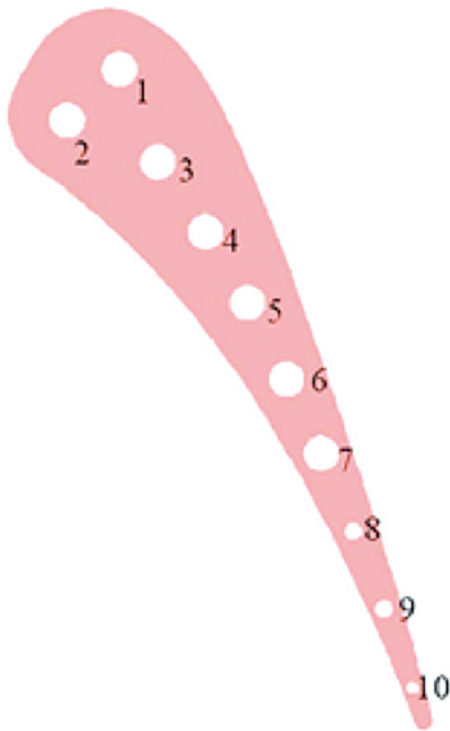


Figure 1. Vane section with ten cooling channels

Channel number	1	2	3	4	5	6	7	8	9	10
D, mm	6.3	6.3	6.3	6.3	6.3	6.3	6.3	3.1	3.1	3.1
G, g/sec	7.79	6.58	6.34	6.66	6.52	6.72	6.33	2.26	1.38	0.68
T, K	371	375	360	364	344.5	399	359	358	418	450

Table 1. Parameters of cooled channels

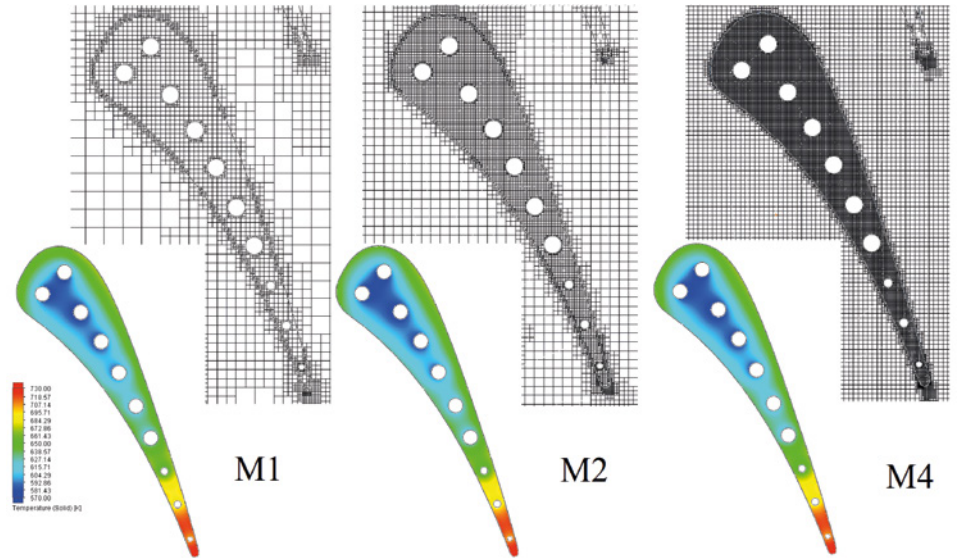


Figure 2. Temperature distribution computed for each mesh configuration

Maximum and average values of calculation discrepancies are showed in Table 2. The results obtained even for the coarse mesh have a good agreement with experimental data.

The second study consisted of a showerhead film cooled vane, five rows of staggered cylindrical cooling holes is used in Nasir et al (2008). The vane cascade consists of four full vanes and two partial vanes. The number of cooling holes on the stagnation region row is 17. Cooling flow is injected at 90° angle to the freestream and 45° angle to the span of the vane. Overview and dimensions of the test vane is presented in Figure 5.

The computational mesh with about 133,000 cells was used.

Figure 6 shows the local Mach number distributions on the vane without film cooling holes. It is plotted against non-dimensional surface distance s/C . The Mach number distribution varies smoothly along the pressure side. The flow on the suction side continuously accelerates up to the throat area ($s/C = 0.51$).

Figure 7 shows the distribution of the gas temperature (left) and cooling air streamlines with the Mach number distribution on the air-gas channel (right).

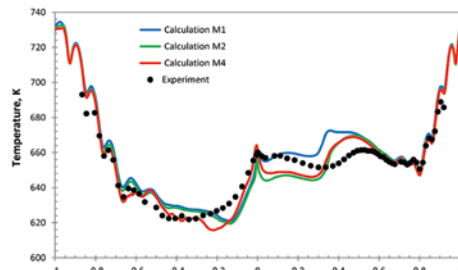


Figure 3. Comparison of calculations with measurements for temperature distribution

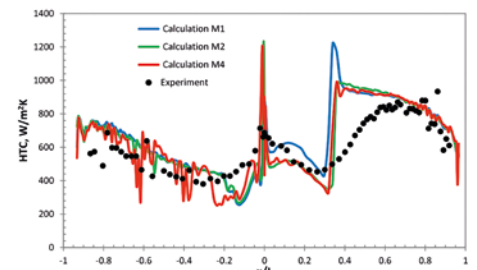


Figure 4. Comparison of calculations with measurements for heat transfer coefficient distribution

	Mesh (M1)		Mesh (M2)		Mesh (M4)	
	Suction Side	Pressure Side	Suction Side	Pressure Side	Suction Side	Pressure Side
Max. error, %	7.79	6.58	6.34	6.66	6.52	6.72
Aver. error, %	371	375	360	364	344.5	399

Table 2. Surface temperature calculation discrepancies

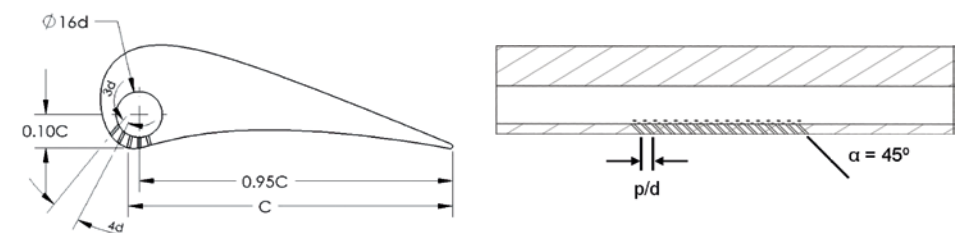


Figure 5. Profile view of showerhead film cooled vane (left) and section view of stagnation row of holes (right)

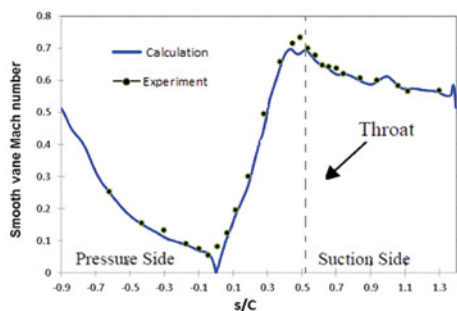


Figure 6. Comparison of computed and measured smooth vane Mach number

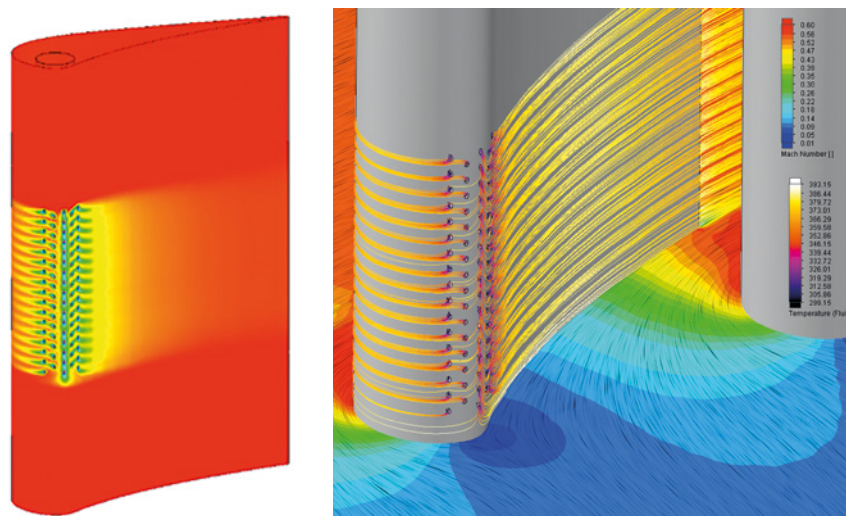


Figure 7. Gas temperature distribution (left) and cooling air streamlines with the Mach number distribution (right)

The final case is a rotor blade used by NPO Saturn. The detailed description of similar blade can be found in Vinogradov et al (2016). General view of the blade and the internal channels are shown in Figure 8. The blade is made of heat-resistant alloy ZS32. Ceramic coating (a thickness of 0.02-0.03 mm with thermal conductivity $\lambda=2-3$ W/(m·K)) serves to insulate components from large and prolonged heat loads by utilizing thermally insulating materials.

Relatively cold air is passed through the passages inside the turbine blade. Complicated internal cooling system includes serpentine channels with rib turbulators. Then coolant goes out the blade through holes located on the blade tip. The remaining coolant is ejected from the trailing edge of the profile.

As for previous test cases evaluation of the temperature distribution of the blade was made by means of conjugate heat transfer simulation. Ceramic heat barrier coating was taken account as the thermal resistance with equivalent parameters. Numerical simulation included modeling of mainstream gas flow, air flow through the internal channels of the blade as well as heat transfer in solid and between fluid and solid by convection. The computational mesh with about 944 000 cells was used.

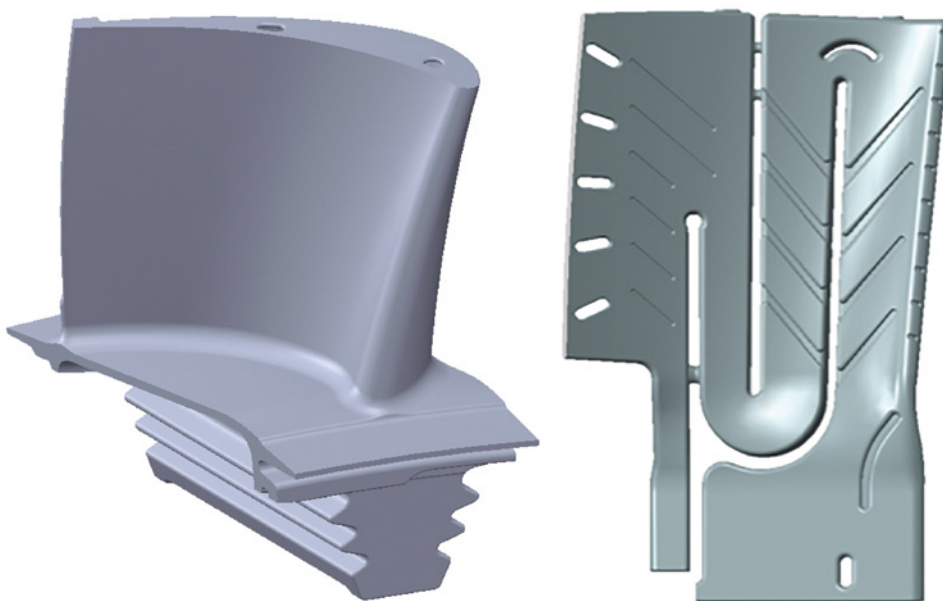


Figure 8. CAD model of simulated blade (left) and its internal passages (right)

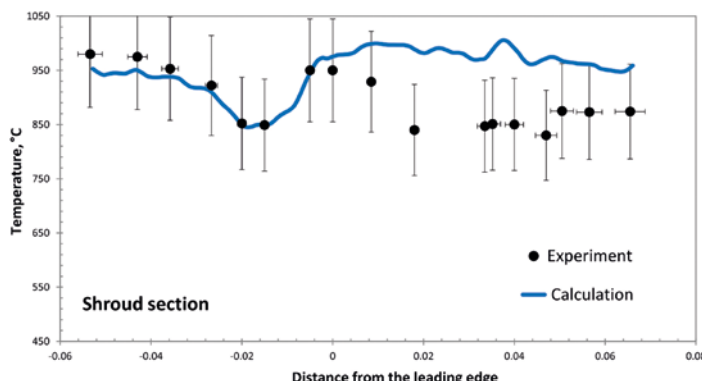
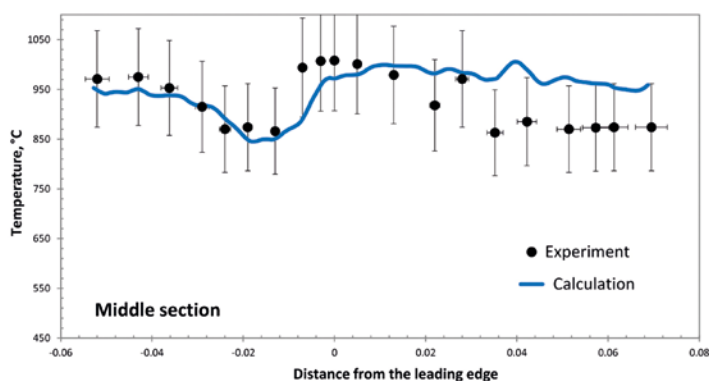


Figure 9. Comparison of computed and measured surface temperature along the profile in shroud section and middle section of the blade

Shroud and middle sections of the blade were taken for comparison of numerical simulations with experimental data (see Figure 9). Marked on the Figure range of ratio error is 10%. One can see that difference between computations and experimental data is within this ratio for pressure side of the blade both for shroud and middle section. For suction side of the blade agreement with the experimental data is a bit worse particularly in shroud section. Calculation discrepancies are estimated at the level of 15% there.

Shown in Figures 10 and 11 pressure and cooling air temperature distributions along flow streamlines as well as surface metal temperature field on both side of the blade are in a good concordance with qualitative evaluations.

Calculated gas mass flow rate through blade row is equal to 29.94 kg/sec. Mass flow rate through one blade is equal to 0.027 kg/sec. Caused by heat exchange with hot metal blade coolant air temperature increment is about 110°C. Obtained results are also in a good agreement with qualitative estimations.

Obtained computation results for these test models are in a good agreement with experimental data. The predicted blade temperature distribution and flow through the blade for industrial convective cooled turbine blade are also in a good agreement with available experimental data in the qualitative and quantitative aspects.

It shows that with FloEFD users can achieve acceptable accuracy on far coarser meshes when compared with traditional CFD approaches. Therefore computations of fluid flow and heat transfer for even complex 3D cases take relatively modest computational resources making FloEFD a useful CFD tool for engineering numerical simulation of heat transfer in vanes and blades.

This article is a summary of the paper: Using Modern CAD-Embedded CFD Code for Numerical Simulation of Heat Transfer in Vanes and Blades. A.V. Rubekina, A.V. Ivanov, G.E. Dumnov, A.A. Sobachkin, Mentor Graphics Corp., Russia; and K.V. Otryahina, PAO NPO Saturn, Russia

References

- [1] Hylton, L.D., Mihelc, M.S., Turner, E.R., Nealy, D.A., and York, R.E. (1983) 'Analytical and Experimental Evaluation of the Heat Transfer Distribution Over

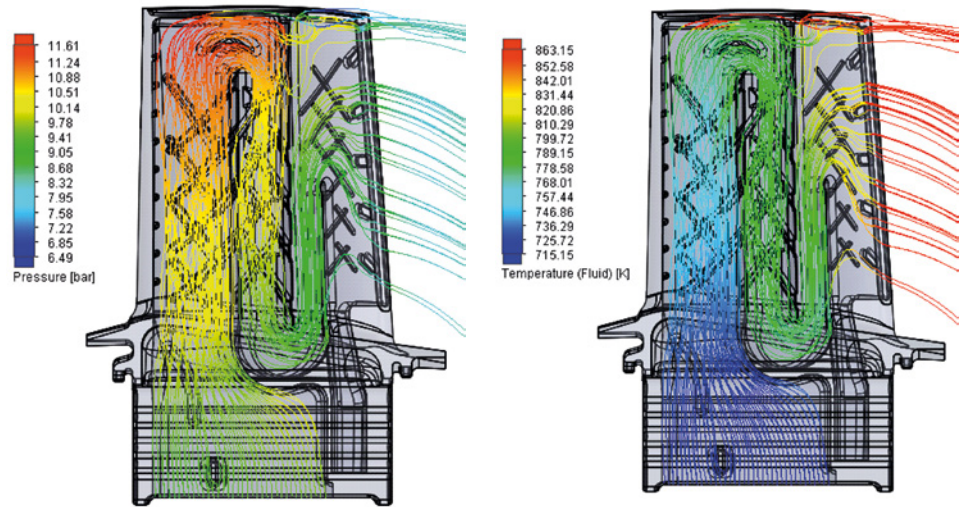


Figure 10. Flow streamlines colored by pressure (left) and the cooling air temperature (right) into passages

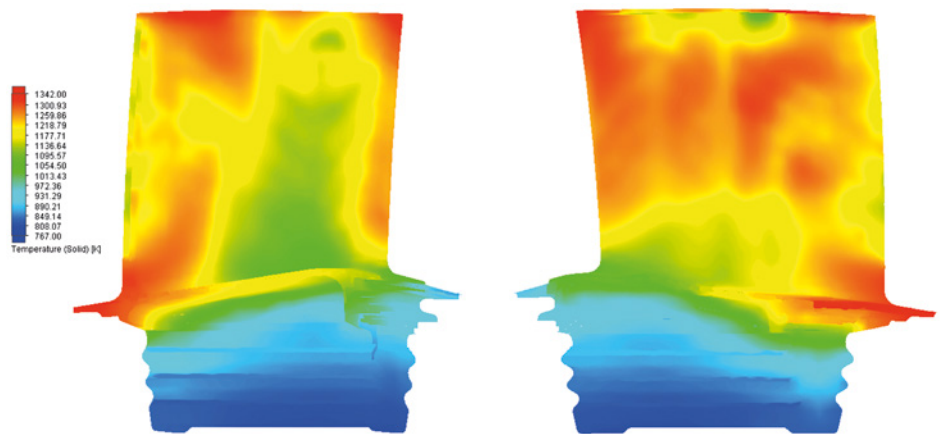


Figure 11. Distribution of solid temperature on the pressure side (left) and on the suction side (right)

the Surface of Turbine Vanes', NASA Paper No. CR-168015.

- [2] Nasir, S., Bolchoz, T., Ng, W.F., Zhang, L.J., Moon, H.K., Anthony, R.J. (2008) 'Showerhead Film Cooling Performance of a Turbine Vane at High Freestream Turbulence in a Transonic Cascade', ASME IM-ECE-2008-66528, 2008.
- [3] Sobachkin, A.A., Dumnov, G.E. (2013) 'Numerical Basis of CAD-Embedded CFD', Proceedings of NAFEMS World Congress NWC 2013, Austria, Salzburg, June 09-12, 2013.
- [4] Vinogradov, K.A., Kretinin, G.V., Otryahina, K.V., Didenko, R.A., Karelin, D.V., Shmotin, Y.N. (2016) 'Robust optimization of the HPT blade cooling and aerodynamic efficiency', ASME GT2016-56195, 2016.

Ask The GSS Expert



How does the Pressure Potential and the coordinate system effect the pressure in FloEFD?

For several application areas, it is crucial to consider the hydrostatic height, for example for the design of pumps or fans. For models of high geodetic head and/or for fluids with high density, the gravitational head is significant. It is important to understand how FloEFD works to avoid any mistakes.

Setting up a FloEFD project user may ask himself the following questions:

- Do I need to correct the environment pressure (to take into account the piezo pressure) for FloEFD models of a high geodetic head, if there are openings at different heights?
- Does FloEFD take into account gravitational head correctly?
- How do you define the pressure at these openings?
- My pressures are too low or too high in the equipment. Is it normal?

FloEFD takes into account the gravitational head when the "gravity" option is enabled. When the "Pressure potential" check box is selected, the specified static pressure is assumed to be piezometric pressure (Figure 1). The "Refer to the origin" option allows the definition of a user defined coordinate system for the reference point of pressure. If this box is unchecked, the global coordinate system is considered.

The hydrostatic pressure is defined as:

$$p(h) = \rho \cdot g \cdot h + p_0$$

The pressure at the origin of the Global Coordinate System (ambient pressure) is defined on the General Settings dialog box. FloEFD automatically adds the $\rho \cdot g \cdot h$ term to any Environment Pressure boundary condition.

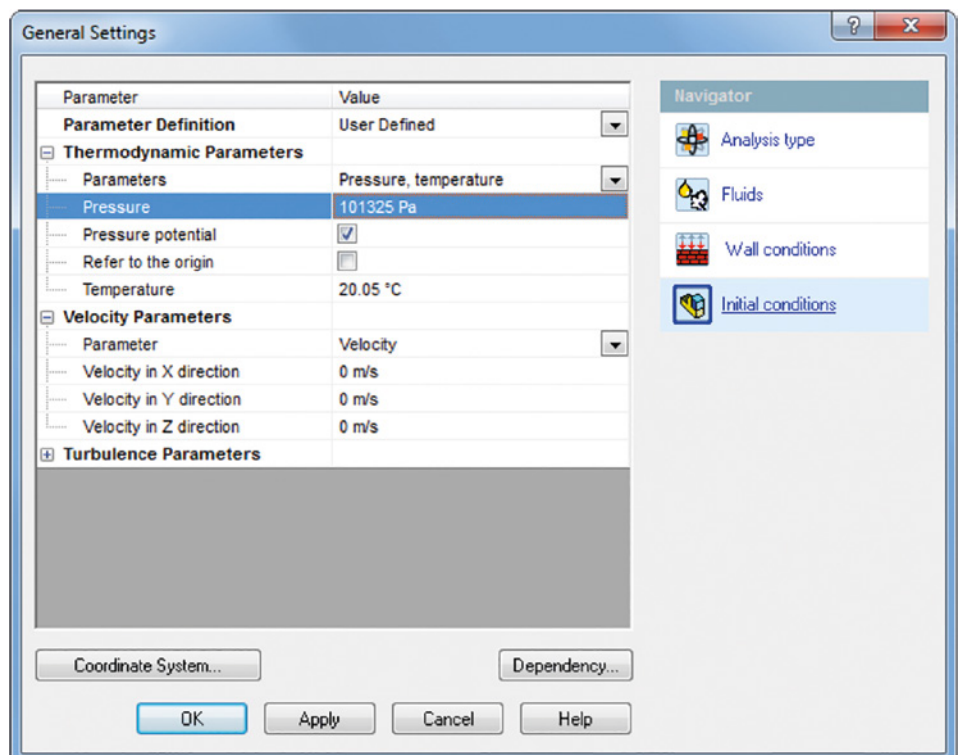


Figure 1. General, ambient settings

For example, a building with a height of 50 m and openings at a height of 10 m each. A boundary condition "ambient pressure" is specified for each opening with the value of the ambient pressure, for example 101325 Pa. The hydrostatic pressure must not be added manually, as this would wrongly increase the resulting pressure (Figure 2).

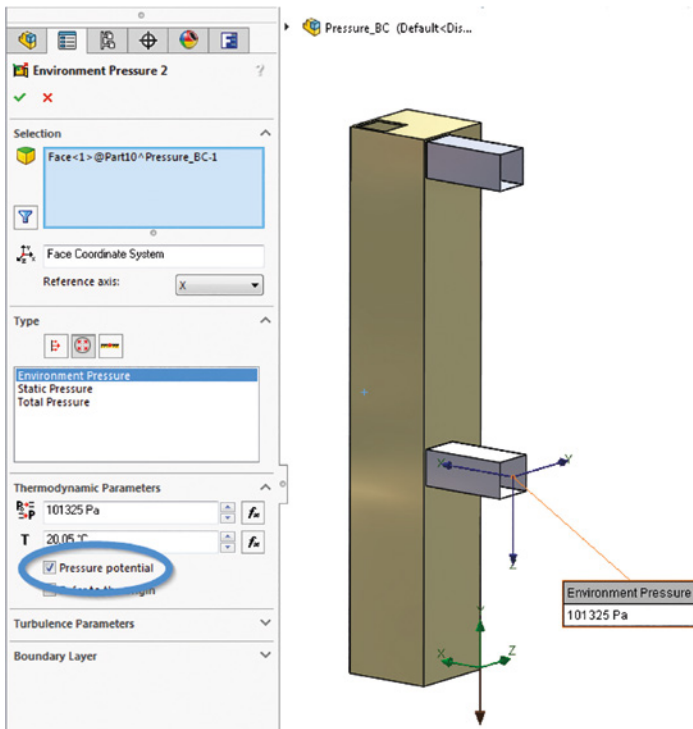


Figure 2. Pressure potential checkbox at pressure boundary condition

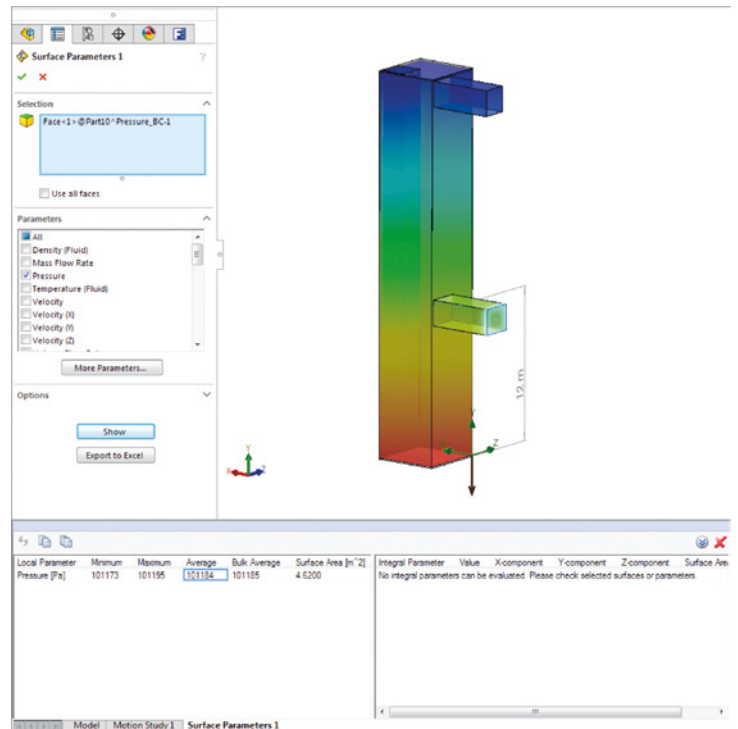


Figure 3. Pressure gradient for reference coordinate system at the bottom

A surface Goal "Total Pressure" on each of these openings' surface will show a value of $p = 101325 \text{ Pa} \pm \rho \cdot g \cdot h$ (This is to check and verify the validity of the data). The + or - sign determines the direction depending on the location of the Global Coordinate System.

The Surface parameter refers to the Total pressure. Notice, for the example shown in Figure 3, that the average value of total pressure is the reference pressure of 101325 Pa minus the $\rho \cdot g \cdot h$ term's value.

With an increasing height from the coordinate system, the resulting pressure decreases compared to the reference pressure (Figure 3).

With a decreasing height from the coordinate system, the resulting pressure increases compared to the reference pressure (Figure 4).

On the results side (Figure 5), due to the location of Global Coordinate System, the pressure field is changing. This difference in the pressure field can be important in some cases where your results directly depend on the pressure value.

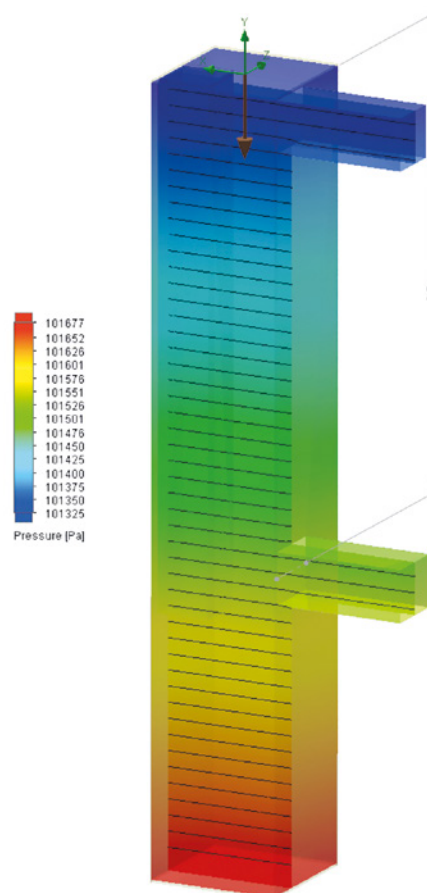


Figure 4. Pressure gradient for reference coordinate system at the top

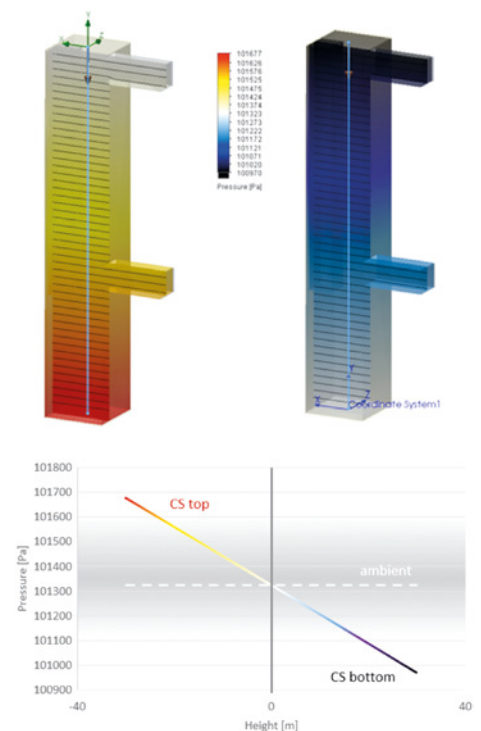


Figure 5. Result for reference Coordinate system at the top (left) and bottom (right)

Knowledge Base Content on Support Center

Mentor launched the new Support Center in July, replacing SupportNet. Support Center is a new, easy-to-use, online support experience, focused on your Mentor products. With its improved search engine it collates content from across Mentor into one convenient place for greater success troubleshooting problems.

Support Center gives access to personalized content for your installed Mentor product(s). The interface allows you to customize your view so that resources and support for the relevant products and software versions applicable to you are displayed on your homepage.

Support Center provides quick access to all the resources you need to support your Mentor products including:

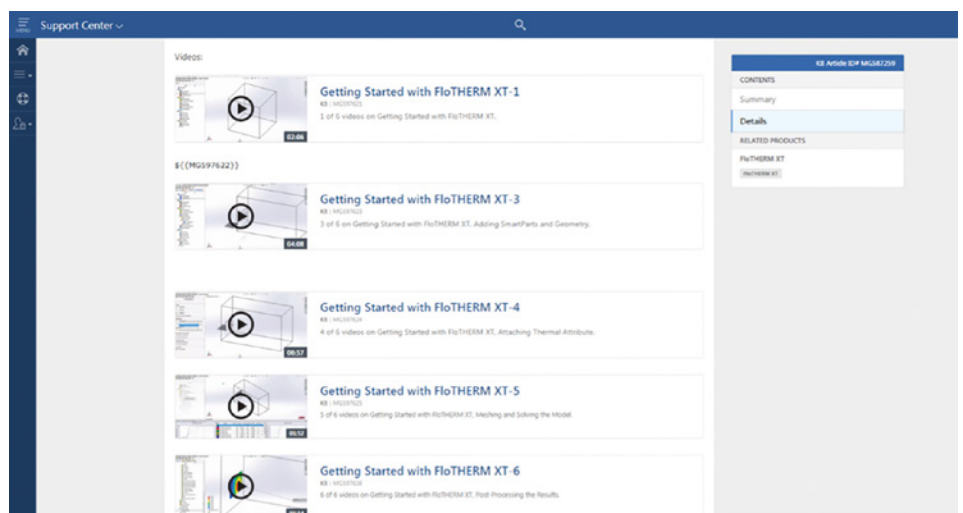
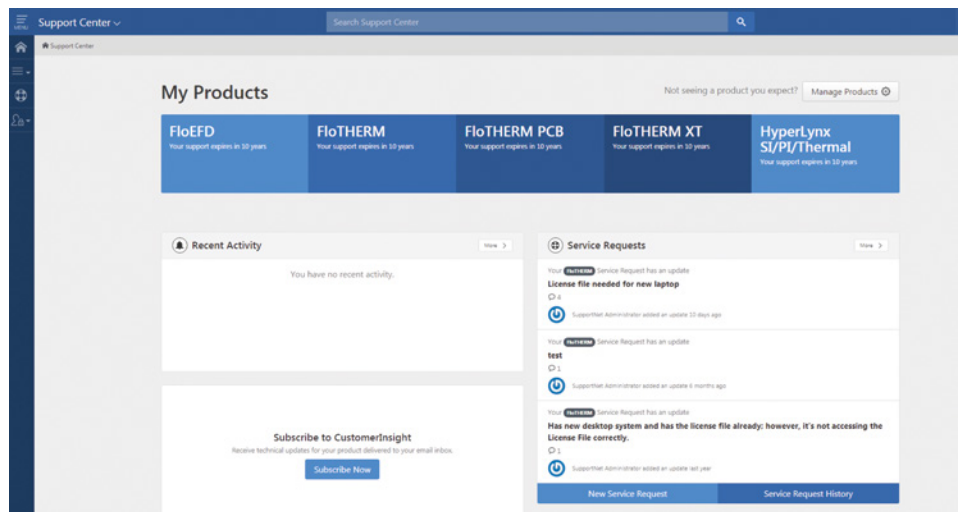
- Browse Troubleshooting Technical Topics,
- Download the Latest Releases,
- Submit & Managing Service Requests,
- Manage Product Licenses,
- Access System Administration Information,
- Quick link to Mentor Training Courses and On-Demand libraries, and
- Easily access resources like Mentor Forums and Mentor Ideas

Content Management in Support Center

Knowledge in Support Center is written and managed by experts of your product(s). At Mentor Support, we add to the contents of Support Center on a regular basis.

All content is reviewed and published with the knowledge that is created for Support Center. Our goal is provide answers to commonly asked questions and make them available to the users in Support Center. This includes Knowledge-Base Articles (KB Articles), videos, documentation, etc.

Another important feature in Support Center is the ability to view SRs across company site(s). You can see and read through the SRs history created by you and your colleagues. This provides easy access to the solutions you and others at your company have obtained in the past.



Design for Six Sigma in Electronics Cooling

By Wendy Luiten, Principal, Wendy Luiten Consulting

Temperature problems are well known in the high-tech industry. Everyone knows of cases where overheated products stopping working and in the best case scenario, resume their function, but only after an extensive period of cooling down.

In past years, electronics cooling was very much about cooling consumer electronics, mainly TVs, computers and networking devices. Nowadays we see the focus shifting towards smartphones, tablets, smart watches and other wearable electronics but also towards all other transitional fields in our society. Energy savings? Cooling of LED lighting is a hot item. Energy transition? Cooling of power electronics, for example in automotive electronics, for solar cells and inverters, or in fast chargers for electric cars and electric buses. Also, the trend towards more and more data communication is enabled by cooling of electronics. One can think about cooling of datacenters, servers and telecom equipment for 5G, and the Internet-of-Things

Everywhere energy is stored or transformed, part of it is released as heat. Higher operating temperatures impact reliability, lifetime and safety, hence embedded control algorithms are increasingly used, dialing back performance or switching off once a measured temperature exceeds a threshold value. A good thermal design will keep your product cool and its performance up. For many product developers, the temperature of their product is something that just happens, and they discover only at the stage that the total product has been realized in hardware and software and is tested for the first time. At that point it is far too late for a cost-effective solution. In addition, problems are difficult to solve, solutions often comprise multiple parts, and are difficult to realize, requiring multiple prototypes and may also involve further fixes when production starts (Figure 1). In the worst case scenario, problems are found in

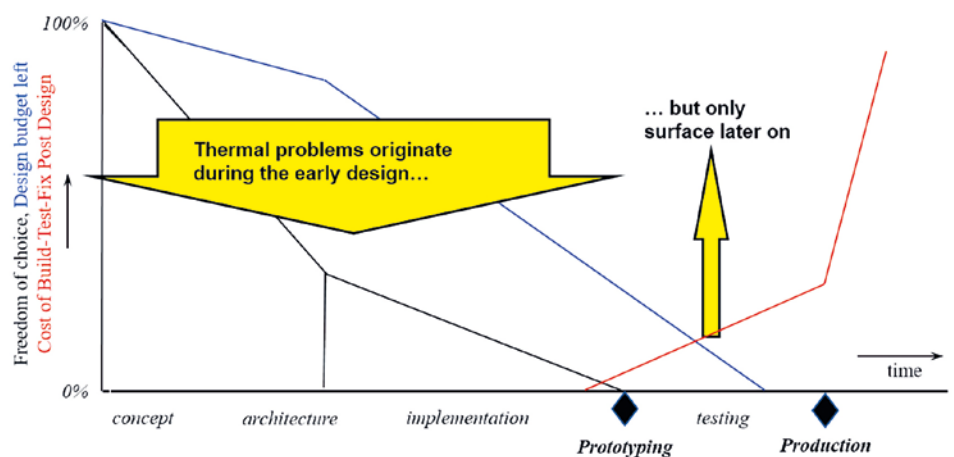


Figure 1. Typical development trajectory

the field with product reliability being impaired due to thermal reasons.

Why are thermal problems so difficult to solve? Simply put, it is because heat flows are so elusive. A typical product has multiple, often interconnected heat flow paths each consisting of multiple steps, and each step represents a thermal resistance. A high source temperature is the result of a high heat dissipation, a high thermal resistance or a combination of both. The heat dissipation is a direct consequence of the functional performance, and usually this cannot be lowered without a performance penalty. This leaves low thermal resistances and short paths as the preferred option to control temperature.

In the ideal case, each heat path from each source to the environment is formed through

a chain consisting of a low number of low thermal resistances. But this is not easy to realize. Part of the thermal resistances is either air-related or infra-red radiation related, which makes them invisible to the human eye. While air might be the primary cooling medium, it does not appear on the Bill-Of-Materials (BOM) for the product, and so far not tracked through the normal change request procedures. Changes that affect the air flow are unseen, and so also likely to recur in the next design iteration, and indeed in the next product development.

Design for Six Sigma (DfSS) is a design philosophy aimed at improving the success of innovation processes. The method is very well suited to the thermal field. Thermal design starts with identification of the product requirements (Define Phase), and flows down to how this translates to the thermal requirements, usage conditions, magnitude and location of heat sources, environment, and the location of temperature critical components (Identify Phase). A good thermal

design then provides a robust solution to heat removal, in close collaboration with the mechanical design and electrical design flows (Design Phase) Identification of input parameters, exploration of the solution space and making a conscious design choice are key concepts.

In the very early design phases thermal concept design can be done analytically, using hand calculations and estimations. This has the advantage of additionally identifying the key input parameters that influence the thermal behavior of the total product, but requires experience and engineering judgement. For more complex cases computer simulations are increasingly used, both in the architecture phase and in the implementation phase. For air-cooled products, use of CFD is the highly preferred option, as in this approach both the heat transfer coefficient and the temperature of the cooling air are calculated as a function of the air flow, rather than assumed to be a generic value to a constant air temperature.

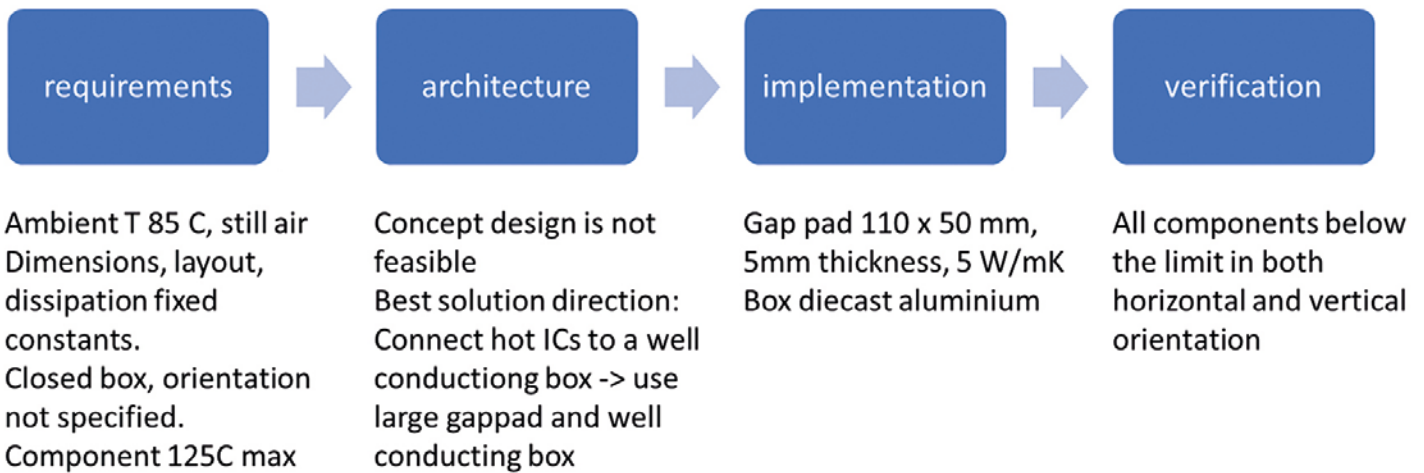


Figure 2. Example of the thermal design process of an automotive electronic box

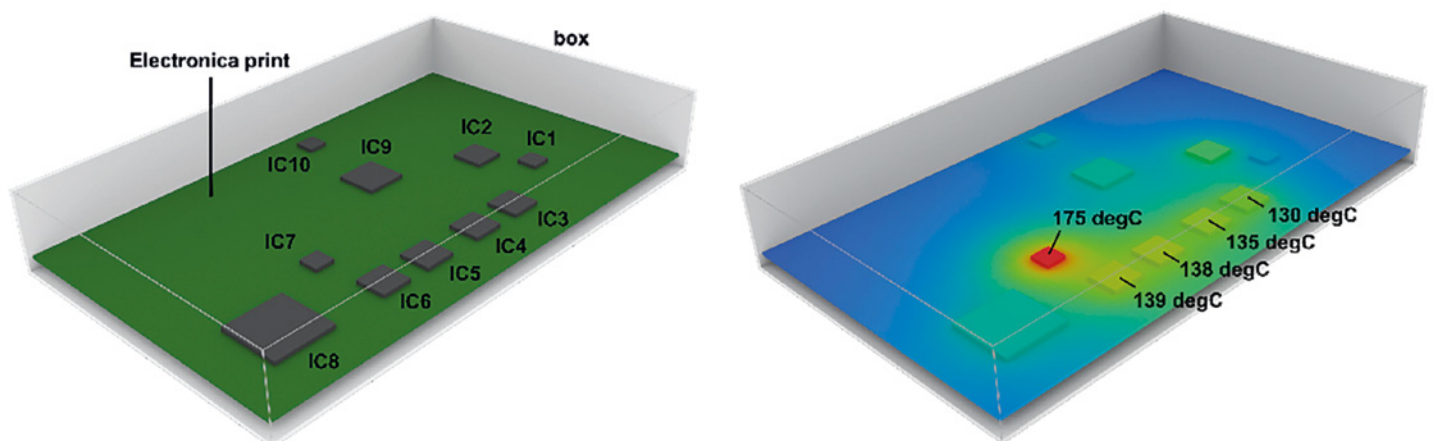


Figure 3. Left: Geometry, Right: Simulated temperature field with the first concept

	0	1	2	3	4	5	6	7	8	9	10	11
Gravity Direction	Negative Z	Negative X	Negative Z	Negative X								
box material : Conductivity (W/(m K))	0.2	0.2	0.2	0.2	2	8	15	15	15	130	130	130
gappad for IC7 : Activated	No	No	No	Yes	Yes	Yes	Yes	Yes	No	Yes	No	No
large gappad for hot area : Activated	No	Yes	No	Yes	Yes							
board : Conductivity (W/(m K))	10	10	10	10	10	10	10	20	10	10	10	10
Heat Sink for IC7 : Activated	No	No	Yes	No								
IC7 : Temperature (degC)	175.6	174.6	148.2	163	154.7	144.2	138.2	129.4	137.1	122.1	121.3	121
IC3 : Temperature (degC)	130.8	128.2	130.6	130.8	130.2	129.8	129.6	122.5	112.6	128.8	103.4	103
IC4 : Temperature (degC)	135.7	133.1	135	135.6	134.7	134.2	133.8	126	115.2	132.4	104.3	103.9
IC5 : Temperature (degC)	138.7	136.4	136.7	138.2	136.7	135.4	134.4	126.9	117.3	131.5	104.9	104.6
IC6 : Temperature (degC)	139.8	138.7	135.9	138.8	136.4	133.9	132.3	125	117.8	127.5	105	104.7

Figure 4. Scenario table with all virtual experiments

In fan-less products the magnitude and the topology of the air flow field and the heating of the cooling air flow are non-trivial and can have very significant impact on the temperature behavior of a product.

In many cases the true power of computer simulation is not in number crunching the detailed mechanical and electrical CAD design as a final check just before production. Rather the true added value is in the use of a series of numerical experiments in the early architecture phase. Choosing the right architecture from the start can free up design space to pursue the most desirable product from the earliest stage. Using computer simulations one can virtually explore the solution space and choose the most appropriate solution direction without incurring the large cost in time and financial resources that would be needed to pursue a similar goal through testing hardware. In the author's experience it would be very common to perform between 10 and 40 computer simulations to finally get to the most optimal architecture for the design. After choosing the most appropriate architecture – tailored to the specific product requirements and usage conditions – detailed design can then follow, often helped by additional computer simulations on the CAD data.

Figure 2 shows the thermal design process of an automotive electronics box as an example. The concept design starts from a closed plastic box containing a Printed Circuit Board (PCB). The thermal requirements are that the box is placed inside a non-ventilated environment of 85°C with a maximum allowed component temperature of 125°C. In the architecture phase, CFD simulations start from this concept design, and an aggressive estimate for the powers to ensure that design is robust enough to deal with the anticipated worst case power consumption.

Figure 3 shows the geometry (left). Note that this concept simulation is performed with only a very rough mechanical/electrical model, and without using mechanical or electronic CAD files or data. Rather, these

architecture-stage simulations precede the detailed mechanical and layout CAD design which take place after the architecture is chosen. The results of the simulations are shown in the calculated temperature field in Figure 3 (right) show that the proposed concept design is not thermally feasible. Multiple ICs are above the 125°C temperature limit, and the hottest component being 50°C higher.

In this product, the key parameters for the thermal resistances consist of the dimensions and material properties of the box, the layout and heat dissipation of the PCB, and the mounting of the PCB inside the box. The size of the box, the fact that the box needs to be closed, the layout of the PCB and the heat dissipation are fixed. Parameters that can be changed can all be investigated in the architecture phase of the thermal design. These are:

- The material of the box, especially the thermal conductivity (normal plastic k=0.2 W/mK, thermal plastic – low budget k=2 W/mK, electrically insulating k=8 W/mK or electrically non-insulating k=15 W/mK, or die-cast aluminum k=130 W/mK) are all discrete options
- Thermal management products: using a heatsink and/or a gap pad – a thermally conductive solid material bridging the air gap between the PCB and the box can be investigated, with
 - a) Location limited to the hottest component, IC7
 - b) Distributed over the entire hot zone
- Thermal conductivity in the printed circuit board itself (layout and construction related, e.g. number of layers, buried power and ground planes).

Another aspect of DfSS is de-risking the potential influences of causes of variation. As the orientation of the box is not prescribed in the product requirements, the box must be simulated both in horizontal and in vertical orientation, since its mounting is under the control of the end user company.

I find FloTHERM's Command Centre indispensable for running the many scenarios that I need to make sure that I do not just have a working design, but the best working design possible for my circumstances.

Figure 4 shows FloTHERM's scenario table with all the calculated cases and corresponding results. In the scenario table, each column represents a virtual experiment. In total, the table shows 12 different virtual experiments. In the top blue part of the table the chosen key design parameters are shown. The bottom, orange, part shows the corresponding calculated temperatures for the key ICs on the PCB.

Scenario 0 is the original concept design. In this design IC7 is 50°C above spec and IC3 to IC6 are also above spec. Scenario 1 shows the results for the vertical orientation. It shows that the horizontal orientation can be considered worst case, and we continue subsequent scenarios with horizontal orientation. In scenario 2, a heatsink is used on IC7, and this is not a viable solution. Scenario 3 – 6 virtually explore the use of a gap pad in conjunction with a closed box of increasing thermal conductivity. The results show that a small gap pad to a plastic box does not work, also not if the box is made of thermal plastic and also not if the PCB itself is better conducting (scenario 7). Scenario 8 shows that also a large gap pad to a thermal plastic box does not solve the thermal problem – clearly a metal box is needed.

Scenario 9 shows that a local gap pad on IC7 to an aluminum die cast box solves the problem for IC7, but IC3 is still above specification. Finally, scenario 10 shows that to apply a gap pad over the hot zone in conjunction with a die-cast aluminum box is a feasible solution, and scenario 11 shows that this solution is also robust with respect to different orientations: in vertical orientation, this solution also fills all requirements.

Figure 5 shows the calculated temperature and flow fields for scenario 10, the final solution, in horizontal orientation. The layout of the board is unchanged, and applying a gap pad of sufficient size bridging the air gap between PCB and box in conjunction with an aluminum die-cast box, a thermal design is realized that will keep all temperatures within the specified boundaries irrespective of the orientation of the final product.

The automotive box example illustrates the importance of a good thermal design and a methodical exploration of the solution space.

Using a heatsink on IC7 was not a solution because the heatsink lowered a resistance in a path that contains a very large second and third thermal resistance: the heat transfer of the air inside the box to the wall of the box, and the heat transfer of the box to the environment. In the chosen solution, multiple

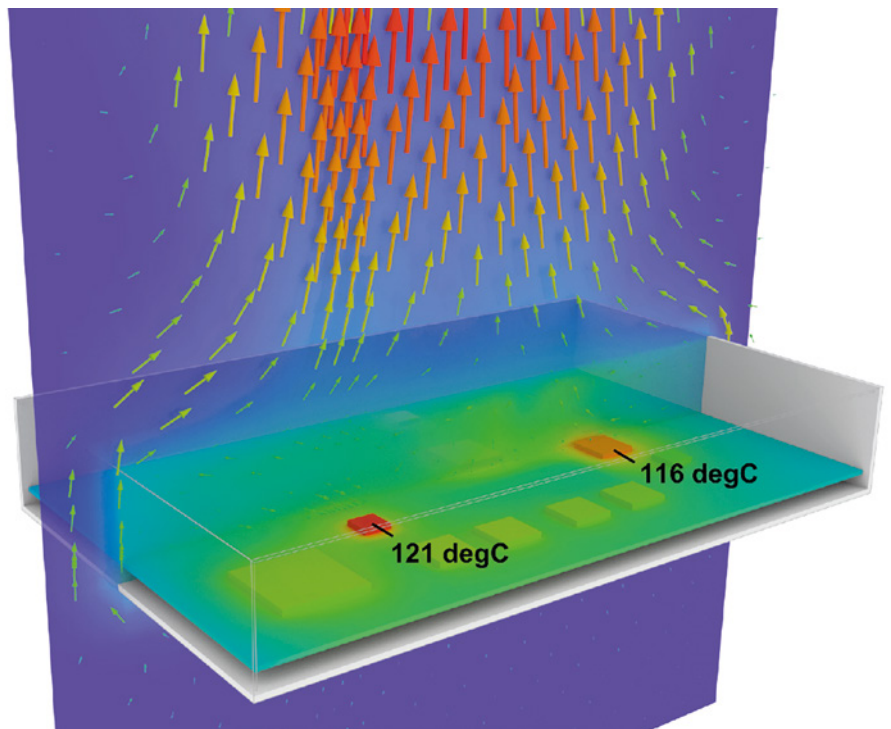


Figure 5. Surface temperature, air temperature and flow field for the final chosen architecture

resistances in the same heat path are lowered through a strategic choice of thermal input parameters.

In the case of the simple automotive box example, purchasing can now proceed to source a supplier for a die-cast box and the gap pad, while in parallel the mechanical developer can proceed to implement the detailed CAD design for a die-cast box. Thermal design in the pre-CAD phases was sufficient to make informed thermal design choices and lower the risk of wasted time and project resources by detailing an unfeasible design to a significant degree. Rather, having de-risked the project from the outset, as more becomes known about the component placement, board layout, component powers etc. the detailed design can explore ways in which the cost can be reduced. In this example, a smaller gap pad may be possible, or a cheaper material with a lower thermal conductivity might perform adequately. Exploration of the solution space is one of the pillars of Thermal Design for Six Sigma as it allows thermal solutions to be found that potentially free up design space to increase product desirability as well. As an example, avoiding the use of the heatsink potentially enables the box to be flatter and reduce its volume claim. It is not limited to the architectural design phase and can be used to very good effect from both engineering and financial standpoints throughout the development.



Liquid Cooled Computing

Enabling The Digital Enterprise In The Advent Of Industry 4.0

By Jon Halestrap, Business Development Director, ICEOTOPE, UK

One of the core tenets of mass manufacturing is centralization. It's an idea pretty much as old as the Industrial Revolution itself. Putting everything in one place – raw materials, workforce, machines, post-production – enabled scale and scale meant efficiency.

The advent of Industry 4.0 has disrupted these long established paradigms. Smart factories are challenging the accepted thinking underpinning volume manufacturing.

- **Innovative manufacturing techniques** – 3D printing has undermined the relationship between volume and cost efficiency. The significant capital expenditure of investing in new tooling meant that any part had to be produced in high volumes to be justifiable.
- **Increasing automation** – factories of the future will be ever less reliant on a local workforce to staff the production line. Factories will be part of a distributed network and contain machines that are more capable of intelligent operation independent of human interaction.
- **Autonomous vehicles** – automated machines will shift the logistics of manufacturing. Rather than relying on a centralized distribution network, manufacturers will use autonomous vehicles, robots and drones to move parts between factories or deliver products directly to retail and even end-users.
- **The “Digital Twin”** – from initial designs through to simulation, materials and production, the digital twin concept will accompany every machine in order to create, test and build products. Taking a digital approach for critical parts of production will open new ways of productivity and efficiency.

This fundamental shift from centralized manufacturing to a flexible network of smart factories is supported by micro and edge data centers. Just as factory hardware no longer

has to sit under a single roof, IT systems will also be spread across a network.

Datacenters and high performance processing systems will sit throughout a manufacturer's network, perhaps on the factory floor itself. Through wireless technology, computers will be in constant communication with other smart factories in the network, the cloud, and a range of connected devices.

Digitalization Puts Strain On Existing Infrastructure

Despite these exciting advances in automation and communications, let's not forget that manufacturing is still about making products – it's a physical business. Machining parts can generate huge amounts of noise, heat, and dust which combine to create a very challenging environment for IT systems.

As systems will be 'edge' deployed as part of a decentralized network they could well exist in remote locations where local on-hand IT support is not guaranteed. Therefore it is paramount that smart factory devices are easy to manage, secure, and resilient to the environmental challenges of the factory floor.

As new technologies such as the Internet of Things (IoT) are driving volumes of data, along with substantial investment at the Edge of Network, it's clear that cost effective and efficient cooling technology is needed.

Cooling is essential to high powered electronics and should not burden your IT investment. Traditional air-based cooling equipment cannot cope with ever-increasing

heat loads that hotter processors and applications demand. Sticking with the legacy approaches will only lead to larger footprints and increasing cost and complexity, with no competitive benefit.

Roughly 25% of datacenter unplanned outages are caused by weather, water, heat or air-conditioning related issues. Combine this with air cooling equipment being bulky, power-hungry and costly, sufficient cooling methods are crucial for business operation and continuity.

Redefining The Cooling Landscape For Industry 4.0

Liquid cooling has been around for many years but, until now, has been regarded as a niche technology with many compromises. However hotter processors and new technologies are driving the need for faster speeds, better flexibility with minimal disruption and downtime.

ICEOTOPE, developers of immersion liquid cooling technology, enables IT infrastructure to operate seamlessly in any environment. The patented technology revolves around immersing and protecting high powered electronics in a specially engineered coolant.

Thanks to Iceotope's total immersion cooling technology, expenses such as chillers, computer room air handling (CRAH) equipment, raised floors or ducting are no longer necessary. The result is an advanced product portfolio ranging from tower to server-level to suit a range of computational demands and environments.

EdgeStation™ - Fan-Free, Resilient Workstation

EdgeStation adds robust, portable powerful computing resource to the digital enterprise. Bringing critical applications closer to the manufacturing operation reduces latency, therefore improving your time-to-market.

Without the industrial drone of fans and pumps, you can put a high performance machine to work side-by-side with your team. Removing the fans ensures a sealed system which protects critical IT components from hot, harsh or contaminated environments delivering reliable performance.

ICEOTOPE has worked with the Advanced Manufacturing Research Centre (AMRC) to solve the problem of dust particles from its carbon fiber facility. This caused continuous IT equipment failure and unscheduled downtime. The AMRC deployed an EdgeStation™ system, which fully encloses and protects



Figure 1. ICEOTOPE EdgeStation™ fan-free resilient workstation



Figure 2. EdgeStation™ deployment at the AMRC carbon fiber laboratory

high-powered electronics to sustain performance and therefore increase product lifespan.

EdgeRack - Simplified Edge Data Center Deployment

EdgeRack is the modern data center to deliver more power in significantly less space so your business can scale one rack-at-a-time.

ICEOTOPE uses a two-stage cooling process – the first stage being a specially engineered liquid to cool all components with the second stage transferring the heat away using a coolant loop. Consider that EdgeRack saves up to 80% energy consumption, and you can reuse the waste heat for district heating, liquid cooled datacenters become a sustainably smart business model.

Summary of ICEOTOPE liquid cooling:

- **Double-digit capex savings** – Iceotope’s technology requires next-to-no additional infrastructure leading to significant capex reductions for datacenters..
- **Significant floor space reduction** – using anywhere between 50% - 75% less floor space, savings for customers are substantial. This leads this need to defer or obviate major capex in extending or building new datacenter space.
- **Full integration** – Iceotope can retrofit their servers into existing infrastructure meaning you can get immediate opex benefits without having to redesign your entire datacenter, alter your supply chain or retrain your staff.
- **Consumes less energy** – without the need for power-hungry computer room air handling equipment and zero fans inside the

servers, Iceotope’s technology can reduce energy bills by up to 80%. Iceotope also allows the recapture and reuse of waste heat leading to an improved corporate risk and social responsibility strategy.

CFD Is Vital For Product Development

The combination of network modeling and CFD are vital to our engineering design processes and greatly reduce the cost and time for development. From prototypes, to performance optimization and design approval, CFD modeling is used for a range of features within the immersion cooling system from natural convection of IT components to forced convection of pipe networks and heat exchangers.

Liquid is 1,000 times more effective at transferring heat than air, however, using liquid comes with challenging physical behaviors. To overcome this, ICEOTOPE uses CFD software to analyze the natural convection inside our server blades, providing details of flow distribution.

To deliver significant energy and cost savings to our customers, we also use CFD to characterize hydraulic resistance in our manifolds to achieve sufficient coolant flow while limiting the operating pressure.

Harnessing the power of digitalization, ICEOTOPE can now utilize its CFD design simulations to create their own “digital twin” to validate and optimize designs.



Figure 3. From one to three chassis, ICEOTOPE delivers business scalability



Kehoe Myers and JS Pump Team up to Design the **Water Supply System** for **Australia's Newest Airport**

By Terry Kehoe, Director, Kehoe Myers Consulting Engineers and Jurgen Sprengel, Principal, JS Pump and Fluid System Consultants

Brisbane West Wellcamp Airport is the first international airport built in Australia in the last 50 years. The site is approximately 839ha in area and is located in hilly terrain with an elevation range of some 90m, this creates a challenging pressure distribution envelope while complying with town water supply design guidelines. The challenge is further exacerbated by water flow from the deeper supply network being limited to 60L/s while the maximum town water system demand is 163L/s.

The airport includes the Wellcamp Business Park (WBP) which comprises industrial zoned allotments of varying sizes, distributed around the airport as shown in Figure 1. The ultimate site development will consist of an airport and mainly industrial uses in the WBP area.

The source of water for the Water Supply System will be the local town water network. It will provide water take-off points shared between two adjacent allotments with fire hydrants provided at the service branches. The water supply system will follow the road easements within the Wellcamp precinct and will form ring mains, where possible, to enable continuous supply to customers in the event of component outages.

The current system comprises of a single water main connecting the trunk main with the airport terminal located some 4.2km downstream. Transitioning the site to its final development is an ongoing process. The ultimate site development will incorporate site water storages and backup supply options in order to achieve maximum flexibility and reliability in town water supply.

For the final development of the business park and Wellcamp Airport, the following water usage rates were projected:

- Average Day Demand: 41.3L/s
- Peak Day Demand: 70.2L/s
- Peak Hour Demand: 133.4L/s

Demand for firefighting of 30L/s is in addition to above demand figures and applies for a nominal duration of four hours. Therefore the key design objectives are:

- To enable gravity water supply where possible,
- Ensure site water storages are of sufficient capacity to manage a firefighting event when coinciding with peak day and peak hour demand,
- Provide sufficient redundancy in water storage to enable any water supply source to be taken out of service,
- Ensure pressure distribution is maintained within the acceptable envelope, and
- Incorporate existing water infrastructure of the current system.

In the ultimate design, water supply pipelines were arranged in ring main arrangements where possible. Two independent water storage reservoirs will provide a fully redundant water supply and will form the predominant source of system pressure and flow. The secondary reservoir with a 1200kL capacity will be located at a higher level than the main Reservoir and will supply the elevated parts of the development. It will also provide full back up to the main reservoir.

Network supply to the main reservoir is via a DN200 branch line connected to the incoming trunk main. Because of the higher elevation of the secondary reservoir, two transfer pumps are required to provide the necessary lift which the trunk main may not be able to achieve at times of high system demand. In the event that the main reservoir is out of service then the feed from the two transfer pumps, and the secondary reservoir will be able to maintain sufficient water supply. In the event the secondary reservoir

is out of service, the transfer pumps will enable the main reservoir to also service the elevated part of the development.

The Hydraulic Model Development

A hydraulic model comprising the ultimate development was created in FloMASTER in order to achieve the right proportions in the overall model design. A current development model was also prepared by cutting down the ultimate development model. Specific sub-models were created to enable the case specific script for each modeling scenario. Steady state simulations were used to establish the flow and pressure distribution in the water supply system.

The variation in elevation and subsequent high pressures in lower lying areas required the water supply system to be divided into 6 separate supply zones. Zones in lower lying areas were protected by pressure reduction valves (PRV) in order to maintain pressure within acceptable limits. Also, backup supply points from the Trunk Main were also protected by PRVs.

Each supply zone was tested for a firefighting event with the other zones operating at peak hour flow. In a conservative approach, the location of the fire was assumed to be at the most disadvantaged location in the zone, such as the highest elevation, thus resulting in the lowest supply pressure.

The Firefighting Simulations

Transient simulations were required to model fire pump start up and shut down. This was to confirm that pump supply pressure would not result in loss of pump suction due to excessive cavitation. Fire pump modeling requires short time steps of about 0.1s in order to follow the transient operation of components, the simulation running for 250 seconds.

The fire pump was equipped with suction valve, discharge piping and variable speed controller. The suction valve was actuated to enable the simulation of a realistic pump start up.

The simulation of a fire pump start up and stop event is shown in Figure 3. The graph illustrates the dynamic flow rates from different flow paths (C9 & C18) and how they affect the fire pump flow rate (C20).

Shown in Figure 5 is the dynamic pressure response at critical locations in the deeper town water supply system (Node 49 & Node 86) and at the fire pump suction (Node 91). It



Figure 1. Locality Map

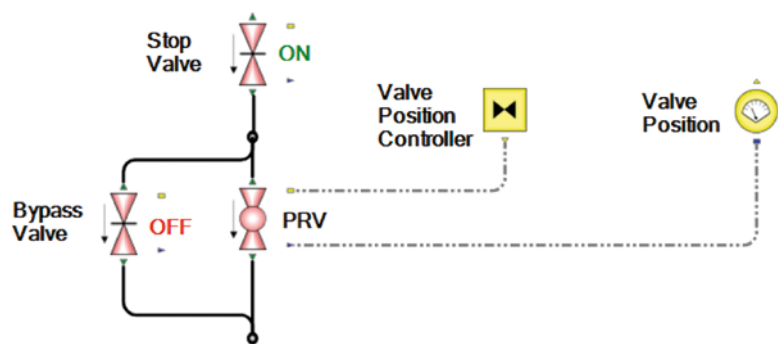


Figure 2. Typical Pressure Reduction Valve (PRV) Arrangement

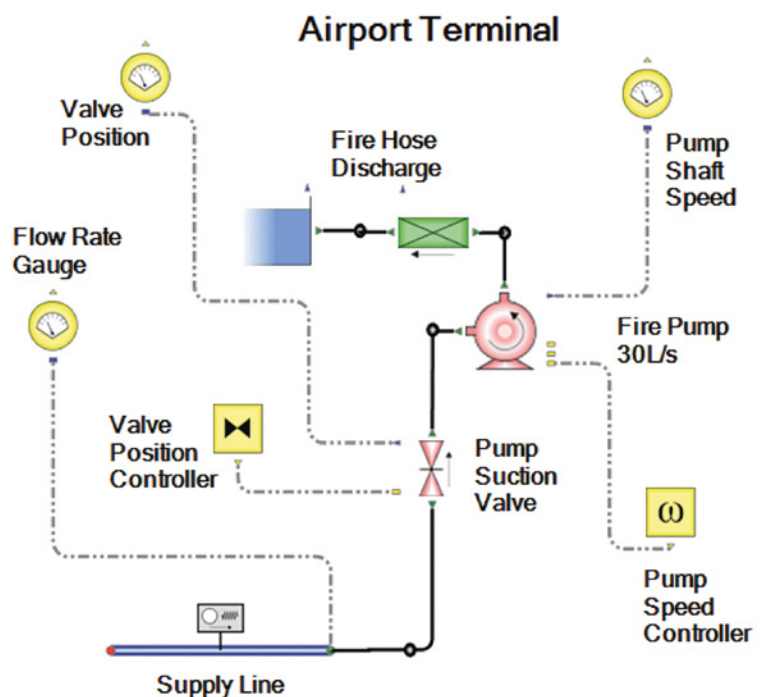


Figure 3. Typical Fire Pump Arrangement

confirms that down surge on pump start up is contained within acceptable limits.

The Storage Tank Capacity Simulations

Transient simulations were required to model reservoir level behaviour under extreme draw-down scenarios. Reservoir level modeling allows for a time step of up to 10s and has to run for a period of two days (173,000s) to provide the desired result graphs.

The simulations assume the worst draw-down scenario where peak day demand and peak hour demand coincide with a firefighting event. The design guidelines require the firefighting event to run for a nominal period of four hours. The goal is to confirm the capacity of the Main Reservoir being sufficient to manage this extreme event, while assisted by the supplement supply of 60L/s from the TRC Trunk Main and secondary reservoir out of service.

The Main Reservoir, Valve and Transfer Pump Arrangement in Figure 6 shows the piping arrangement around the Main Reservoir. The model was set up for time based draw-offs in each zone operating at peak day and peak hour demand. In addition, a firefighting event was initiated in Zone 5. After working hours the zonal draw-offs were reduced to 50% of the average day demand. Supply from the Trunk Main replenishing the Main Reservoir was controlled by a level control valve, its maximum flow rate limited to 60L/s.

The result graph in Figure 7 shows outflow from the Main Reservoir and inflow from the TRC Trunk Main. The firefighting event occurs during peak day and peak hour demand on the first day only while peak day and peak hour demand also occur on the second day.

The useful level range of the Main Reservoir extends from 0.3m to 5.3m. When the level reaches 5.3m, the inlet control valve matches inflow with outflow and thus keeps the level steady. Following rapid draw down during the firefighting event, the level recovers sufficiently fast after working hours with enough storage capacity available for another firefighting event on the next day if required.

The FloMASTER V8 software has enabled the complete hydraulic design of the Wellcamp Town Water Supply System and has confirmed its operational capabilities by static and dynamic model simulations and all design objectives of this project have successfully been achieved. This includes verification of low and high flow demand scenarios (except for firefighting events). In

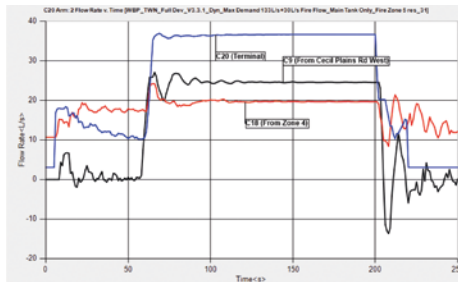


Figure 4. Flow Rates in Fire Pump Area

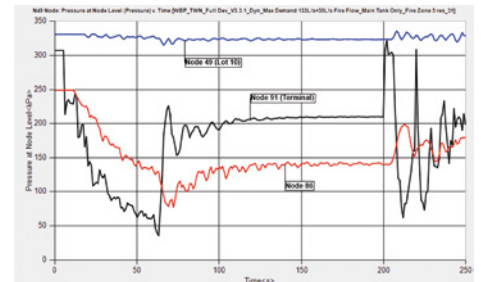


Figure 5. System Pressure Response

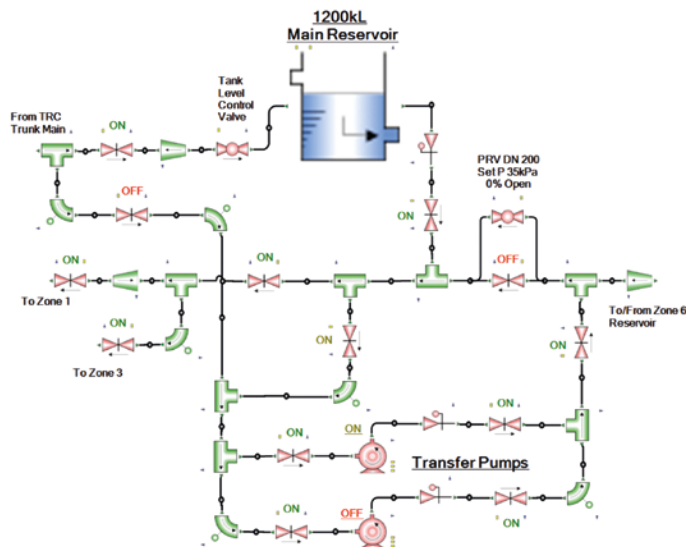


Figure 6. Main Reservoir, Valves and Transfer Pump Arrangement

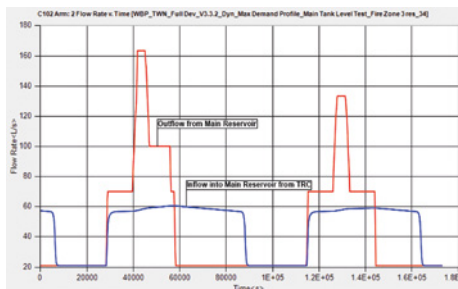


Figure 7. Main Reservoir Inflow and Outflow over Two Day Period



Figure 8. Main Reservoir Water Level Response over Two Day Period

the current development, a firefighting incident in the airport area (Zone 5) requires the resetting of the incoming PRV from 500 kPa to 650kPa in order to provide sufficient supply pressure. Following completion of firefighting event, the PRV has to be reset to 500kPa as otherwise the pressure would be excessive in lower parts of the system. Modeling of fire pump operation has confirmed sufficient supply pressure being available to avoid loss of prime when the system is operating at maximum flow demand. It has also confirmed that water levels in the reservoirs are being maintained above low level thresholds while being supplemented from the Trunk Main for a period of 48 hours when operating under extreme water demand

The Evolution of **One-dimensional Simulation for Automotive Thermal Management Systems**

By Giancarlo Gotta, Virtual Analyst, Fiat Chrysler Automobiles Italy



The origin of one-dimensional simulation of engine cooling systems can be placed in the early 80's when **two important events occurred: increased use of test rigs for testing vehicle thermal performance on one side and beginning of large use of computer science for simulating complex physical systems.**

In order to explain the evolution of one-dimensional simulation for automotive thermal management systems, consider a very popular car, the Fiat Panda. The first generation of this city car was introduced in 1980. The second generation was awarded European Car of the Year in 2004. The third generation debuted at Frankfurt Motor Show in September 2011. In over 31 years over 6.5 million Pandas were sold globally, 4.5 million being the first generation. Original Fiat Panda and elder sister Fiat Uno were both a commercial success and a turning point for automotive design process, starting the search for industrial efficiency by anticipated validations and reduced development time.

The first generation Panda was equipped with a simple engine cooling system whose purpose was cooling the engine, heating the cabin and defogging / defrosting windshield in colder environments. The system was not designed to cool the cabin in warm summer months, nor did customers' expectations ask for this function, now considered as mandatory. Original Panda had in the past fewer requirements for thermal control and validation needs by simulation than her current, younger sibling.

Nevertheless, the performance simulation of these simpler engine cooling systems was feasible only by large, clumsy hardware use or a simplified numerical-graphical approach. Due to the lack of commercial codes, the former option required dedicated programs written in complex languages such as FORTRAN, as well as specific skills and knowledge that were not easily available at that time. The latter option, on the contrary, was rather effective but very time consuming when applied to the early stages of the vehicle design, when multiple configurations have to be evaluated.



Figure 1. Fiat Uno marked a breaking point in subcompact car European market, answering customer request for improved fuel economy and available internal volumes, without paying a price for reduced performances or ugly apparel. These results were achieved through technical innovation and stimulated application of system design approach by virtual analysis.

The progress of computer science produced more powerful and smaller machines that could be used directly by engineers. One-dimensional simulation or 1D was one of the techniques that took advantage of this progress. One-dimensional fluid-dynamic codes were designed similarly to the equivalent electric circuit method. As voltage (electric potential difference) induces a current in an electric circuit, pressure differences induce a flow in a fluid system. The fluid flow in turn transports heat from one node to another, e.g. from the engine to the radiator, to be transferred to cooling air flow generated by either radiator fan action or vehicle speed.

The use of these simulation models allowed an important change: compare simulation results and experimental data, creating a quick and cost effective communication link between two different engineer populations. Connection between two "alien" worlds created a beneficial interaction, enabling the optimization of efficiency of the engine cooling system.

The simple cooling system of small gasoline engines mounted on the original Panda includes all automotive basic cooling parts. And the minimal configurations of 1D system modeling '90s engineering is still good for today's applications, comprised the following components:

- An internal combustion engine generating heat, removed by engine coolant,
- A coolant pump producing coolant flow rate through the engine,
- Ducts and pipes to transport coolant and heat to a heat exchanger or "radiator",
- A radiator that exchanges heat with an external cooling air flow,
- An electric fan supplementing vehicle motion to generate cooling air flow at low speeds, and
- A cabin heater providing passengers an adequate thermal comfort during winter.

This basic 1D engine cooling system model is then integrated with boundary conditions that produce the required cooling air flow rate over the heat exchangers, namely the radiator and the cabin heater. Radiator boundary conditions simulate vehicle speed by specifying pressures at vehicle front end and vehicle bottom. These pressures drive the air flow rate through the radiator and inside the engine bay. Cabin heater boundary conditions simulate passenger compartment warming air flow and are not used, unless winter season climate is considered.

In these models, coolant loop expansion tank (hot bottle) is omitted due to its complexity. The expansion tank is used to fill and pressurize cooling system while vehicle and engine are running, in order to guarantee operating conditions above boiling temperature at ambient pressure. Although the expansion tank plays a crucial role in real-life cooling systems, the first simplified models neglecting it were still capable of providing adequate thermal results. For this reason these basic models have been very useful for a long time and can be still implemented nowadays starting a new project, acting as pathfinders and paving way for subsequent, more refined studies to be run when a larger amount of information is available.

Increasing Complexity

Vehicle complexity increased together with customer requirements leading to the addition of more and more functionalities. One example is the use of an air conditioning system capable of maintaining thermal comfort conditions inside passenger cabin during summer time.

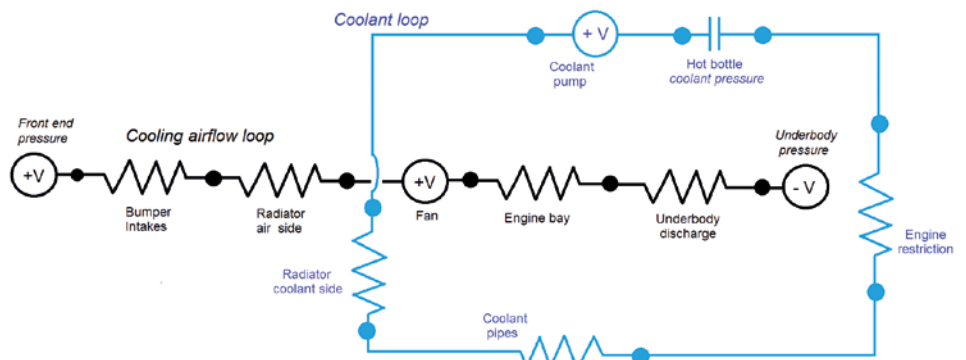


Figure 2. Engine cooling system can be ideally modeled as a pair of electrical circuits. An open end circuit describes cooling air flow loop, a closed ring circuit describes coolant loop.

AC introduced an additional variable, the presence of a gas condenser, usually placed upwind right in front of the radiator and then creating important challenges for engineers.

The condenser removes heat by the passenger compartment rejecting it to the external cooling air flow, dropping coolant radiator efficiency in the process. 1D simulation approach has proved to be very useful to investigate this topic even if the whole air conditioning system and thermal loop is not detailed: it is always possible to evaluate AC system impact on the engine cooling system by setting the condenser permeability to cooling air flow and estimated passenger cabin thermal power removed. These two parameters influence velocity and temperature of the cooling air flow crossing main radiator and their effects can be easily tracked by 1D models. This in turn allows thermal engineers to improve specifications for fan and radiator, getting better supplier feedbacks and parts tailored to their needs. Final result is a more balanced, lighter, cheaper or smaller automotive engine cooling system.

For this purpose new generation of 1D simulation models became slightly more complex than the basic one, well suited to take care of small gasoline engine and their coolant loops from Panda onward. But most important, increased complexity tied together engine systems and AC engineers: their common needs triggered a sharp turn in automotive thermal system development and were the seed generating current design and simulation platforms, capable to handle and integrate requirements by different thermal department.

Scalable Engine Cooling Module

The spreading of supercharged and diesel engines in the '90s required automotive engine cooling systems to provide even more functionalities, integrating different heat exchangers together in a "cooling pack" or

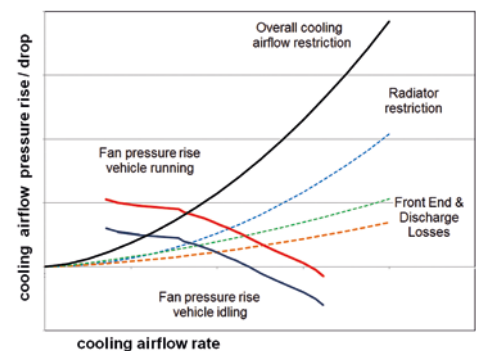


Figure 3. Classical numerical-graphical estimation of cooling air flow for automotive engine cooling systems. All cooling air flow restrictions due to pressure losses through vehicle bumper intakes, radiator and other heat exchangers, engine bay and underbody discharge are compounded in a single, overall pressure drop curve. Fan pressure rise curve, supplemented by vehicle speed ram effect, activates cooling air flow..

“cooling module”. Thermal engineers were thus confronted with a new challenge: the need of understanding the performances and mutual feedback of different arrangements for three, sometimes four stacked heat exchangers. Additional capabilities were required by one-dimensional simulation tools. In the ‘90s FloMASTER delivered the AVS module (Airside Visualizer and Segmenter) capable of modeling the position and mutual interactions of different components inside the cooling pack. This new capability allowed engineers to understand quickly and easily how and how much more efficiently a complex, layered engine cooling module works. Additionally, the engineers could perform parametric analyses where dimensions and positions of the different heat exchangers, as well as fan power and fan blade diameter, can be changed and re-sized up or down. The interactions of original and modified components of the cooling pack are automatically computed by FloMASTER and the user was not required to make any assumption or perform complex procedures that were prone to error. This new functionality allowed for a step change in the accuracy of 1D models as well a more creative use of thermal simulation. For the first time it was possible to scale cooling packs and evaluate a large number of configurations in a small time frame. Since then the scalability of vehicle engine cooling modules became more and more important, allowing release of different and customized solutions according vehicle mission: this is a strong enabler to ride current competitive automotive market, allowing car makers to introduce the same model in many countries, each one different for climate, customer vehicle usage and road patterns. The scalability of 1D simulation models supports both development time and research cost reduction and has potential to maintain high vehicle quality standards.

The Original Concept of Vehicle Thermal Management

As previously discussed, the increased complexity of simulation models required a closer collaboration among different departments involved in vehicle development. In particular, the AVS module implemented in FloMASTER enables the user to consider the three dimensional arrangements of cooling pack components as well as non-uniform air velocity distribution as a result of the vehicle aerodynamic studies. In this framework the collaboration between thermal and aerodynamic engineers, the last ones responsible to set up and run three-dimensional CFD simulation, was particularly important and gave birth to the concept of Vehicle Thermal Management at the start of the new millennium.

From Mechanical to Electronic Control Systems

While in the past components of engine cooling systems were controlled by simple mechanical controllers, in the new millennium the control systems evolved to use more electronic based controllers. An example is the fan control system. Early cooling fans could be triggered by the equivalent of a bimetallic strip, running a single speed: later on electrical resistors were introduced allowing two, three or more fan speed matching cooling needs and current usage. Today, PWM controls and brushless fan motor guarantee an infinite number of combinations of vehicle speed and fan rotational speeds. A similar functionality is found in the valves controlling coolant flow. Alongside with traditional wax and spring thermostatic valves, the cooling system is now

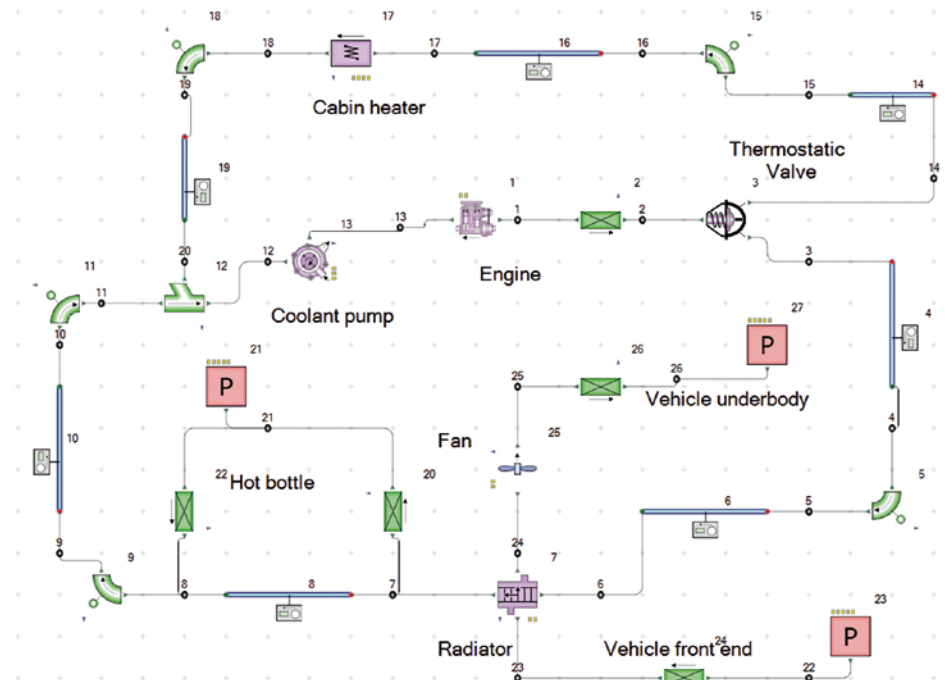


Figure 4. A classical automotive engine cooling system arrangement can be investigated by a classical 1D FloMASTER model. According needs and purposes each engine cooling system model can be simplified further on, or introduce more elements: here you can find a fair enough hydraulic description, a basic cooling air flow set up, most recent components for engine, coolant pump, fan and thermostatic valve and a low level, yet effective hot bottle.

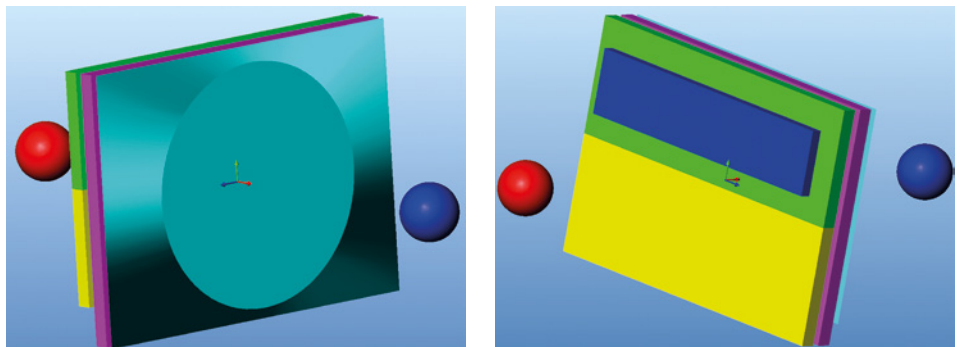


Figure 5. A single automotive project has to take care of many engine and drive configurations. 1D simulation models investigate engine cooling module performances according parts capacity and layout, taking into account mutual airside pressure drop and thermal feedbacks.

equipped with electronically controlled servovalves granting continuous and permanent modulation of flow. These two functionalities together allow for the maximization of the amount of heat removed by the cooling system to optimize cabin comfort and obtain faster engine warm up. The latter enables the reduction of fuel consumption and meets the increasingly demanding regulations for reduced pollutants and greenhouse gas emissions.

New Approach, New Skills

In order to properly model these new thermal management systems where electronics plays a crucial role, controller components need to be introduced into the one-dimensional models. These components are capable of modulating the behavior of valves and fans in response to coolant pressure and temperature. At the same time, traditional steady state simulations capable of verifying system performance capacity searching for thermal equilibrium need to be integrated with transient simulations: and these ones need new data, such as component thermal capacity and road pattern checks to get time histories for vehicle and engine speed.

This additional knowledge allow preliminary studies of both thermal systems and their controls and only these parallel developments produce an efficient automotive thermal management. This comes for a price: new skills to be developed. Today, engineers in charge of thermal management need to be able to account for the interaction of the engine cooling system with the engine control system and passenger thermal comfort control system; they have to be proficient in vehicle dynamics too. But only communication, both between engine cooling system parts and engineers of different disciplines, is the real key for success.

The Simulation of the Future

It's now clear that the near future simulation of engine cooling systems will still be based on the knowledge of traditional thermal and mechanical systems, but will be required to model engine cooling system calibrations much more than today. We can thus dare to define the future 1D simulation as a "smart" analysis of processes and controls rather than a "dull", robot-like thermal analysis. And this is more and more true as hybrid and electric vehicles are developed and sold into the market and new technical solutions are introduced. An example is the so defined "dual loop cooling system" in which not only the engine, but also the passenger air conditioning and the engine air induction systems are liquid cooled by at least two separate systems, working with totally different

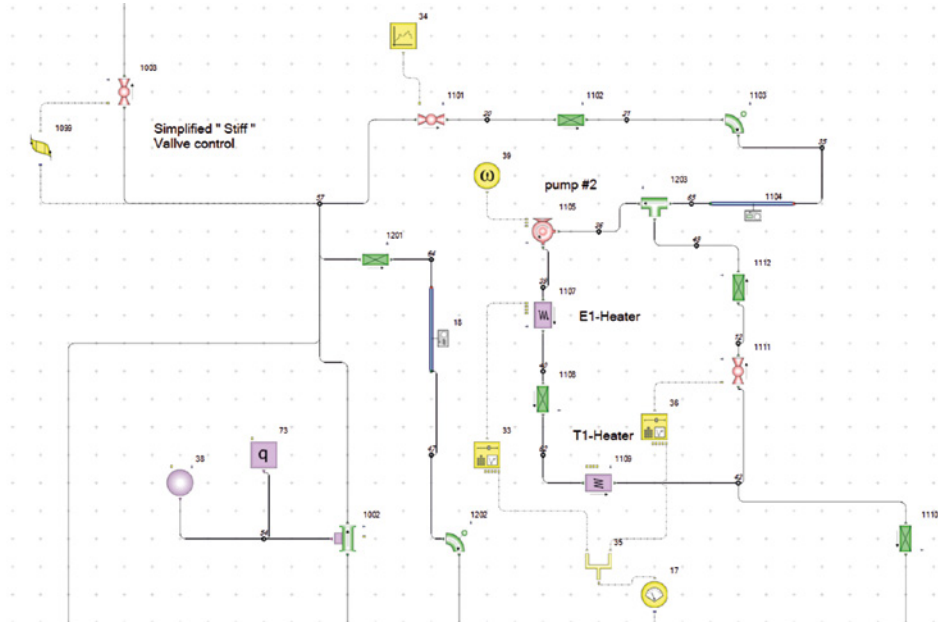


Figure 6. Automotive industry have to comply with most severe environment regulations. To meet these standards all vehicle systems, including engine cooling systems, will be run "on demand" by programmed calibrations. This trend is hastened by introduction of hybrid and full electric traction vehicle: then future 1D simulation models have to investigate transient operations and will be populated by a good share of sensor and control elements.

temperature, heat transfer capacity and coolant flow rates. Hybrid and electric vehicles most challenging function is battery thermal management: their efficiency is granted inside a narrow temperature operative window, so they have to be either cooled or heated and thermally robust enough to withstand quick and Ampere-intensive recharging cycles.

In the near future of automotive engineering, synthesis and judgment developed by the sum of individual experiences and extremely deep knowledge of their components will lead engine cooling system teams. They will have to interact more than today with other departments, sharing information and solving potential conflicts, accepting compromises and performance trade-off. In order to minimize arguments, achieve effective development time reduction but adding quality and build environmentally friendly vehicles, they will be required to take part in a final project: a collaborative development process, including in a common design and virtual analysis environment their parts and elements to perform vehicle-wide engine cooling checks with all other R&D automotive departments.

1D simulation approach is well suited for this task. Provided future engineers don't forget a venerable yet effective guideline, dating back to Aristotle: "Superiority of demonstrations by fewer postulates or hypotheses". In a nutshell: Keep Things Simple and Work Hard.

CAD-Embedded **Battery Pack Design Optimization** for Mobilis Electric Vehicle

By Vitor Straub, CFD Specialist and Guilherme Tondello, Engineering Director, Creative Solutions



“We were very insecure about the operating conditions of our battery pack. We couldn't know for sure if the cooling solutions adopted would suffice in the most diverse climatic conditions we can find in the country. Thankfully, with FloEFD™ and the expertise of Creative Solutions, it was possible to develop a good model of our battery pack. Numerous situations were simulated and with this, we were able to optimize the design in order to guarantee the perfect operation of the batteries in different conditions”

Thiago Hoeltgebaum, R&D Director, Mobilis

Creative Solutions is a customer-centric group which offer computational design and simulation services to its clients in diverse areas such as automotive, aerospace, energy generation, oil and gas, and telecommunications among others and have customers spread throughout Latin America. Recently, we engaged Mobilis, a Brazilian company, to develop small electric vehicles (EV) for recreational use. The purpose of this work was to optimize the battery pack geometry in Mobilis to avoid problems caused by insufficient refrigeration, while maximizing the internal air flow and keeping the system under ideal operation conditions, extending the life of the equipment. CAD-embedded simulation capabilities of FloEFD were central to our work for battery design optimization.

Figure 1 shows the battery pack design and its location on the floor, underneath the driver seat of the vehicle. The battery pack has 4.1kWh of total energy and peak power of 12.3kW with 32 cells in a 16S2P configuration (two cells in parallel and 16 of such units connected in series). The battery pack weighs 60kg, has a volume of approximately 30 liters and is air-cooled. Cells were supplied by GB Systems in China and have Lithium Iron Phosphate (LFP) based chemistry.



The work was done in two parts:

- In the first stage, temperature distributions in the battery pack were simulated with the original pack design to examine the severity of thermal issues in the pack, and
- In the stage two, CAD-embedded battery pack design optimization was pursued to reduce maximum temperature and to deliver more uniform temperature distribution among cells during operation.

A more uniform temperature distribution and lower maximum, as is well-known by now, results in longer battery life. Simulation studies were conducted in two distinct operating conditions, see Table 1. The FloEFD-driven redesign of battery pack, as showcased in this article, resulted in significant improvements in the thermal behavior that guarantees thermal comfort of the batteries under very critical conditions.

Battery Pack Design Exploration

The original battery pack design, as shown in Figure 1(b), consisted of one inlet and outlet for air with an outlet port on the side with smaller diameter than the inlet port. Although the calculated Reynolds number didn't exceed transition value for turbulence, in this work turbulent flow is assumed for aluminum base plate (enclosure of the battery pack) due to the likely interactions between air and uneven ground underneath the vehicle. Since the battery pack is air-cooled, air flow distribution within pack has a strong impact on battery thermal behavior. This section discusses results based on steady-state simulations to assess thermal behavior of battery pack. Figure 2 shows air pressure distribution in the pack. Figure 3 shows temperature distribution in the pack with the peak temperature of 84°C, significantly higher than maximum recommended temperature (60°C) from the cell manufacturer. Further analysis showed that the air outlet location rendered low volumetric flow and its reduced diameter in relation to the entrance was a limiting factor. However, the barrier formed because of the air outlet port being very close to the battery cells was the most impacting factor in the thermal performance of the system, motivating change in geometry. Essentially, the constrained space between the cells and the air outlet port rendered insufficient air flow.

Through a couple of design iterations, modifications were made to:

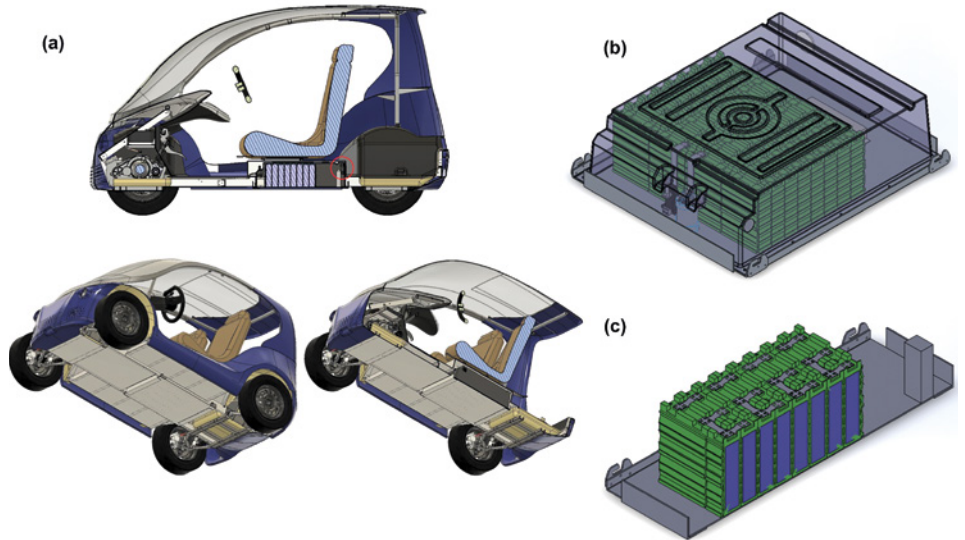


Figure 1. (a) Battery pack housed at the floor of Mobilis vehicle (b) Battery pack design (c) Cells configurations in the battery pack

1. Increase the number of inlets and outlets to two,
2. Shift air outlet ports to the front face of the pack from the side, and
3. Increase outlet ports diameter to match with inlet ports.

The resultant CAD design is shown in Figure 4. Figure 5 shows air flow (pressure distribution) in the re-designed pack. Flow constriction near the outlet (see Figure 2) from the original pack design was eliminated with very few areas of flow stagnation compared to the original design. Also, the new design improved air flow rate in the narrow area of battery cells and battery pack enclosure to aid in convective heat transfer. Figure 6 shows the resulting temperature distribution in the new pack. As can be seen, maximum temperature is 54°C (compared to 84°C for the original design) and is well within the maximum recommended temperature by the cell manufacturer.

Operational Viability of Redesigned Battery Pack under Critical Conditions

Once the redesigned, battery pack operated within the battery manufacturer-recommended temperature limits, we simulated the thermal response of the redesigned battery pack under the critical conditions. Critical conditions (Table 1) are defined as the conditions vehicle may get exposed to for short periods of time but is not designed to operate continuously. Our analysis showed the redesigned pack will reach very unsafe temperatures

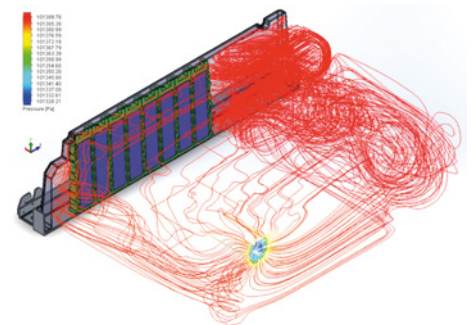


Figure 2. Air pressure distribution inside original battery pack

Status	Nominal Operation	Critical Operation
Ambient temperature (°C)	30°	38°
Average heat generation (W/cell)*	4.06	12.8
Average vehicle speed (mis)	6.94	2.78
Reynolds Number	307,971	119,718
Average convective heat transfer coefficient for A1 base plate (W/m2-K)	23.7364	11.4465
Air inlet	Positive static pressure of 64 Pa	
Air outlet pressure (kPa)	101.325	

Table 1. Summary of operating conditions

of up to 110°C, if operated under such critical conditions continuously, as shown in Figure 7. The focus, however, was to estimate temperature ramp up in the battery pack once it's subjected to such extreme conditions and if it would be enough for the system to react.

Figure 8 shows the temperature rise in the battery pack when subjected to these critical operating conditions. Under such conditions, the battery pack can operate for ~78 minutes from rest conditions before the battery pack temperature rises beyond the maximum recommended temperature of operation (60°C). Thanks to battery's large thermal mass, this slow temperature rise rate offers reasonable time to take necessary actions to avoid safety or battery life-limiting damages to the battery pack.

Impact on Mobilis EV Development

For any industry, disruptive technology such as with electric vehicles, it is very important for a company to take all steps to assure there are no design flaws, unpredicted use conditions, and limit liability risks. With the help of FloEFD's unique CAD-embedded simulation capabilities, we were able to quickly simulate dozens of scenarios and explore the battery thermal behavior with change in battery CAD design. This opened many battery design optimization possibilities for Mobilis EV. Through FloEFD-driven design exploration simulations, we could obtain an optimized battery pack design and assured the cooling system was adequate for the harshest cases, such as driving on a long steep uphill with the vehicle loaded, when the asphalt is hot, or starting the vehicle when it has been parked outside on a sunny summer day. The simulations were instrumental for Mobilis to understand if there are use conditions that can negatively impact battery life and should be avoided by customers as well as for devising strategies to mitigate liability issues that can be caused by misuse or random unpredictable system failures.

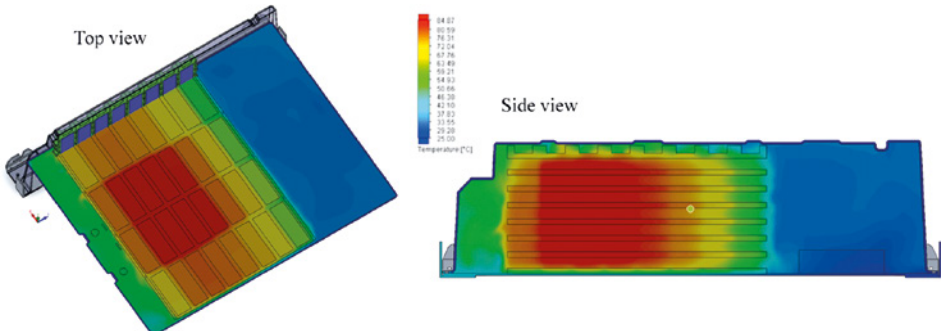


Figure 3. Temperature distribution in battery pack with original pack design. Simulation results are for the nominal operation.

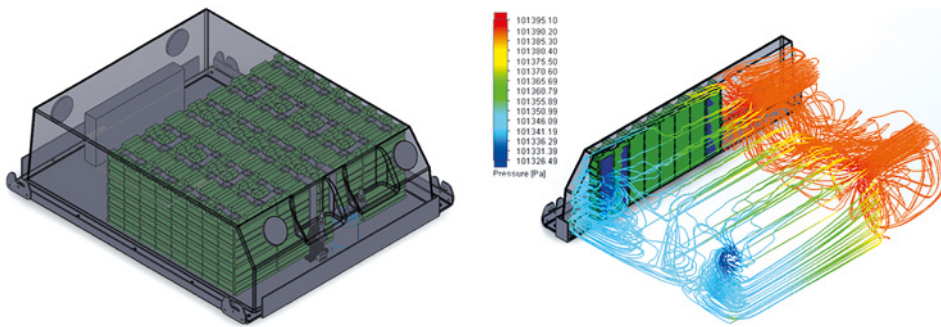


Figure 4. Redesigned battery pack with changes to air inlet and outlet ports location, dimension and numbers

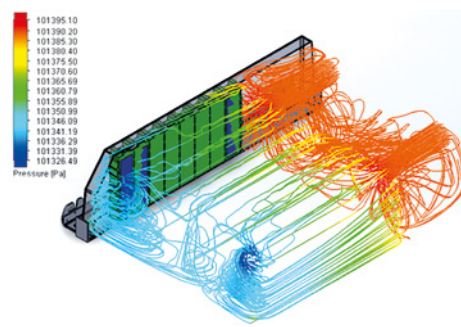


Figure 5. Air pressure distribution inside the redesigned battery pack

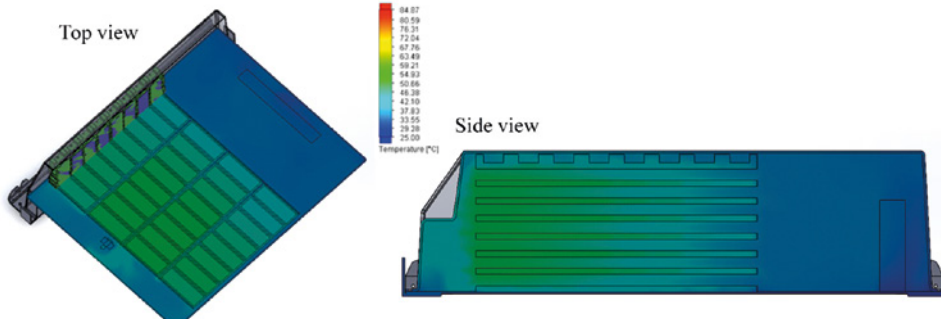


Figure 6. Temperature distribution in the redesigned battery pack for the nominal operating conditions. Maximum temperature in the pack is 54°C. Color legend is kept the same as in Figure 3 for ease of contrast between the original and the redesigned pack

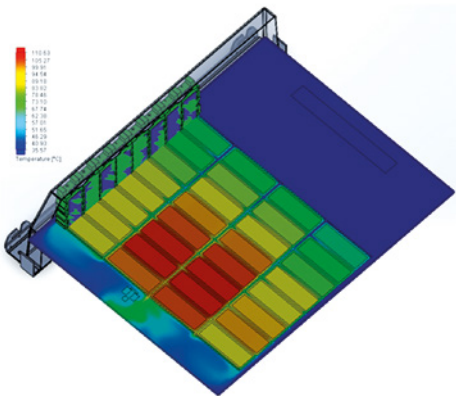


Figure 7. Redesigned battery pack temperature profile if operated under critical conditions continuously. Max temperature reaches unsafe levels of 110°C

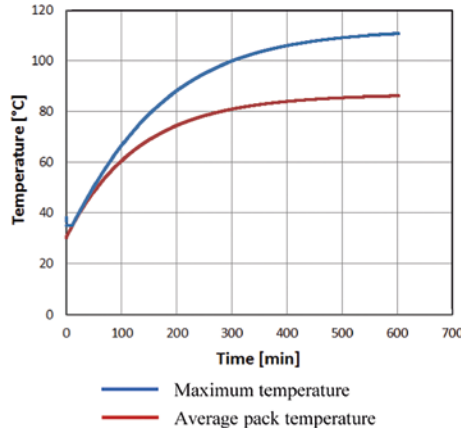


Figure 8. Battery pack temperature rise with time when subjected to critical operating conditions

Geek Hub

An ancient invention suddenly undergoes a renaissance.

By Mike Gruetzmacher, Technical Marketing Engineer, Mentor, a Siemens Business

About 15 years ago, I became aware of the Flettner rotor in a book about “forgotten inventions”. Anton Flettner invented a rotor ship, equipped with the rotors named after him. The rotors use the Magnus effect, named after Heinrich Gustav Magnus. Two ships were built in the 1920s, the Buckau, renamed Baden-Baden, even sailed from Germany to America and back.

The second ship, the Barbara, was equipped with two diesel engines and three rotors and has been used as a commercial freighter in the Mediterranean. With wind force 5, it ran at 13.5 kn operating with diesel engines (which powered the ship propeller) and rotors simultaneously. Without operating the rotors, running with the diesel engines only, it ran at 10 kn. Using the rotors only, without diesel engines, it was almost as fast at 9.5 kn. This means the rotors were able to achieve almost the same ship velocity as the diesel engines. In the single rotor operating condition, the Barbara gained almost the same speed as the single diesel engine operating condition [1]. The economic crisis, cheap oil and the increasing performance of the diesel engines, with which these kind of sails could no longer compete, unfortunately sealed the end of this technology in the 1930s [1].

A few years ago, as a young application engineer, I tried to reproduce this effect, but I did not succeed in successfully simulating this effect. A couple of months ago, my colleague, Jim Petroski, drew my attention to this technology again, because it has again been fulfilled and applied in today's shipping industry [2, 3]. In the meantime, rotating capabilities were developed for FloEFD. Therefore, it is also time for me to pick up this example again.

The Magnus force, which is the main influencing factor, can be simulated in FloEFD. Figure 1a shows a rotating cylinder.

A rotating, round object in an airstream experiences a force transverse to the flow direction. This is illustrated in Figure 1a by the blue low pressure area above the cylinder.

The modern application of the Flettner rotor offers one main advantage. A rotating

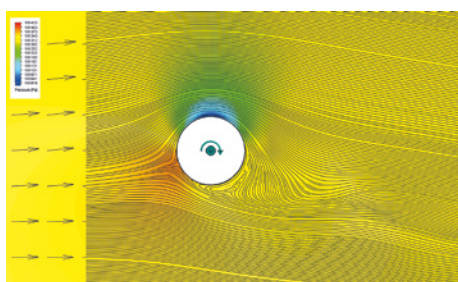
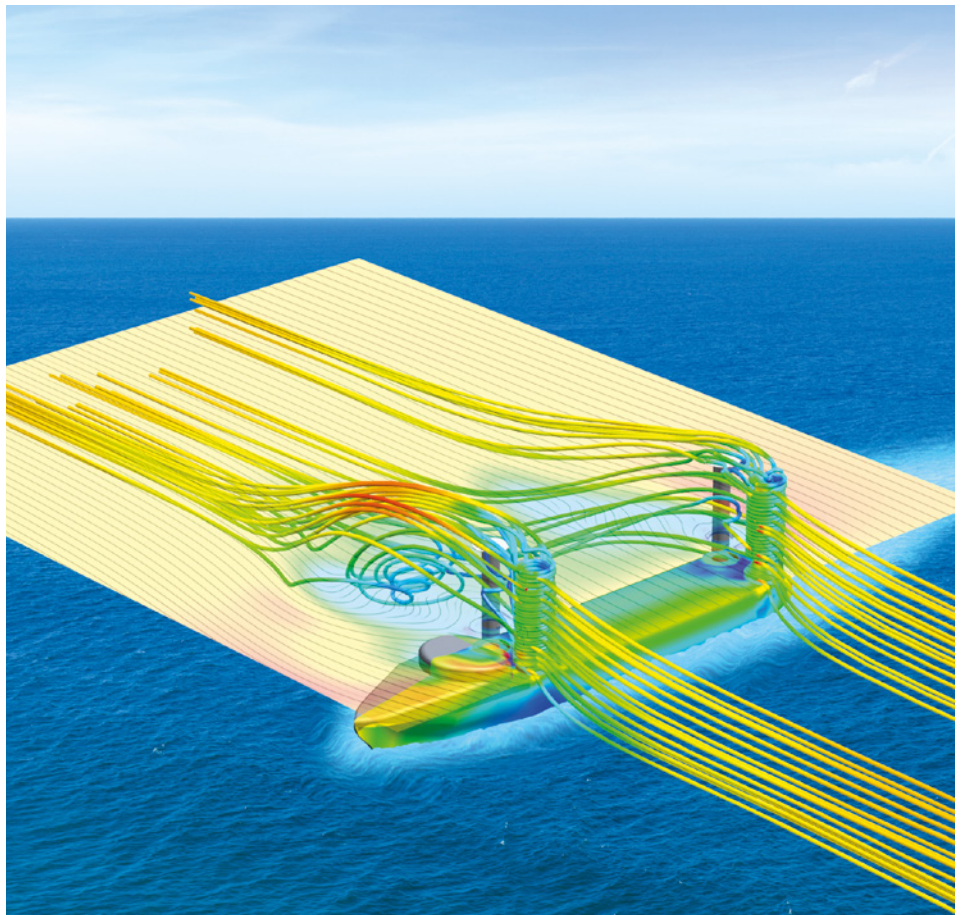


Figure 1a. Rotating cylinder

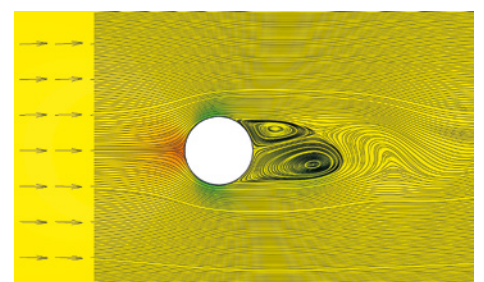


Figure 1b. Stationary cylinder

cylinder produces a force transversely to the air flow direction through the Magnus effect of suction and compression forces. The forces of the rotors are generated by the rotation and act transversely to the wind direction. Hence, they do not generate any savings in situations where the resulting wind direction is directly from the front or from behind, comparable to sailing “in irons” or “running with the wind”. The greatest advantages can thus be achieved when the wind comes from the side. The speed of the rotor must be adapted to the wind speed. At higher wind speeds, the rotor speed is also increased so that high drive energy is also to be provided for the rotors at high wind energy. Modern measuring and control systems allow an efficient adjustment of the rotational speed and direction of rotation and therefore make this technology interesting again in terms of fuel savings.

A simplified example of a vessel equipped with the four shown rotors was used and the forces of the air flow only, are considered. The water forces were neglected for this comparison. The ambient velocity for the simulation is the resultant of the wind speed and the forward movement of the ship.

The goal was to reproduce the influence of the Magnus effect and to visualize it. Even if only qualitative results can be shown, the effect can be illustrated visually. This example is based on a generic, simplified model of a vessel, so there are no real drag coefficients here.

Figure 4 shows the vessel example and the resulting air velocity directions for the study. The air speed is 20 kn, from several directions between 20° and 160°. The height of the rotors is 20m with a diameter of 4m. The rotating speed of the rotors is 100 RPM for the four rotors. A parametric study was applied in FloEFD.

Figure 5 shows a qualitative comparison of the vessel example. As can be seen in the diagram, the resulting drag force on the ships body is less on rotating rotors. Less drag force means a lower fuel consumption, which saves money and protects the environment.

As expected, the highest reduction in the drag force is achieved at approximately 90°. It is not exactly at 90° due to the influence of the vessels shape, which also corresponds to the available public information [4].

Of course, it is also necessary to consider the weight of the vehicle, the maintenance, the control technology, the possibly lost freight capacity etc. in order to be able to evaluate

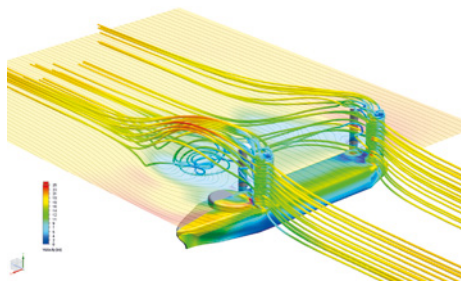


Figure 2. Vessel simulation with FloEFD

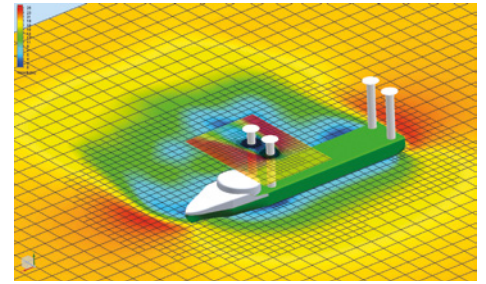


Figure 3. Vessel simulation with FloEFD

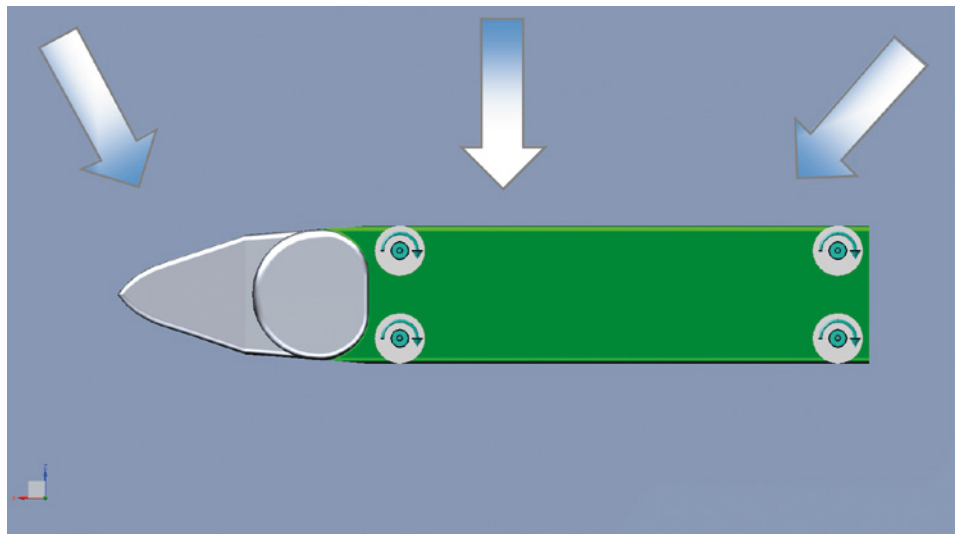


Figure 4. Vessel example with resulting air directions

the savings. According to public operators' information, the fuel savings are estimated to be about 25% due to the use of Flettner rotors. Considering the high utilization rates in shipping industry, it is certainly an attractive and environmentally friendly measure. Maybe we will see similar approaches in future for ferries and cruise liners.

Further approaches to fuel economy can be found on the Internet, e.g. Container ships with sails or the Vidskip [5], Many opportunities for further geek hub studies...

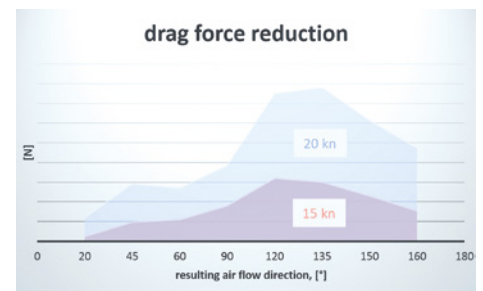


Figure 5. Drag force reduction

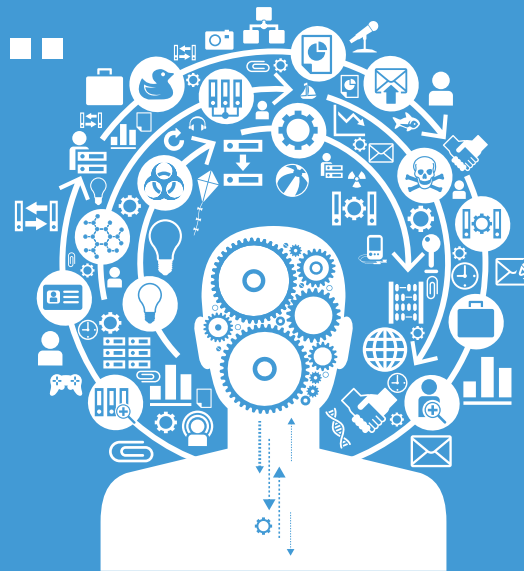
References

- [1] Christian Maehr, „Vergessene Erfindungen: Warum fährt die Natronlok nicht mehr?“, DuMont 2002, ISBN 3-8321-7816-3
- [2] https://www.youtube.com/watch?v=kDyBrSW1_Og
- [3] <https://www.youtube.com/watch?v=2pQga7jxAyc>
- [4] <https://www.youtube.com/watch?v=aQXp75Qt99M>
- [5] <http://www.ladeas.no/>
<http://www.auerbach-schiffahrt.de/>
<http://go.mentor.com/4NmtM>

Brownian Motion...

The random musings of a Fluid Dynamicist

Brownian Motion or **Pedesis** (from Greek: πήδησις Πεδε:σις 'leaping') is the presumably random moving of particles suspended in a fluid (a liquid or a gas) resulting from their bombardment by the fast-moving atoms or molecules in the gas or liquid. The term 'Brownian Motion' can also refer to the mathematical model used to describe such random movements, which is often called a particle theory.



From here to Autonomy

I am just about coming to terms with autonomous vehicles, it seems it will happen in my lifetime and I perhaps could use the extra time to learn to play Bridge. I was listening to the radio earlier and heard that by 2050 (hope I hold out that long) we will likely be traveling on pilot-less aircraft. Now that made me feel uncomfortable.

Air travel is very safe, just 1.25 accidents per million jet flights, so what would be the benefit to me as a passenger? Apparently this is a cost and resource issue – fares would decrease by an average of 10%, and also there is a long-term pilot shortage.

The announcement when you sit down and prepare for take-off would be very different, 'Hello, this is your Captain speaking', would seem rather hollow. Perhaps instead it might boast about how many miles it has flown, with how little rest and the size of the hard-drive. Somehow though a 'real' pilot has been elevated to a mystical status, helped by Chesley Sullenberger landing his plane safely on the Hudson. It is hard to imagine holding an auto-pilot in such high esteem.

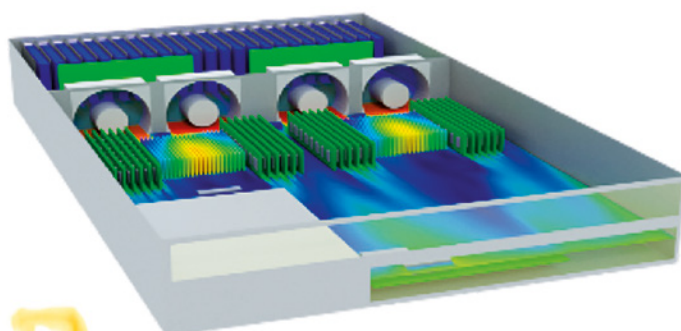
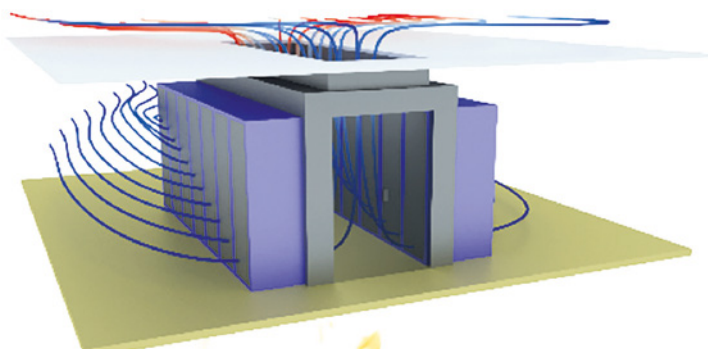
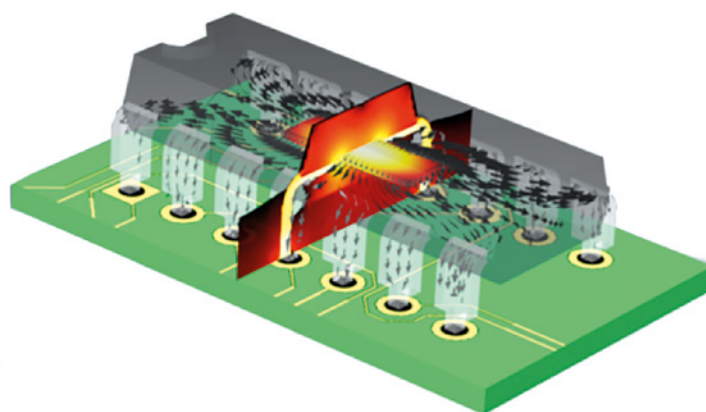
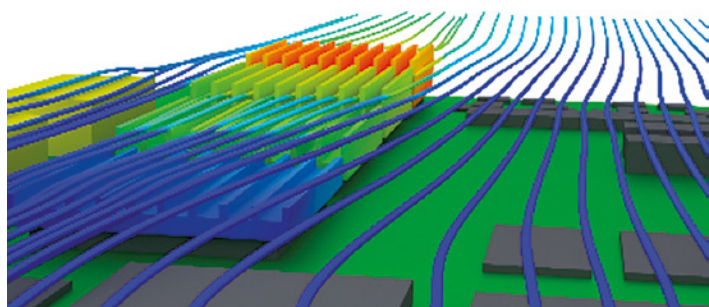
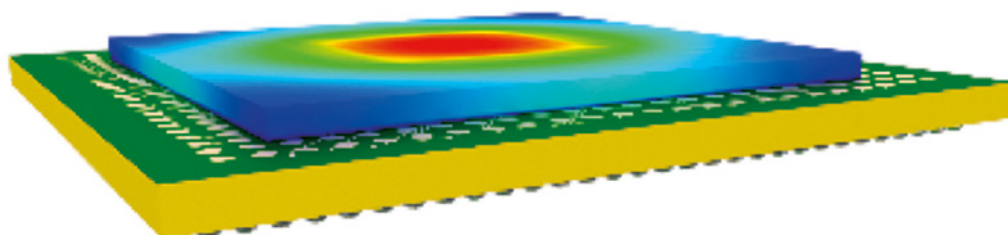
Less well-known is that autonomous ships already cruise our oceans and it seems likely that crew-less will regularly set sail long before either vehicles or aeroplanes become routine. Directed from land-locked control centers, they are the perfect career option for those who suffer from motion sickness!



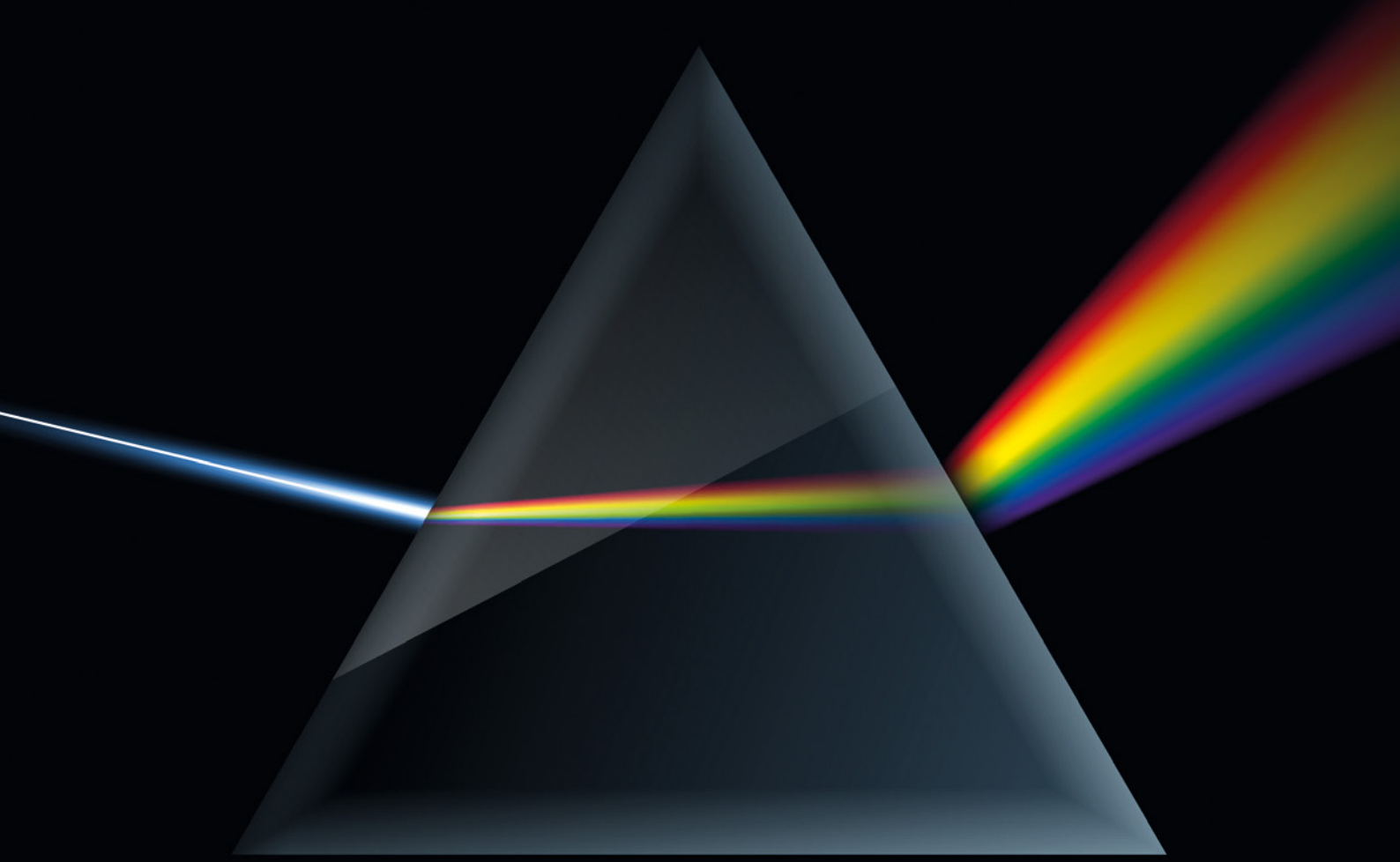
FlOThERM™ - when the

HEAT IS ON

WE DELIVER ELECTRONICS COOLING



Full Spectrum CFD



Designers

Engineers

Analysts

With the acquisition of CD-adapco and Mentor Graphics, Siemens PLM now has the most comprehensive suite of CFD solutions in the marketplace today serving all use profiles in modern product development and PLM workflows, from R&D Specialists to Designers. We embrace CFD-focused integrated multi-physics to frontloading via MCAD-embedding, including design space exploration, yielding proven accuracy and unprecedented productivity benefits to all users.

www.mentor.com

Mentor[®]
A Siemens Business